

Modulation of Brain Activity and Networks by Deep Brain Stimulation of the Subthalamic Nucleus and L-DOPA Therapy in the 6-OHDA-Hemiparkinsonian Rat

INAUGURAL-DISSERTATION

Zur Erlangung des Doktorgrades der
Mathematisch-Naturwissenschaftlichen Fakultät
der Universität zu Köln



Vorgelegt von
NADINE APETZ
aus Bonn

Digital Express²⁴, Köln
2022

Berichterstatterinnen:
Prof. Dr. Heike Endepols
Prof. Dr. Silvia Daun

Tag der mündlichen Prüfung:
08.06.2022

Eidesstattliche Erklärung

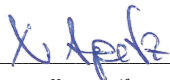
gemäß der Promotionsordnung vom 12. März 2020

Hiermit versichere ich an Eides statt, dass ich die vorliegende Dissertation selbstständig und ohne die Benutzung anderer als der angegebenen Hilfsmittel und Literatur angefertigt habe. Alle Stellen, die wörtlich oder sinngemäß aus veröffentlichten und nicht veröffentlichten Werken dem Wortlaut oder dem Sinn nach entnommen wurden, sind als solche kenntlich gemacht. Ich versichere an Eides statt, dass diese Dissertation noch keiner anderen Fakultät oder Universität zur Prüfung vorgelegen hat; dass sie - abgesehen von unten angegebenen Teilpublikationen und eingebundenen Artikeln und Manuskripten - noch nicht veröffentlicht worden ist sowie, dass ich eine Veröffentlichung der Dissertation vor Abschluss der Promotion nicht ohne Genehmigung des Promotionsausschusses vornehmen werde. Die Bestimmungen dieser Ordnung sind mir bekannt. Darüber hinaus erkläre ich hiermit, dass ich die Ordnung zur Sicherung guter wissenschaftlicher Praxis und zum Umgang mit wissenschaftlichem Fehlverhalten der Universität zu Köln gelesen und sie bei der Durchführung der Dissertation zugrundeliegenden Arbeiten und der schriftlich verfassten Dissertation beachtet habe und verpflichte mich hiermit, die dort genannten Vorgaben bei allen wissenschaftlichen Tätigkeiten zu beachten und umzusetzen. Ich versichere, dass die eingereichte elektronische Fassung der eingereichten Druckfassung vollständig entspricht.

Teilpublikation: Apetz N, Paralikar K, Neumaier B, Drzezga A, Wiedermann D, Iyer R, Munns G, Scott E, Timmermann L, Endepols H. Towards chronic deep brain stimulation in freely moving hemiparkinsonian rats: Applicability and functionality of a fully implantable stimulation system. J Neural Eng. 2021 March 18(3) 036018

__Köln, den 22.03.2022

Ort, Datum



Unterschrift

Table of Contents

Eidesstattliche Erklärung.....	3
Table of Contents.....	4
List of Abbreviations.....	6
Kurzzusammenfassung.....	8
Abstract.....	10
General Introduction.....	11
Aim of this study.....	24
Data Availability Statement.....	25
Inclusion of a Publication.....	25
CHAPTER ONE: Towards chronic deep brain stimulation in freely moving hemiparkinsonian rats: Applicability and functionality of a fully implantable stimulation system.....	26
Abstract.....	26
Published Chapter.....	26
CHAPTER TWO: Comparing acute and chronic deep brain stimulation of the subthalamic nucleus in a rat hemiparkinson model: a [¹⁸F]FDG PET study.....	27
I. Introduction.....	27
II. Materials and Methods.....	28
II.i Animals.....	28
II.ii Stimulation System.....	28
II.ii.i Electrode.....	28
II.ii.ii Stimulation System.....	28
II.iii Surgical Procedures.....	28
II.iv Treatment Regimes.....	29
II.iv.i Deep Brain Stimulation.....	29
II.v Cylinder Test.....	30
II.vi Positron Emission Tomography.....	30
II.vi.i [¹⁸ F]FDG.....	30
II.vi.ii [¹⁸ F]FDOPA.....	30
II.vii Statistical Analysis.....	31
II.vii.i Behaviour.....	31
II.vii.ii [¹⁸ F]FDG PET.....	31
II.vii.iii [¹⁸ F]FDOPA PET.....	31
III. Results.....	31

III.i Dopaminergic Lesion and Electrode Placement	32
III.iii Effects of Acute and Chronic STN DBS on Cerebral [¹⁸ F]FDG Uptake	33
III.iv Effects of Acute STN DBS on Brain Networks.....	34
IV. Discussion.....	38
CHAPTER THREE: Comparing the effects of DBS of the subthalamic nucleus and systemic L-DOPA treatment on brain (network) activity and motor performance in hemiparkinsonian rats.....	47
A. Introduction.....	47
B. Material and Methods.....	48
B.a Animals	48
B.b Stimulation System and Surgical Procedures	49
B.c Treatment Regimes.....	49
<i>B.c.a Deep Brain Stimulation</i>	<i>49</i>
<i>B.c.b L-DOPA Injections.....</i>	<i>49</i>
B.d Cylinder Test.....	49
B.e Positron Emission Tomography.....	50
<i>B.e.a [¹⁸F]FDG PET</i>	<i>50</i>
<i>B.e.b [¹⁸F]FDOPA PET</i>	<i>50</i>
B.f Statistical Analysis.....	50
<i>B.f.a Behaviour</i>	<i>50</i>
<i>B.f.b [¹⁸F]FDG PET.....</i>	<i>50</i>
<i>B.f.c [¹⁸F]FDOPA PET.....</i>	<i>51</i>
C. Results.....	51
C.a Dopaminergic Lesion and Electrode Placement	51
C.b Effects of DBS and L-DOPA on Behaviour.....	51
C.c Effects of DBS and L-DOPA on Cerebral [¹⁸ F]FDG Uptake	52
C.d Effects of DBS and L-DOPA on Brain Networks.....	54
D. Discussion	57
Conclusion	63
References	65
Acknowledgements.....	91

List of Abbreviations

[¹⁸F]FDG	=	2-deoxy-2-[¹⁸ F]fluoroglucose
[¹⁸F]FDOPA	=	L-3,4-dihydroxy-6-[¹⁸ F]fluorophenylalanine
6-OHDA	=	6-hydroxydopamine
AADC	=	aromatic amino-acid decarboxylase
BNST	=	bed nucleus of stria terminalis
CF	=	contralateral (affected) front paw
COMT	=	catechol-O-methyltransferase
CPu	=	caudate putamen
DA	=	dopamine
DAT	=	dopamine transporter
DBS	=	deep brain stimulation
fMRI	=	functional magnetic resonance imaging
GABA	=	γ-aminobutyric acid
Glu	=	glutamate
GPe	=	globus pallidus externus
GPi	=	globus pallidus internus
IF	=	ipsilateral (non-affected) front paw
L-DOPA	=	3,4-dihydroxy-L-phenylalanine/levodopa
LRRK2	=	gene coding for leucine-rich repeat kinase 2
M1	=	primary motor cortex
MAOB	=	monoamine oxidase type B
MFB	=	medial forebrain bundle
MPPP	=	1-methyl-4-phenyl-4-propionoxy-piperidine
MPTP	=	1-methyl-4-phenyl-1,2,5,6-tetrahydropyridine
MRI	=	magnetic resonance imaging
MSN	=	medium spiny neuron
Nac	=	nucleus accumbens
NaCl	=	sodium chloride
OCT	=	optical coherence tomography
PAG	=	periaqueductal grey
PARK7	=	gene coding for DJ-1
PD	=	Parkinson's disease
PDCCP	=	PD cognition-related covariance pattern
PDRP	=	PD motor-related covariance pattern
PET	=	positron emission tomography
PINK1	=	gene coding for PTEN-induced putative kinase 1
PPTg	=	pedunclopontine tegmental nucleus
PRKN	=	gene coding for parkin
SN	=	substantia nigra
SNARE	=	soluble N-ethylmaleimide-sensitive-factor attachment receptor
SNc	=	substantia nigra pars compacta
SNCA	=	gene coding for synuclein alpha (α-synuclein)

SNr	=	substantia nigra pars reticulata
SPECT	=	single-photon emission computed tomography
STN	=	subthalamic nucleus
SUV_{cer}	=	standardised uptake value ratio normalised to cerebellar mean
SUV_{wb}	=	standardised uptake value ratio normalised to whole brain mean
THS	=	tiefe Hirnstimulation
TFCE	=	threshold-free cluster enhancement
VIM	=	nucleus ventralis intermedius
VOI	=	volume of interest
VTA	=	ventral tegmental area

Kurzzusammenfassung

Morbus Parkinson (PD) ist eine fortschreitende neurodegenerative Erkrankung, die durch einen selektiven Verlust dopaminerger Zellen in der Substantia nigra pars compacta verursacht wird. Sie äußert sich durch zahlreiche motorische und nicht-motorische Symptome wie Tremor, Bradykinesie, Steifheit, autonome Funktionsstörungen, Schlafstörungen oder psychiatrische Symptome. PD ist für Patienten aber auch deren Angehörige sehr belastend und strapaziert als die nach Morbus Alzheimer zweithäufigste neurodegenerative Erkrankung weltweit zudem auch das Gesundheitssystem stark. Da die Goldstandardtherapie, d.h. die Verabreichung des Dopaminvorläufers 3,4-Dihydroxy-L-Phenylalanin (= Levodopa = L-DOPA) oder dopaminerger Agonisten, nach mehrjähriger Behandlung zu unerwünschten Dyskinesien und Wirkungsschwankungen führt, wurden in den letzten Jahrzehnten Anstrengungen unternommen, Alternativen zu finden. Die tiefe Hirnstimulation (THS) des Nucleus subthalamicus (STN) ist eine sichere und gut verträgliche Lösung, die die Parkinson-Symptome verbessern und die Einnahme dopaminerger Medikamente erheblich reduzieren kann. Obwohl sie sich in den letzten 35 Jahren in der klinischen Anwendung bewährt hat, sind die genauen Mechanismen, durch die die THS im Gehirn wirkt, noch nicht vollständig geklärt. Ein großes Problem ist der Mangel an gut übertragbaren präklinischen Studien. Die meisten Tierstudien sind durch die Einschränkung der Tiere durch Kabel, Rucksäcke oder Kopfstücke von externen Stimulationssystemen eingeschränkt, die zusätzlich eine Einzelhaltung der Tiere erfordern und somit die normale motorische Leistung und das Verhalten beeinflussen. Darüber hinaus sind die Stimulationsperioden oft auf Minuten bis Tage begrenzt, während Parkinson-Patienten über Jahre hinweg chronisch stimuliert werden. Auch bildgebende Studien, die die Auswirkungen von THS auf die Aktivität im erkrankten Gehirn untersuchen, sind rar, obwohl sie gut geeignet sind, um das Verständnis für die weiterreichenden Auswirkungen von THS auf die Aktivität pathologischer Netzwerke zu erhöhen. Insbesondere in Kombination mit Verhaltens- und motorischen Leistungstests haben bildgebende Verfahren das Potenzial, die durch THS ausgelösten Veränderungen im gesamten Gehirn aufzuzeigen, und sie mit einer Verbesserung der Symptome in Beziehung zu setzen. Letztlich hilft ein besseres Verständnis der durch eine effektive STN-THS hervorgerufenen Veränderungen der Gehirn(netzwerk)aktivität, dieses therapeutische Instrument weiterzuentwickeln und zu verbessern. Ziel der vorliegenden Studie war es daher, ein vollständig implantierbares Stimulationssystem zu etablieren, das Stimulation in frei beweglichen und in Gruppen gehaltenen Tieren ermöglicht, und dessen mögliche Anwendungsbereiche zu testen. In einem ersten Schritt wurde das entwickelte Standardverfahren für die Implantation des Systems und die Testprotokolle an Hemiparkinson-Ratten validiert, was zur Veranschaulichung der Auswirkungen einer akuten STN-THS auf den Gebrauch der Vorderpfoten und die Stoffwechselaktivität des Gehirns führte. Die akute STN-THS erhöhte vor allem den ipsiläsionalen Hirnstoffwechsel, insbesondere im Striatum, während sie ihn kontralateral verringerte. Sie wirkte somit dem metabolischen Ungleichgewicht entgegen, das durch einseitige 6-Hydroxydopamin (6-OHDA)-Läsionen verursacht wird, was zu einer Verbesserung der motorischen Leistung führte. Alle untersuchten Hirnnetzwerke wurden darüber hinaus durch akute THS verändert. Im nächsten Schritt wurden die unterschiedlichen Auswirkungen akuter und chronischer fünfwöchiger STN-Stimulation auf die Nutzung der Vorderpfoten und den Hirnstoffwechsel untersucht. Die Auswirkungen der chronischen (fünfwöchigen) STN-THS auf den Gehirnstoffwechsel unterschieden sich geringfügig von denen der akuten Stimulation, und waren mit besserer motorischer Leistung verbunden. Im letzten Teil wurden die Auswirkungen der akuten STN-THS auf das Verhalten und die Gehirn(netzwerk)aktivität mit denen der Goldstandardtherapie L-DOPA und einer Kombination beider Behandlungen verglichen. Wie vermutet wirkten sich die verschiedenen Behandlungen unterschiedlich auf den Hirnstoffwechsel und die

Netzwerkaktivität aus, was sich auch in der motorischen Leistung zeigte. Das etablierte Stimulationssystem ist somit bei sorgfältiger Auswahl der Simulationsstellen und -parameter ein nützliches Instrument, um die Auswirkungen akuter und chronischer STN-THS in frei beweglichen Tieren auf die Stoffwechselaktivität und die Netzwerkfunktion des Gehirns zu untersuchen.

Abstract

Parkinson's disease (PD) is a progressive neurodegenerative disorder caused by a selective dopaminergic cell loss in the substantia nigra pars compacta. It manifests through numerous motor and non-motor symptoms including tremor, bradykinesia, rigidity, autonomic dysfunction, sleep disturbances or psychiatric symptoms. While being a wearing condition for patients as well as their friends and family, PD also puts a heavy burden on the health system being the second most common neurodegenerative disorder worldwide following Alzheimer's disease. As the gold standard therapy, *i.e.* administration of the dopamine precursor 3,4-dihydroxy-L-phenylalanine (= levodopa = L-DOPA) or dopaminergic agonists, leads to unwanted dyskinesias and response fluctuations after several years of treatment, efforts have been made during the last few decades to find alternatives. Deep brain stimulation (DBS) of the subthalamic nucleus (STN) is a safe and well-tolerated solution that can improve parkinsonian symptoms and significantly reduce dopaminergic medication intake. However, while it has been well established in the clinical use over the last 35 years, the exact mechanisms by which DBS acts in the brain are yet to be fully elucidated. A big problem is the lack of well transferable pre-clinical studies. Most animal studies are limited by the constraints imposed on animals by cables, backpacks or headpieces of external stimulation systems that additionally require single housing and influence normal motor performance and behaviour. Additionally, stimulation periods often only last minutes to days compared to the chronic stimulation of PD patients over years. Similarly, imaging studies elucidating the effects of DBS on activity in the diseased brain are scarce while they are well suitable to broaden the understanding of the bigger scale impact of DBS on pathological network activity. Especially in combination with behavioural and motor performance tests, imaging studies have the potential to illustrate whole brain alterations elicited by DBS that lead to the improvement of symptoms. Ultimately, a better understanding of the brain (network) activity changes evoked by effective STN DBS helps to further develop and improve this therapeutic tool. The present study therefore aimed at establishing a fully implantable stimulation system that allows for stimulation in group-housed, unrestrained and freely moving animals, and testing out its possible range of applications. In a first step, the developed standard operating procedure for system implantation and testing protocols was validated in hemiparkinsonian rats, resulting in the illustration of the effects of acute STN DBS on front paw use and brain metabolic activity. Acute STN DBS increased mainly ipsilesional brain metabolism, especially in the striatum, while decreasing it contralesionally. It therefore counteracts the metabolic imbalance caused by unilateral 6-hydroxydopamine (6-OHDA) lesions, leading to improvements of motor performance. Additionally, all brain networks analysed were altered by acute DBS. In a next step, the different impact of acute and chronic five-week STN DBS on front paw use and metabolic brain activity was investigated. The brain metabolic effects of chronic (five week) STN DBS slightly differed from those of acute stimulation resulting in a better motor performance. The last part compared the effects on behaviour and brain (network) activity evoked by acute STN DBS with those caused by the gold standard therapy, L-DOPA, and a combination of the two treatments. As hypothesised, the different treatments affected brain metabolism and network activity differently, which also showed in motor performance. Hence, when stimulation sites and parameters are well chosen the established stimulation system is a useful tool to elucidate the effects of acute and chronic STN DBS in unrestrained animals on brain metabolic activity and network functioning.

General Introduction

Parkinson's disease (PD) is a progressive neurodegenerative disorder that is characterised by a loss of neuromelanin-laden dopaminergic neurons in the substantia nigra pars compacta (SNc) and other selective neurons, including aminergic brain stem nuclei and cholinergic neurons, ultimately leading to decreased dopamine (DA) levels in the striatum (1).

With an age-adjusted incidence rate of about 10 to 15 per 100,000 and a crude prevalence of 100 to 200 per 100,000 (2) PD is the runner-up of the most common neurodegenerative disorders worldwide following Alzheimer's disease (3). Age is the most consistent risk factor of PD confirmed by a steadily and rapidly increasing prevalence with age (1,4,5). Accordingly, the sporadic idiopathic form of PD with its late onset (> 60 years of age) makes up about 90 % of all PD cases, while the hereditary, familial form mostly affecting people 40 years of age or younger accounts for the rest (3). Gender has been found to play a potential role in susceptibility as men are roughly twice as likely to suffer from PD as women (6). Several studies have also tried to elucidate the significance of ethnicity in the prevalence of PD. Findings indicate that Caucasians might be more susceptible than Asians or Blacks. However, demographic or methodological differences such as health-care standard, survival rate, or diagnostic criteria may easily confound these results. Hence, the difference in prevalence between ethnic groups cannot be exclusively attributed to genetic or environmental factors between populations (2,3,5,6).

The exact causes and mechanisms of action of PD still remain to be fully elucidated today (7–11). However, there are numerous approaches including cellular, molecular, and biochemical changes as well as environmental risk factors. Studies suggest that one of the environmental risk factors could be the exposure to pesticides and other environmental toxins including illicit drugs. For example, in the 80's the intravenous use of the drug 1-methyl-4-phenyl-1,2,5,6-tetrahydropyridine (MPTP), a by-product in the synthesis of 1-methyl-4-phenyl-4-propionoxy-piperidine (MPPP) also called "synthetic heroin", was found to induce severe parkinsonism in several individuals (12,13). MPTP was therefore later used for animal models of PD (see below) (14). Similarly, Betarbet and colleagues (2000) found, that the chronic systemic exposure of rats to the pesticide rotenone has inhibitory effects on the mitochondrial complex I, leading to a highly selective degeneration of nigro-striatal dopaminergic neurons and therefore PD-like symptoms (11). Other environmental factors examined for being positively or negatively associated with the development of PD include beta-blockers, head injury, consumption of dairy products, high caloric intake (higher risk), physical activity, coffee/caffeine, non-steroidal anti-inflammatory drugs, and smoking (lower risk) (15,16). However, clear causal relationships between these factors and the onset of PD could not be shown to date.

Several genes have been found to cause or at least play a role in the aetiology of familial PD. Spontaneous mutations of these genes, however, can also be seen in patients without a family history of the disease (17). The best studied ones are *SNCA*, the gene coding for the protein α -synuclein, *PINK1*, the gene coding for PTEN-induced putative kinase 1, the protein deglycase DJ-1 gene named *PARK7*, the leucine-rich repeat kinase 2 gene *LRRK2*, and *PRKN*, the gene coding for parkin (18,19). But investigations continue and more and more genetic PD loci are found (20). The dysfunction of many of these genes lead to cellular processes that have been shown to be involved in neurodegeneration like oxidative stress, abnormal cellular pathways, and above all, mitochondrial dysfunction (21–23).

A very big part of the scientific interest is also directed at excessive protein accumulation and aggregation in hereditary as well as sporadic PD. Alpha-synuclein might be the best known of these misfolded and aggregated proteins. It is a small 144-amino acid presynaptic protein that regulates vesicular function by promoting

SNARE-complex assembly (24). It is therefore crucial for neurotransmitter release. In 1997 point mutations of *SNCA* were shown to play a role in some inherited forms of PD (25). Especially dupli- or triplications of the gene that increase levels of the protein rather than changing its function seem to have pathological effects (7,26). Accordingly, the difference in significance for PD pathology between α -synuclein monomers and oligomers has been investigated, finding that oligomerisation caused by excess levels of α -synuclein is the primary cause for its toxicity (27).

Several groups found that α -synuclein constitutes the major part of inclusion bodies called Lewy bodies, one of the main cellular pathological hallmarks of sporadic idiopathic PD (28,29). Apart from α -synuclein, they can contain more than 90 different proteins and other substances many of which, like DJ-1, LRRK2, parkin or PINK1, are linked to PD (see above) (30). Lewy bodies, which can also occur in other neurodegenerative diseases such as dementia with Lewy bodies or the Lewy body variant of Alzheimer's disease, are eosinophilic intracytoplasmic fibrillar inclusions typically found in vulnerable monoaminergic and cholinergic neurons (8,31,32). More specifically, in PD they occur in dopaminergic neurons of the SNC, noradrenergic neurons of the locus coeruleus, cholinergic neurons of the nucleus basalis of Meynert, the hypothalamus, and occasionally in other sites like cerebral cortex or thalamus (31,32). Occasionally, *i.e.* in 10 % of individuals over the age of 60, Lewy bodies occur without diagnosed PD, referred to as incidental Lewy body disease. However, the increase of its prevalence with age and the strong similarities of morphological changes and pathological progression between the two diseases suggests that incidental Lewy body disease is merely a pre-symptomatic phase of PD (8,33). The exact role of Lewy bodies in PD is still under discussion. While it used to be believed that their formation was a cytotoxic process causing cell death, new evidence shows that their formation may be a neuroprotective mechanism in PD (30). For example, it was suggested that Lewy bodies are related to aggregates, cytoprotective inclusions that decompose and remove excess amounts of cytotoxic proteins (32,34). Chen and Feany (2005) found that an increase of α -synuclein aggregation, as found in Lewy bodies, reduces its toxicity in a *drosophila* model of PD (35). Other studies showed that oligomers and protofibrils of α -synuclein are cytotoxic, while its fibrillary aggregates have cytoprotective effects (36,37). Nevertheless, the exact role of Lewy bodies, be it protective or toxic, remains to be elucidated.

Another substance that gained more and more interest over the past decades is neuromelanin. It is a dark intracellular catecholamine-derived pigment found in specific catecholaminergic cells of the SNC (dopaminergic cells), the locus coeruleus (noradrenergic cells) and some other brain areas (38). These specific cells produce and accumulate the black-brownish pigment during their lifetime, which has been associated with a progressive deterioration of cell metabolism, and, therefore, may play a role in neurodegeneration in old age (39). Indeed, it has been found that cells containing greater amounts of the pigment are more prone to cell death in the elderly, that this effect is even aggravated in PD patients (39). Additionally, in a rodent model exhibiting age-dependant increases of neuromelanin, animals developed PD-like pathology after reaching a certain neuromelanin threshold (40). Together with the fact that the loss of cells containing neuromelanin correlates with the loss of dopaminergic innervation in the striatum (41), this suggests a link between neuromelanin and PD. The exact role of the pigment in the pathogenesis of PD, however, remains unknown to date (40). What is known is that there is a delicate equilibrium between iron, neuromelanin, and DA in cells producing the pigment. While being an important player in many redox reactions, abnormal levels of reactive iron, as found in PD, are cytotoxic. Neuromelanin is an effective metal chelator able to trap iron and protect cells against oxidative stress. Excessive amounts of DA can cause cell death but when converted to neuromelanin, the cell is rescued. When released by degenerating neurons, neuromelanin activates microglia that cause further release of the pigment, neuroinflammation, and -degeneration (42). It becomes clear that the right balance between these players needs to be maintained to prevent neurodegeneration. In the state of

PD, some (or all) of these mechanisms could be impaired, leaving neuromelanin-laden cells more prone to cell death (38). Finally, Halliday *et al.* (2005) found the increased levels of neuromelanin in yet healthy SN neurons of PD patients to be associated with α -synuclein accumulating around the pigments' lipid components (43). They suggest these early intracellular changes to render nigral cells more vulnerable to degeneration in PD (43).

As a consequence of the neurodegeneration caused by the multiple factors mentioned above, the transmission of information between brain structures is altered in PD. It was discovered that the dopaminergic depletion occurring in the parkinsonian SNc is accompanied by an increased activity of γ -aminobutyric acid (GABA)-releasing neurons in the basal ganglia output nuclei globus pallidus internus (GPI) and substantia nigra pars reticulata (SNr) (44). To explain these changes of signal transmission and the accompanying pathological changes in voluntary movement, a basal ganglia model including a "direct" and an "indirect" pathway has been employed for a long time (Fig 1 A). According to this model, in the healthy brain GABAergic projections from striatum to GPI and SNr constitute the direct pathway (arrow I. in Fig. 1 A). The indirect pathway between striatum and basal ganglia output nuclei includes GABAergic projections from striatum to globus pallidus externus (GPe), from GPe to subthalamic nucleus (STN), and glutamatergic projections from STN to GPI and SNr (arrows II., III., and IV. in Fig. 1 A) (44).

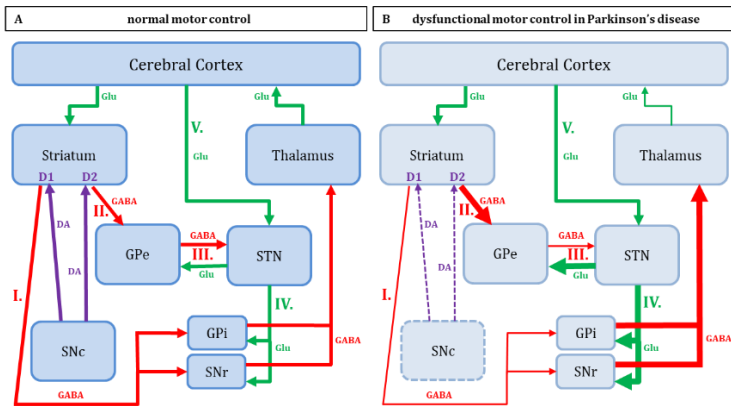


Fig. 1 Schematic illustration of the basal ganglia model suggested for Parkinson's disease including direct, indirect and hyperdirect pathway. **A** Neuronal signal transmission in the healthy brain. **B** Impaired neuronal signalling in the state of Parkinson's disease (PD) with a dopamine-depleted substantia nigra pars compacta. For the sake of clarity, anatomy and interconnections are simplified and incomplete. Purple arrows represent dopaminergic signal transmission; green arrows indicate excitatory signal transmission; red arrows indicate inhibitory signal transmission. Arrow I. represents the direct pathway; arrows II., III., and IV. represent the indirect pathway; arrows IV. and V. constitute the hyperdirect pathway. Dashed lines represent the pathological nigro-striatal dopamine system in PD. The width of arrows indicates the degree of activity, i.e. neuronal firing rate, of each pathway. Abbreviations: D1 = activating dopaminergic D1 type receptors, D2 = deactivating dopaminergic D2 type receptors, DA = dopamine, GABA = γ -aminobutyric acid, Glu = glutamate, GPe = globus pallidus externus, GPI = globus pallidus internus, SNc = substantia nigra pars compacta, SNr = substantia nigra pars reticulata, STN = subthalamic nucleus.

The GABAergic striatal output neurons of both pathways are called medium spiny neurons (MSN) (45). Generalising, those MSNs directly projecting to GPI and SNr predominantly contain D1 type receptors, whereas those projecting to the GPe express mainly D2 type receptors (46). DA provokes different effects on

these receptors and, therefore, on the neurons carrying the respective type. Simply said, the medium spiny neurons with D1 type receptors, constituting the direct GABAergic pathway to GPi and SNr, are excited, and those carrying D2 type receptors, forming the indirect pathway, are inhibited (47,48). However, as a neuromodulator DA is acting on multiple classes of pre-, post-, and extrasynaptic receptors situated on the spines or dendrites of MSNs, glutamatergic presynapses, or striatal interneurons (49,50). Here, DA is able to affect several aspects of synaptic transmission, including ion channels, signalling molecules, vesicular release machinery, or membrane insertion, thereby modulating neurotransmitter release, postsynaptic sensitivity, or membrane excitability of the pre- and postsynaptic neurons (49,50). Additionally, the discovery of MSNs co-expressing D1 and D2 type receptors and forming pharmacologically distinct D1-D2 receptor heteromers stresses the complexity of dopaminergic action on MSN signal transmission, which is most likely exceeding the mere difference in effect between D1 and D2 type receptors (51).

Figure 1 A illustrates the balance between direct and indirect pathway and their inhibitory and excitatory actions on GPi and SNr in the healthy brain. In the parkinsonian brain, DA-depletion disturbs this balance as shown in Figure 1 B. The activity of the direct pathway is reduced (arrow I. in Fig. 1 B), disinhibiting GPi and SNr. The indirect pathway on the other hand is overactive (arrows II. and IV. in Fig. 1 B), further increasing activation of GPi and SNr. Due to the GABAergic projection neurons of these two structures their excessive output then leads to an inhibition of the thalamus and, therefore, less activation of cortical motor areas, impairing the execution of voluntary movements (46).

However, studies in monkeys suggest a third, monosynaptic and, therefore, extremely fast "hyperdirect" pathway between cortex, STN and GPi/SNr (52,53), and its existence in man has been confirmed (54–56). Nambu *et al.* (2005) therefore proposed the "dynamic model" for the regulation of voluntary movements. In short, upon cortical movement initiation, sequential information processing by the three pathways triggers the correct, chosen motor program (direct), while suppressing competing programs (indirect and hyperdirect) (57). Disinhibition is a key mechanism in basal ganglia motor control (58,59). According to the model, the direct pathway facilitates the release of selected motor programs by disinhibiting the target areas of basal ganglia output nuclei. More precisely, the GABAergic MSNs of the striatum inhibit the tonic GABAergic activity of nigral and pallidal neurons projecting to the thalamus. This inhibition of the inhibition, or disinhibition, of the thalamus facilitates its signal transduction to the cortex and, consequently, movement execution (Fig. 2 A) (59). The indirect and hyperdirect pathways suppress competing programs by targeted inhibition of certain neuron populations within the involved brain regions (57). Similar to the other two pathways, the hyperdirect pathway is also pathologically altered in PD (60,61). Hence, in the parkinsonian state, the dynamic model states that signalling of the indirect and hyperdirect pathway increases, leading to the suppression of larger thalamic and cortical areas. In contrast, signalling of the direct pathway is reduced, weakening its disinhibition of the thalamus in a spatial and temporal manner and, therefore, impairing the execution of selected motor programs through cortical areas (Fig. 2 B) (57).

Nevertheless, newer studies found that the mechanisms of the basal ganglia networks are not quite that simple. For example, it has to be taken into account that DA depletion seems to have different effects on striato-pallidal and striato-nigral neurons, causing diverse morphological and physiological changes and effects on their synaptic function (45). It is also criticised that a strict separation of direct and indirect pathways or D1 and D2 type receptors does not exist and that both pathways are interconnected (62–64). The classical model does also not consider abnormal network interactions and possible compensatory mechanisms (62,63). For instance, chronically low levels of DA were found to evoke compensatory cell-type specific, homeostatic changes in MSNs that restore the balance between direct and indirect pathways by adapting their intrinsic excitability (65). Finally, the role of different striatal interneurons, namely GABAergic,

cholinergic, and nitric oxide synthase-positive interneurons, in synaptic cross-talk between direct and indirect pathway MSNs and the concomitant importance of nitric oxide and endocannabinoids in long-term depression has been stressed (64).

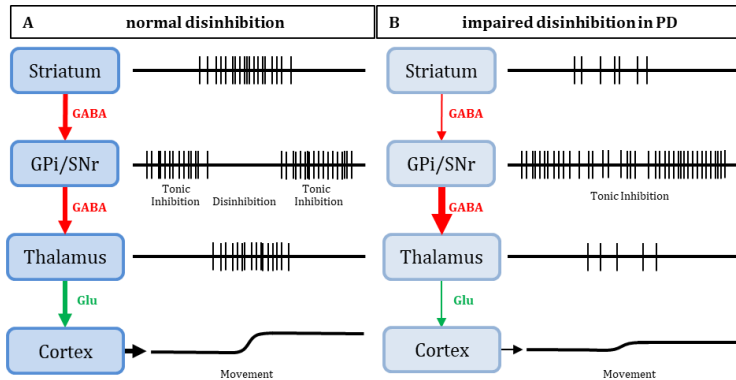


Fig. 2 Illustration of disinhibition as a key mechanism in the motor control of basal ganglia. (adapted [58]) **A** In the healthy brain, phasic activity of inhibitory striatal medium spiny neurons interrupt the tonic inhibitory output of GPi and SNr, therefore disinhibiting the thalamus and facilitating activation of motor areas in the cortex leading to movement execution. **B** In the parkinsonian brain, the pathologically inactive striatum fails to sufficiently inhibit the GABAergic nigral and pallidal projections to the thalamus. Without an adequate disinhibition, the thalamus cannot activate cortical motor areas and the execution of movement is impaired. Green arrows indicate excitatory signal transmission; red arrows indicate inhibitory signal transmission. Abbreviations: Glu = glutamate, GPi = globus pallidus internus, PD = Parkinson's disease, SNr = substantia nigra pars reticulata.

As complex as the mechanisms involved in PD are its symptoms. They comprise motor symptoms and non-motor symptoms, which can be divided into autonomic dysfunction, sleep disturbances, cognitive and psychiatric symptoms, and sensory impairments (66,67). Motor symptoms often first occur when 70 % to 80 % of dopaminergic cells are lost (68). They typically include bradykinesia, meaning the slowness of initiation of voluntary movements, and the decrease of speed and amplitude of repetitive movements. Muscular rigidity, a stooped body posture and freezing of gate are also very common in PD. Some patients develop a shuffling gate with reduced arm swinging, some present with very small and rapid steps that lead to loss of balance and postural instability. Besides micrographia, the tendency for a particularly small handwriting, patients also suffer from a lack of facial expression (hypomimia) and speech impairments (66,67). The probably most prominent motor symptom of PD, occurring in about 80 % of patients, is the 4 - 6 Hz resting tremor, mostly seen in the hands (1,67).

Non-motor symptoms often develop before the start of motor symptoms and can pose an even bigger distress than motor complications. They are highly diverse and differ from patient to patient (67,69). Autonomic dysfunction includes, amongst others, low blood pressure to the extent of dizziness or loss of consciousness, constipation, and excessive sweating (66,67). Fractionated sleep, daytime sleepiness or restlessness in bed are some of the sleep disturbances experienced by roughly two thirds of PD patients (70-73). Cognitive and psychiatric symptoms can manifest as hallucinations or illusions, apathy, anhedonia to the extent of depression, anxiety, impaired memory or cognitive deterioration to the point of dementia (66,67). Lastly, sensory disturbances in PD include the deterioration or loss of smell, abnormal sensation in certain body

parts, *e.g.* restlessness in the legs or numbness, as well as pain that is felt by up to 85 % of PD patients, predominantly in the lower limbs (74–77).

The heterogenic clinical nature of PD that overlaps in parts with other forms of parkinsonism makes a definite diagnosis challenging. To date, there is no specific test for the exclusive diagnosis of PD, and the use of standard clinical criteria does reduce but not prevent misdiagnoses (66,78–80). Hence, PD is mistaken for other diseases like essential tremor, vascular parkinsonism or atypical parkinsonian symptoms in about 25 % of patients (78). The only distinctive features found in PD patients are neuropathological, namely the loss of neuromelanin-laden dopaminergic neurons mainly in the SNc and the formation of Lewy bodies (1,79,80). However, both features have also been shown to occur isolated from one another challenging their causal relationship in PD (80). Hence, the diagnosis of PD often depends on the exclusion of other neurological diseases. Therefore, the presence of a combination of specific cardinal motor symptoms (*e.g.* asymmetric onset of symptoms, resting tremor, bradykinesia, rigidity) together with the absence of exclusionary features, including substantial changes in brain imaging, pyramidal or cerebellar signs, or a history of drug abuse, and good responsiveness to the DA precursor 3,4-dihydroxy-L-phenylalanine (= levodopa = L-DOPA) is assessed (68,79).

Imaging techniques have not played a major role in the diagnosis of PD for a long time but are increasingly employed to support and facilitate diagnostics lately (81–83). The techniques used include optical coherence tomography (OCT), transcranial tomography, magnetic resonance imaging (MRI) and molecular imaging, *i.e.* single-photon emission computed tomography (SPECT) and positron emission tomography (PET) (84,85).

OCT produces cross-sectional images of internal biological tissues (86). Its utilisation in PD diagnostics is based on the finding that retinal nerve fibre layer and macular thickness, both of which can be measured using OCT, are significantly reduced in PD patients, and that the thinning of these structures is associated with disease progression and severity (87,88). Hence, the thickness of the retinal nerve fibre layer or macula can serve as a potential biomarker for the differential diagnosis of PD (85).

Transcranial tomography detects ultrasound echoes thereby assessing the echogenicity of certain brain regions like the substantia nigra (SN). In PD, a hyperechogenicity of the SNc is thought to be associated with increased levels of iron in mesencephalic cells of the nigro-striatal pathway (85,89). During the last 20 years the echofeatures of brain structures of various neurodegenerative diseases including vascular parkinsonism, drug-induced parkinsonism or essential tremor, have been found to differ from one another suggesting transcranial tomography as a potential diagnostic tool. However, the diagnostic accuracy of this method, especially in early stages of PD, is still insufficient for making transcranial tomography a reliable technique to diagnose PD (89).

MRI is based on the principle of nuclear magnetic resonance, *i.e.* the emission of measurable energy in form of radio signals by certain atomic nuclei when placed in a strong magnetic field and stimulated by radio waves of a specific frequency (90). As structural brain imaging of patients in early stages of PD is generally without pathological findings when using conventional MRI, it has been mainly used to exclude other pathologies that do show structural abnormalities (91). Nevertheless, during the last decades, several new techniques and approaches have been explored to improve MRI as a diagnostic tool for PD. In the past, conventional, structural MRI assessed indicators for neurodegeneration like increased cellular levels of iron, changes in tissue volume or other signal change in a qualitative manner. Today, new methodologies have brought advantages that also allow the quantitative analysis of structural alterations and biochemical changes. Magnetic resonance-planimetry and -volumetry, quantitative structural magnetic resonance-based techniques including diffusion imaging and magnetisation transfer imaging are just a few of the newer imaging techniques applied. Furthermore, the development of high-field MRI with higher field strength led to increased signal-to-noise

ratios, spatial resolution, and, therefore, overall better image quality (91). Advances were not only made in the technical aspects of MRI, but also in image analysis algorithms leading to new possibilities like neuromelanin-sensitive MRI showing progressive loss of neuromelanin-containing cells in SNc and locus coeruleus, functional MRI, or multimodal imaging combining information gained from different modalities (81,91,92). Thus, MRI has evolved into a helpful tool not only in PD diagnosis and the monitoring of disease progression, but also in the efforts to further understand this complex disease, its characteristics and its therapeutic approaches (93–98).

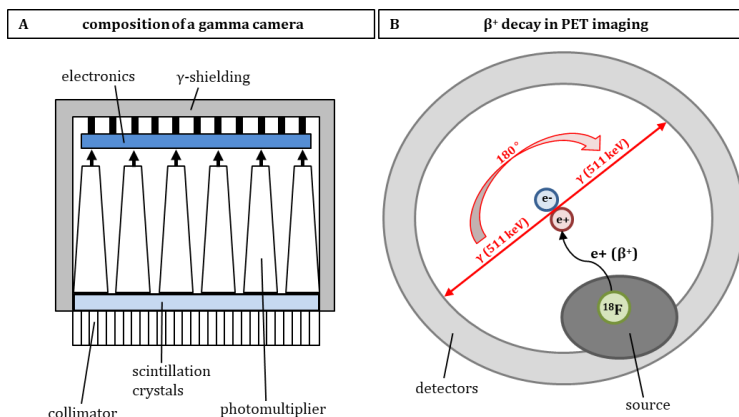


Fig. 3 Composition of a gamma camera and β^+ decay in PET imaging. **A** Schematic illustration of the components of a gamma camera (adapted (102)). When excited by γ -rays, the scintillation crystals emit light photons, which are then converted to electrons and amplified by photomultipliers. The photomultiplier finally gives out an electrical impulse, whose amplitude gives information about the radiation energy and its emission site. Gamma cameras used for SPECT additionally have a collimator in front of the scintillation crystals to only detect rays of a certain direction. **B** Principle of the decay of positron emitting isotopes utilised for PET imaging using the example of ^{18}F (adapted (116)). After being emitted by the radionuclide, positrons travel a short distance (2 – 3 mm) through the tissue before combining with an electron and undergoing annihilation. This produces energy in form of two antiparallel 511 keV photons (γ -rays), which can then be detected in coincidence by the gamma camera.

SPECT, introduced in 1963 (99), and PET, established in the 1970s (100,101), are nuclear medical imaging techniques that have become standard methods for diagnosis, treatment evaluation, and intervention (102). Both methods are based on the principle that radioisotopes that decay via beta emission are introduced into an organism (patient or laboratory animal), and the γ -rays (photons) produced during the beta plus (β^+) decay, i.e. positron emission, are detected (102,103). This is achieved with so called "Anger" or gamma cameras (102). They consist of several parts (Fig. 3 A). First comes the γ -ray detection medium, i.e. scintillation crystals of thallium-doped sodium iodide (NaI[Tl]) for SPECT (104), and cerium-doped lutetium oxyorthosilicate ($\text{Lu}_2\text{SiO}_5[\text{Ce}]$) for PET imaging (105). They emit light following the fluorescence process occurring through the excitation produced by entering γ -rays. The resulting light photons are converted to electrons and amplified in a downstream photomultiplier tube, which finally gives out an electrical impulse. The gamma camera can then use the amplitude of this impulse to determine the radiation energy and its emission site. As the emission of gamma photons is isotropic, gamma cameras for SPECT imaging, detecting single photons, have a collimator preceding the scintillation crystals that only permits rays of a certain

direction to be detected by the crystals (102). The spatial resolution of PET and SPECT is limited by several factors, including the physics of β^+ decay, the technology for the detection of two γ -rays in coincidence (PET), or the trade-off between spatial resolution and sensitivity caused by the collimator used (SPECT) (106). Today, modern small-animal-PET and -SPECT scanners can reach spatial resolutions up to ~ 0.7 mm (107,108). Typical γ -ray emitting radionuclides used for SPECT are for example iodine-123 (^{123}I) or technetium-99m ($^{99\text{m}}\text{Tc}$). In general, SPECT tracers have lower emission energies (usually around 150 keV) and longer half-life times than the isotopes used in PET (109). In PD diagnostics, SPECT imaging is mainly used with radiotracers binding to the DA transporter (DAT), a protein exclusively expressed on presynaptic dopaminergic nerve terminals. The so called DAT-SPECT is therefore able to show the integrity of dopaminergic nerve terminals, or the loss thereof, in the striatum (110). Although its use has been debated, a majority of studies found SPECT imaging to be beneficial in the differential diagnosis of PD (111–115). Hence, it is an established method especially to detect premotor and early PD and distinguish it from other neurodegenerative diseases like essential tremor or non-neurodegenerative parkinsonism (110,114).

Similar to SPECT, in PET imaging a radiopharmaceutical or so called PET tracer labelled with a positron-emitting isotope (typically ^{18}F , ^{11}C , ^{13}N , or ^{15}O) is introduced into an organism, *i.e.* patient or laboratory animal, and accumulates according to the tracer's properties (117,118). During its decay, the isotope then emits positrons (β^+ decay) (119) that travel a few (2 – 3 mm) millimetres through the tissue before combining with an electron, undergoing annihilation and producing energy in form of two photons/ γ -rays, each with an energy of 511 keV, travelling in opposite directions (Fig. 3 B) (118,120). These photons can then be detected and the point of annihilation reconstructed (118,120). In sum, a picture of the tracer's distribution within the body can be reproduced (117). Since many of the radioactive tracers are or resemble organic molecules like glucose, amino acids, or neurotransmitters that naturally occur in an organism, PET imaging allows for the targeting, quantification, and illustration of specific metabolic processes. It can therefore shed light on the integrity and functionality of certain organs, including the brain, and biochemical processes while other imaging techniques are limited to the illustration of physical structures (121–125).

In matters of PD, two tracers in particular have won recognition over the last decades: 2-deoxy-2- ^{18}F fluoroglucose (^{18}F FDG) and L-3,4-dihydroxy-6- ^{18}F fluorophenylalanine (^{18}F FDOPA) (Fig. 4). ^{18}F FDG is a fluorinated radioactive substitute for glucose. It has been applied to measure regional cerebral glucose consumption, *i.e.* brain energy metabolism, *in vivo* for over 40 years (126,127). ^{18}F FDG crosses the blood brain barrier using the same transporters as glucose. Once in the neuron, the enzyme hexokinase phosphorylates it irreversibly to ^{18}F fluorodeoxyglucose-6-phosphate, which is then not further metabolised. Hence, it accumulates in metabolically active cells resulting in PET images representing brain activity patterns (128). As changes thereof can help identify characteristic pathological patterns, ^{18}F FDG PET imaging is a widely used tool in the differential diagnosis of PD (129). However, the purpose of ^{18}F FDG PET exceeds that of a diagnostic method and it is also used to gain further insight into the nature of a disease or the potency of therapeutic procedures. Numerous groups therefore employ ^{18}F FDG PET to investigate different aspects of PD in patients as well as animal models. To better understand the disease, Lozza *et al.* (2004) investigated the pathological disorganisation of brain networks in PD and their relationship to executive processes (130). Other studies aimed at mapping the brain metabolic patterns of animal models of PD. They also correlated the impaired glucose metabolism measured with the degree of dysfunctional motor behaviour finding similarities between animal model and patients (131,132). Other groups focused on treatment strategies and their effects on brain networks or general cerebral activity. For example, Berding and colleagues (2001) looked at resting regional cerebral glucose metabolism in advanced PD comparing the naïve condition (OFF) with that under

dopaminergic treatment (ON) (133). Other groups studied the modulating effects of deep brain stimulation (DBS) on functional networks to better understand the impact it has on a whole brain level (134–139). [¹⁸F]FDOPA is able to cross the blood brain barrier by active transport and is therefore generally injected intravenously (85). It is a fluorinated form of L-DOPA, the precursor for DA, and used to visualise the dopaminergic system *in vivo*. More specifically, it reflects the integrity and function of dopaminergic presynaptic nerve terminals, *i.e.* L-DOPA transport into the terminal, the conversion of L-DOPA to DA or [¹⁸F]FDOPA to [¹⁸F]fluorodopamine, respectively, via the enzyme aromatic amino-acid decarboxylase (AADC), and dopamine storage capacity (140,141). Interestingly, striatal, but not nigral [¹⁸F]FDOPA uptake has been shown to linearly correlate with nigral dopaminergic cell count (140,142,143). This suggests that [¹⁸F]FDOPA is not taken up by the dopaminergic cell bodies in the SNc, but only by their pre-synaptic terminals located in the striatum. Accordingly, [¹⁸F]FDOPA PET images of PD patients show specific regional, meaning striatal, reductions in tracer uptake that correlate with motor symptoms (144–146). The method has therefore become established in the differential diagnosis of PD as tracer accumulation patterns vary between PD and other neurodegenerative diseases like progressive supranuclear palsy or multiple system atrophy (147,148). Besides diagnostics, similar to [¹⁸F]FDG PET, [¹⁸F]FDOPA PET imaging has also proven helpful in other areas. For example in displaying the rate of progression of PD or in comparing early and advanced stages of the disease as shown by several groups (149–152).

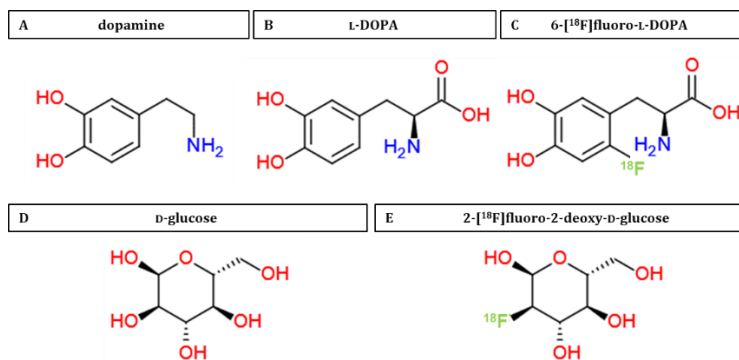


Fig. 4 Structural formulas. **A** The neurotransmitter dopamine, an important player in basal ganglia-mediated motor control. **B** The dopamine precursor levodopa (L-DOPA). The enzyme aromatic amino-acid decarboxylase converts it to dopamine by splitting off CO₂. **C** The fluorinated form of L-DOPA, 6-[¹⁸F]fluoro-L-DOPA, used display dopaminergic integrity in PET imaging. **D** Glucose, an important part of energy metabolism. **E** The fluorinated form of glucose, 2-[¹⁸F]fluoro-2-deoxy-D-glucose, used to for glucose metabolism PET imaging.

Some researchers take advantage of a combination of [¹⁸F]FDG and [¹⁸F]FDOPA PET to better understand PD (153). For instance, in a previous study, a combination of [¹⁸F]FDG and [¹⁸F]FDOPA PET was used to gain a better understanding of the correlations between dopaminergic depletion severity, brain metabolism, and motor impairment in a rat model of PD (154). Nagano-Saito *et al.* (2003) also used [¹⁸F]FDG and [¹⁸F]FDOPA to investigate the relationships between pathological cerebral activity (glucose metabolism), impairment of the dopaminergic system, and motor and cognitive symptoms (155). Holtbernd and his team (2015) obtained similar results when investigating the connections between nigro-striatal dopaminergic integrity and PD-specific metabolic brain networks responsible for behavioural and cognitive impairments, namely the PD

motor-related covariance pattern (PDRP) and the PD cognition-related covariance pattern (PDCP) (156). In a recent PET/computed tomography study, Emsen and colleagues (2020) found both tracers to favourably complement each other in the diagnosis and management of PD (157). Thus, both [¹⁸F]FDG and [¹⁸F]FDOA PET imaging are not only invaluable tools in the diagnosis and management of PD, but also help to broaden the understanding of its underlying processes and mechanisms, and facilitate the exploration and improvement of existing and future therapeutic possibilities.

The multi-factorial and multi-systemic nature of PD makes it difficult to pinpoint an exact origin or cause. Hence, to date there is no neuroprotective therapy available that is able to modify the disease progression and most established treatment strategies are symptomatic (158–162). For many years, the intervention with L-DOPA has been the gold standard in the treatment of PD since it is well able to improve motor symptoms (158,163). DA agonists like pramipexole or ropinirole complement the dopaminergic treatment options. They tend to have a longer half-life than L-DOPA, which decreases the motor complications seen in L-DOPA therapy, and act more specifically on the D2 type dopaminergic receptors (164). Because of the different physiological actions of L-DOPA and DA agonists, they have different sets of side effects while both show good efficacy in treating motor symptoms. Hence, they are often given in combination in low dosages (165). It has also been suggested to start early treatment with agonists before later adding L-DOPA to delay the onset of dyskinesias and motor-fluctuations seen with prolonged L-DOPA treatment (166,167). Similarly, other compounds increasing DA concentrations in the brain like monoamine oxidase type B (MAOB) inhibitors or catechol-O-methyltransferase (COMT) inhibitors are applied to manage motor fluctuations (158,168).

While initially offering great improvements, long-term treatment with L-DOPA, other dopaminergic substances or combinations of them leads to severe motor complications and side effects in most cases, as mentioned above. For example, many patients suffer from motor response fluctuations within a few years of disease progression. Phases of good drug effect and reasonable mobility alternate with unpredictable hyperkinesia and phases of poor mobility despite regular medication intake (169–171). It has been suggested that these fluctuations appear due to a decreased ability of the parkinsonian brain to buffer shifts in administration-dependent L-DOPA availability with progressing dopaminergic neurodegeneration (172). Treatment with L-DOPA for several years can also lead to so-called levodopa-induced dyskinesia, putting an additional burden onto patients (173,174). Furthermore, the necessity to increase drug doses over time to compensate for the worsening of symptoms due to an advanced disease state also increases the risk of behavioural side effects including hallucinations, delusions, mania, impulsive disorders or anxiety (175–178). Alternative approaches in the pharmacological treatment of PD and treatment-induced motor and non-motor symptoms include antioxidants, adenosine A2A antagonists, modulators of glutamatergic or serotonergic receptors, mitochondrial enhancers, antidepressants, trophic factors, β -blockers, amantadine, anticholinergics, phytotherapy and several more (158,159,179–182). However, especially for the management of non-motor symptoms the amount of high quality studies to date is scarce or their results not promising.

A newer strategy aiming at modifying the disease rather than the symptoms is stem cell and gene-based therapy. Preclinical stem cell therapy research started about 40 years ago using rat foetal dopaminergic neurons with promising results (183–186). However, when transferring the procedure to clinical studies using human foetal mesencephalic transplants, problems like high variability and low availability of cells as well as ethical concerns arose despite providing proof-of-principle (187–189). Thus, successful efforts were made to establish authentic mesencephalic dopaminergic neurons from pluripotent human embryonic stem cells and clinical trials are underway (190–194). Gene therapy is looking at introducing genes like the one for AADC (the enzyme converting L-DOPA to DA) or for glutamic acid decarboxylase into PD patients using an

adeno-associated viral type 2 vector (195–198). The potential disease modifying properties of several growth/neurotrophic factors are also being investigated. Although promising results exist, more data is needed to estimate the full potential of these newer therapies (199,200).

Besides the transplantation of cell grafts, surgical interventions for the treatment of PD comprise ablative techniques like pallidotomy, thalamotomy, or subthalamotomy as well as DBS of GPi, STN or thalamus (201). The ablative techniques are well effective long-term in treating motor symptoms while not sharing the unwanted motor side effects seen with prolonged dopaminergic medication (202–204). When performed unilaterally, pallidotomy shows the same efficacy as is seen with STN or GPi DBS, however, none of the ablative strategies comes without side effects, especially when performed bilaterally (201,205). Although these techniques have been deployed for decades, their exact mechanisms of action are yet to be fully understood (206–208).

DBS is a reversible, adaptable and generally well-tolerated yet very costly alternative to the irrevocable ablative options mentioned above. Similar to those, DBS is also applied in different brain target areas, the most prominent ones being the thalamic nucleus ventralis intermedius (VIM), the GPi and the STN. While stimulation of the VIM mainly reduces or abolishes tremor, the GPi is targeted predominantly to treat bradykinesia/akinesia, rigidity and dyskinesia (209–211). The STN seems to be the best target for the treatment of PD as its stimulation is able to improve all parkinsonian symptoms and significantly reduce dopaminergic medication intake (212–215). It is safe and has been well established over the last 35 years (216–218). In the last decade, advancements have been made regarding DBS technology. For example, new electrodes with multiple independent sources have been developed that allow for more specific steering of stimulation currents towards the target region (219,220). Advantageous over conventional spherical stimulation, the more selective stimulation of target regions leads to increased current thresholds for side effects and, therefore, bigger therapeutic windows (221,222). Another approach is the so-called closed-loop or adaptive DBS. It is based on the principle that the stimulation parameters autonomously adjust in real-time based on constant feedback input signals representative of the patient's clinical state (223). Nevertheless, despite the long period of research and the technical advancements, the exact mechanisms by which DBS acts in the brain are yet to be fully elucidated.

Animal models are an important and helpful tool in experimental medical sciences. They not only help to understand diseases by mimicking the specific features like pathogenic mechanisms and their behavioural outcome, they also help to discover and develop new therapeutic strategies (224). There are numerous animal models for PD that can be divided into two categories. The first category includes models using synthetic or environmental neurotoxins to simulate pathological, phenotypic and symptomatic characteristics of the disease. Rats and monkeys are the preferred species for this category (225–227). Acute exposure to the neurotoxins causes prompt nigro-striatal dopaminergic cell death and motor impairments, whereas chronic exposure induces a more realistic progressive model that may also include α -synuclein aggregates (17). The second category comprises transgenic and viral vector-mediated models based on knocked out genes or overexpressed PD-related gene mutations or the manipulation of dopaminergic transcription factors (17). They either disrupt the nigro-striatal pathway or reveal specific cellular and molecular pathogenic features potentially responsible for cell death. These models are most commonly implemented in mice, zebra fish and flies (225–227).

The first animal model of PD ever designed was the 6-hydroxydopamine (6-OHDA) rat model belonging to the first category (228,229). It is based on the specific uptake of the hydroxylated analogue of DA and noradrenaline, 6-OHDA, by catecholaminergic neurons via the DAT (17,225). As 6-OHDA does not cross the blood brain barrier, it needs to be injected intracerebrally (230,231). Once in the neuron, 6-OHDA accumulates

and leads to the formation of free radicals/reactive oxygen species. It has also been shown to enter mitochondria where it inhibits complex I adding to the oxidative stress and finally causing cell death (232,233). 6-OHDA fails to provoke the formation of protein aggregates or inclusion bodies but has been reported to interact with α -synuclein (234). The magnitude of dopaminergic lesion depends on the amount of 6-OHDA injected, the site of injection, and the species used. Mice, rats, cats, dogs and monkeys are all sensitive to 6-OHDA (235–238). However, rats are often the species of choice for this model. Three sites have proven most effective for the generation of Parkinsonian models, namely the SNc, the medial forebrain bundle (MFB) and the striatum (239). While injections into SNc and MFB have been shown to cause a progressive loss of nigral dopaminergic neurons over time (240,241), results for injections into the striatum have been inconclusive, as progressive and non-progressive cell loss has been observed (241,242). Irrespective of the injection site, a degeneration of 50 % to > 90 % of dopaminergic cells of the SNc can be achieved (241,242). Bilateral injections result in profound behavioural and motor deficits that can lead to animals' death as they are unable to sufficiently care for themselves (225,243). Therefore, injections are mostly applied unilaterally. As they induce asymmetric motor deficits, unilateral injections also have the big advantage that the contralateral hemisphere can serve as an internal control. Furthermore, the typical stereotypies produced by unilateral lesions like amphetamine-induced rotational behaviour correlate well with the extent of the lesion and, hence, the amount of 6-OHDA (229,244). This quantifiability of lesion and symptoms together with its high reproducibility and versatility therefore make the 6-OHDA model a great choice to test new therapeutic strategies and treatments (234,245).

Another common toxin model is the MPTP model. It is predominantly used in mice and non-human primates as rats are highly resistant to the substance (246). After passing the blood brain barrier, MPTP is transformed to its active and toxic metabolite 1-methyl-4-phenylpyridinium (MPP⁺) by MAOB. MPP⁺ is then selectively transported into dopaminergic cells via the DAT. Here, it blocks mitochondrial complex I, thereby lowering ATP levels, increasing oxidative stress and ultimately causing neuroinflammation and cell death (247). MPTP can be administered acutely or chronically via systemic or intracerebral injections (248,249). Thus, depending on the dosing route, regimen and the species or strain used, different stages and aspects of PD can be modelled from pre-symptomatic to late-stage complications (248). For example, the acute administration of MPTP in mice causes dopaminergic neurodegeneration that correlates well with motor impairment. However, these effects can improve within a few days post-injection (250). Chronic low-dose administrations on the other hand cause a delayed nigro-striatal degeneration of dopaminergic neurons and α -synuclein aggregation while missing motor impairment (251,252). Chronic models in non-human primates with repeated bilateral intracarotid injections are able to mimic L-DOPA-responsive parkinsonism comprising all the main features like progressive nigro-striatal dopaminergic cell loss, α -synuclein aggregates, and motor deficits. Despite its weaknesses, like the reversibility of symptoms after cessation of treatment, the MPTP model therefore is the best resembling the clinical syndrome of PD to date (17,225,226).

For the sake of completeness, pesticides and herbicides like paraquat, rotenone or maneb are also employed in toxin-based animal models for PD. They are able to induce dopaminergic degeneration, motor deficits and α -synuclein accumulation, albeit not with the same success and reliability as MPTP or 6-OHDA. Hence, they are primarily used to investigate the effects of certain environmental risk factors and their interplay with other factors like genetic predisposition or age (17,225).

The genes *SNCA*, *PINK1*, *PARK7*, *LRRK2*, and *PRKN* that are most frequently targeted in PD animal models of category two are all found in the familial form of the disease. Nevertheless, they are also thought to help explain pathological cellular mechanisms of idiopathic PD as both forms may share several genetic features (225,253). *SNCA*, the gene encoding α -synuclein, was the first gene to be associated with PD (17). Hence, by

now there are numerous transgenic α -synuclein animal models that develop different features of PD, *e.g.* the formation of inclusion bodies, degeneration of dopaminergic neurons or motor deficits (254–257). Nevertheless, despite the usefulness in understanding the pathological contributions of this protein in PD, the transgene rather affects, and therefore these models represent, early developmental stages than late onset neurodegeneration of PD, and potential compensatory mechanisms are not considered (17,258). Despite some good results in mutant *LRRK2*^{R1441G} BAC transgenic mice, most models using mutations in this gene have been unsuccessful in simulating main hallmarks of PD (17,259,260). Similarly, models using the knock out, silencing or overexpression of *PARK7*, *PINK1*, or *PRKN* show only limited changes in dopaminergic nigrostriatal system, motor functioning, and protein aggregation (17,225). The combination of different transgenes, viral vector-mediated models, or the modulation of transcription factors, however, may well be able to add to our knowledge about PD, its aetiology and the underlying mechanisms (17).

With so many different models available, nearly all hallmarks of PD can be replicated. However, despite great efforts none of the models mentioned above gives a full picture of the disease's neuropathology or represents the complete clinical syndrome (17). While toxin-based models obtain great dopaminergic cell loss and the development of according motor symptoms, they lack the formation of inclusion bodies. In turn, transgenic models enable detailed insights into the role of certain genes in PD or specific cellular and molecular mechanisms and pathways of the pathogenesis, whereas the dopaminergic neurodegeneration is inconsistent and not all models develop motor deficits (225). Hence, researchers have to choose the species as well as their models based on the scientific question they are trying to answer while keeping the specifications and limitations of each model and species in mind (17,225,226).

In conclusion, PD is an encumbrance for patients and the health system worldwide, while the search for a superior remedy continues. It is therefore of greatest importance to keep investigating approaches that aim at preventing, halting or modifying disease progression, and to keep improving the therapies that are already established. DBS of the STN is one of these established methods that is not yet used to its full capacity as mechanisms of action are not sufficiently understood to date. This is where this study spuds in.

Aim of this study

Numerous studies have investigated the effects of various aspects of DBS in the treatment of PD: from the exploration of acute vs. long term effects (218,261), over the impact on non-motor symptoms (262,263), the interaction with and difference to L-DOPA treatment (134,263–265), to the benefits of electrodes with multiple independent contacts and current steering (266). PET imaging has thereby been an important instrument to visualise the impact of STN DBS on brain overall functioning (135,139). However, similar to the multi-systemic nature of PD, the mode of action of DBS is a multi-factorial neuromodulation and, hence, still not completely understood to date (267,268).

Animal studies are frequently used to shed further light on DBS in PD, its mechanisms of action, and its effects on symptoms (269–273). Some researchers also looked at the interrelation of DBS and L-DOPA in animal models of PD (274). In these studies, stimulation times usually did not exceed several minutes to a few days (275,276). Attempts were made at introducing chronic DBS in animal models. However, parts of the stimulation systems remained external and therefore hazardous and restraining for the animals (277–280). To our knowledge only Harnack and colleagues (2008) developed a fully implantable system, yet, limited themselves to testing its safety and applicability in naive animals (281).

There are some studies combining PET imaging and DBS in various animal models of disease (282–284), the amount of PET research specific to DBS in animal models of PD, however, is rare (285,286). Our group has already used the combination of DBS, [¹⁸F]FDG and [¹⁸F]FDOPA PET imaging in the 6-OHDA rat model, though using an external stimulation system. For instance, it could be shown that 6-OHDA lesions cause ipsilesional hypo- and contralesional hypermetabolism, which both contributed to motor impairment as well as compensation (154). This metabolic imbalance was then shown to be normalised by STN DBS (137). Some DBS effects were found to depend on the severity of the dopaminergic lesion, and both 6-OHDA lesions and STN DBS altered striatal functional connectivity, especially interhemispheric networks (138).

With the present study, we therefore aimed at establishing a fully implantable DBS system with the potential for chronic DBS and test its range of applications in illustrating the effects of STN DBS on brain (network) activity and motor performance in a rat model of PD using a behavioural test and functional [¹⁸F]FDG PET imaging.

The work was divided into three consecutive parts: In CHAPTER ONE we aimed at establishing a standard operating procedure for the use of the new, fully implantable DBS system for rodents in the 6-OHDA rat model (287). Therefore, components of the system and its assembly, surgical procedures, stimulation settings and timing, as well as time points of behavioural tests and imaging were worked out and optimised. As a result, effects of acute STN DBS on pathological brain activity and motor performance are shown. In CHAPTER TWO we then sought to compare the effects of acute (~24 h) and chronic (five weeks) STN DBS on behaviour, metabolic cerebral activity and pathological brain network functions in the unilateral 6-OHDA rat. Finally, in CHAPTER THREE, we compared the impact of STN DBS on motor performance, brain metabolic activity, and networks compared to the classical L-DOPA treatment.

We hypothesised that DBS would either normalise the lesion-induced metabolic and network changes or influence them differently to compensate for the alterations caused by 6-OHDA and recover behavioural performance. We also assume that the various forms of therapy, *i.e.* acute and chronic DBS as well as L-DOPA treatment, will influence behavioural and metabolic changes differently.

Data Availability Statement

Raw data of this work were generated in the Institute for Radiochemistry and Experimental Molecular Imaging in the Clinic for Nuclear Medicine at the University Hospital Cologne. The data that support the findings of this study are available from the corresponding author, Nadine Apetz, upon reasonable request.

Inclusion of a Publication

CHAPTER ONE of this dissertation, “Towards chronic deep brain stimulation in freely moving hemiparkinsonian rats: applicability and functionality of a fully implantable stimulation system”, has been published in the Journal of Neural Engineering 18 (2021) 036018 by IOP Publishing (<https://doi.org/10.1088/1741-2552/abe806>). It has been submitted for publication on the 21st of December 2020, revised on the 4th of February 2021, accepted for publication on the 19th of February 2021 and published on the 16th of March 2021 (288).

Since the fully implantable stimulation system provided by Medtronic® was a newly developed tool, at the beginning of this project, the experiences with the device of our group as well as in general were very limited. After initial pilot experiments, the purpose of the first part of this dissertation was therefore to establish a functional standard operating procedure with the new device and test its ability to generate reliable data sets. Accordingly, in the methodological paper, it could be shown that the system is well tolerated and prior results achieved with external stimulation systems could be largely reproduced (138). Collecting a solid and reliable acute data set was a necessary first step to later expand the study with chronic experiments and compare the method to other, established treatment options for PD, *i.e.* L-DOPA. The first, acute tests with the new stimulation system presented in the publication are therefore the logical basis for the following two chapters, making it a suitable first chapter for this dissertation.

As also mentioned in the acknowledgements, together with professors Endepols and Timmermann, I took part in designing the study. I executed all experiments including surgeries, MRI/PET scans, and behavioural tests, and analysed and interpreted the data. Professor Endepols supported me with her advice, experience and expertise, especially regarding MRI and PET scans, as well as the statistical analyses and interpretation of the data. I wrote the manuscript and made the figures, while co-authors had the opportunity to edit the draft. Hence, I contributed the lion's part of this study.

CHAPTER ONE: Towards chronic deep brain stimulation in freely moving hemiparkinsonian rats: Applicability and functionality of a fully implantable stimulation system

Nadine Apetz¹, Kunal Paralikar², Bernd Neumaier^{1,2}, Alexander Drzezza^{3,7,8}, Dirk Wiedermann⁴, Rajesh Iyer⁵, Gordon Munns⁶, Erik Scott⁵, Lars Timmermann² and Heike Endepols^{1,2,3}

¹ Forschungszentrum Jülich GmbH, Institute of Neuroscience and Medicine, Nuclear Chemistry (INM-5), Wilhelm-Johnen-Straße, 52428 Jülich, Germany

² University of Cologne, Faculty of Medicine and University Hospital Cologne, Institute of Radiochemistry and Experimental Molecular Imaging, Kerpener Str. 62, 50937 Köln, Germany

³ University of Cologne, Faculty of Medicine and University Hospital Cologne, Department of Nuclear Medicine, Kerpener Str. 62, 50937 Köln, Germany

⁴ Department of In-vivo NMR, Max Planck Institute for Metabolism Research, Gleueler Str. 50, 50931 Köln, Germany

⁵ Medtronic, Rice Creek East 7000 Central Avenue NE Minneapolis, MN 55432, United States of America

⁶ Medtronic, Rice Creek East 7000 Central Avenue NE Minneapolis, MN 55432, United States of America

⁷ German Center for Neurodegenerative Diseases (DZNE), Bonn-Cologne, Germany

⁸ Forschungszentrum Jülich GmbH, Institute of Neuroscience and Medicine (INM-2), Molecular Organization of the Brain, 52428 Jülich, Germany

E-mail: nadine.apetz@uk-koeln.de

Keywords: Parkinson's disease, deep brain stimulation, 6-OHDA rat model, subthalamic nucleus, cylinder test, [¹⁸F]FDG PET

Abstract

Objective. This study aimed at investigating a novel fully implantable deep brain stimulation (DBS) system and its ability to modulate brain metabolism and behaviour through subthalamic nucleus (STN) stimulation in a hemiparkinsonian rat model. **Approach.** Twelve male rats were unilaterally lesioned with 6-hydroxydopamine in the medial forebrain bundle and received a fully implantable DBS system aiming at the ipsilesional STN. Each rat underwent three cylinder tests to analyse front paw use: a PRE test before any surgical intervention, an OFF test after surgery but before stimulation onset and an ON test under DBS. To visualise brain glucose metabolism in the awake animal, two [¹⁸F]FDG scans were conducted in the OFF and ON condition. At least 4 weeks after surgery, an [¹⁸F]FDOPA scan was used to check for dopaminergic integrity. **Main results.** In general, STN DBS increased [¹⁸F]FDG uptake ipsilesionally and decreased it contralesionally. More specifically, bilateral orbitofrontal cortex, ipsilateral caudate putamen, sensorimotor cortex and nucleus accumbens showed significantly higher tracer uptake in ON compared to OFF condition. Contralateral cingulate and secondary motor cortex, caudate putamen, amygdala, hippocampus, retrosplenial granular cortex, superior colliculus, and parts of the cerebellum exhibited significantly higher [¹⁸F]FDG uptake in the OFF condition. On the behavioural level, stimulation was able to improve use of the contralesional affected front paw suggesting an effective stimulation produced by the implanted system. **Significance.** The fully implantable stimulation system developed by us and presented here offers the output of arbitrary user-defined waveforms, patterns and stimulation settings and allows tracer accumulation in freely moving animals. It is therefore a suitable device for implementing behavioural PET studies. It contributes immensely to the possibilities to characterise and unveil the effects and mechanisms of DBS offering valuable clues for future improvements of this therapy.

Published Chapter

The chapter "Towards chronic deep brain stimulation in freely moving hemiparkinsonian rats: applicability and functionality of a fully implantable stimulation system", has been published in the Journal of Neural Engineering 18 (2021) 036018 by IOP Publishing (<https://doi.org/10.1088/1741-2552/abe806>). It has been submitted for publication on the 21st of December 2020, revised on the 4th of February 2021, accepted for publication on the 19th of February 2021 and published on the 16th of March 2021 (288).

CHAPTER TWO: Comparing acute and chronic deep brain stimulation of the subthalamic nucleus in a rat hemiparkinson model: a [¹⁸F]FDG PET study

I. Introduction

Most studies investigating DBS in animal models of PD applied acute stimulation lasting for minutes to hours in animals that were anaesthetised or restrained by cables to external stimulators (270,272,275,305,306). In contrast, DBS in PD patients is applied continuously over years and some symptoms may further improve or deteriorate in time. Therefore, many human studies investigate the effects of DBS months to years after surgery, when the stimulation is well adjusted and established. For example, bradykinesia and rigidity were measured to improve up to 63 % and 52 %, respectively, twelve months after DBS onset (320). The positive effects of STN DBS on gait and freezing do not always remain long-term and axial motor features are known to decline over time (215,321–324). More than a third of patients show relevant deterioration of postural stability only between five and eight years after implantation (261). Similarly, DBS effects on non-motor symptoms can change over time. For example, a gradual decline on phonological and semantic verbal fluency tasks has been reported a few months after surgery, which further progressed over several years (261,263). Long-term follow ups also revealed a significant decline in tasks of episodic memory, executive function, and abstract reasoning (261). While some of these long-term changes can be attributed to the progression of disease, others might actually depend on the duration of DBS.

Accordingly, a handful of animal studies found changes in therapeutic outcome depending on DBS duration. For example, Salin *et al.* (2002) discovered that STN DBS for two hours changed 6-OHDA lesion-mediated changes in neurotransmitter-related gene expression only in output structures of the basal ganglia, namely SNr and entopeduncular nucleus (325). In a following study, the same group showed that continuous DBS for four days additionally affected metabolic changes in globus pallidus and striatum. They therefore suggest that STN DBS has both, instant and delayed effects on 6-OHDA lesion-induced cellular changes that need to be fully characterised using chronic stimulation patterns (326). Another group showed that STN DBS influenced neurotransmitter levels in several basal ganglia structures of a 6-OHDA hemiparkinsonian rat model differently depending on whether stimulation was applied acutely (1 to 3 h), subchronically (7 days), or chronically (5 weeks). They conclude that there is a progressive metabolic impact of STN DBS in the basal ganglia and that long-term benefits of this therapy are based on both acute and delayed actions of DBS (279,327).

Against this background, the applicability of results of animal studies using acute STN DBS is limited showing an incomplete picture, and those investigating chronic stimulation effects are scarce (278,279,328). Hence, there is a great need for experiments particularly in rodent models investigating the impact of chronic DBS on a behavioural, cellular and network level. To our knowledge, this is the first study investigating behaviour and changes of cerebral activity in acutely and chronically stimulated hemiparkinsonian rats using [¹⁸F]FDG PET.

II. Materials and Methods

II.i Animals

A total of eight male Long-Evans rats (Janvier Labs, Le Genest-Saint-Isle, France) were kept in groups of two to four in individually ventilated cages with free access to standard rodent chow and water at a reversed day-night-cycle (lights on 8:30 pm to 8:30 am). Room temperature was 22 ± 1 °C and relative humidity averaged out at 55 ± 5 %.

All animals received unilateral 6-OHDA injections and ipsilateral DBS electrode implantation. After being tested in the OFF condition and one day prior to the first experiment with STN DBS, stimulation was turned on for the acute test battery. Four rats then continued to receive chronic DBS treatment continuously for a period of five weeks.

All experiments took place in the dark (active) phase of the animals at approximately the same time each day to avoid changes caused by their circadian rhythm. Experiments were carried out in accordance with the EU directive 2010/63/EU for animal experiments and the German Animal Welfare Act (TierSchG, 2006) and were approved by regional authorities (LANUV NRW; application number 84-02.04.2012.A304).

II.i Stimulation System

II.i.i Electrode

Concentric bipolar platinum/iridium electrodes as used in CHAPTER ONE were also implemented in this study (Fig. 5 B).

II.i.ii Stimulation System

For acute and chronic STN DBS, the fully implantable stimulation system introduced in CHAPTER ONE was used. To make the whole system more sturdy and durable to sustain five weeks inside the rats' bodies, the extension leads as well as the pin connectors attached to the electrode were insulated with silicone tubing (Fig. 9). Additionally, all connecting points between stimulator, extensions and pin connectors were sealed with sterile medical adhesive silicone type A (Silastic®, Dow Corning Corp., Midland, MI, USA).

II.iii Surgical Procedures

Surgeries were executed as described in CHAPTER ONE. In brief, in a first surgery, animals received the unilateral 6-OHDA lesion, and a guide cannula was implanted. A computer assisted stereotactic drill and microinjection robot (Neurostar®, Tübingen, Germany) was used to drill holes for the guide cannula to the STN (-3.6 mm posterior, ± 2.8 mm lateral) and for the ipsilateral 6-OHDA injection into the medial forebrain bundle (-4.4 mm posterior, ± 1.2 mm lateral). For each animal, the side of catheter and lesion was chosen in a randomised fashion. A total of 14 µg of 6-OHDA free base (21 µg of 6-Hydroxydopamine hydrobromide containing ascorbic acid as stabiliser, Sigma Aldrich®, St. Louis, USA) in 3 µl of NaCl was injected at a total depth of 7.9 mm below the *dura mater*. After slowly being inserted, the guide cannula's tip reached a depth of 7.6 mm below the *dura mater* at its final position. Once in place, the catheter was embedded in dental cement to lock its position. The catheter was closed using a nylon dummy until the electrode would be inserted.

To confirm the correct placement of the catheter above the STN, MRI scans were performed before the second surgery as described in CHAPTER ONE. The electrode insertion depth for each animal then resulted from the distance between catheter tip and STN. A dental cement stopper at the respective length of each electrode was formed to prevent an insertion beyond the defined point.

The day following catheter implantation and 6-OHDA lesion, animals received electrode and stimulation system in a second surgery. The stimulator was implanted dorsolaterally and connected to the electrode via subcutaneous extension leads. The concentric bipolar electrode was inserted into the catheter and fixed with dental cement. After connecting the two electrode contacts with the sockets coming from the extensions, they were covered with more dental cement until everything was stable and bonded. Animals were allowed a minimum recovery time of five days.

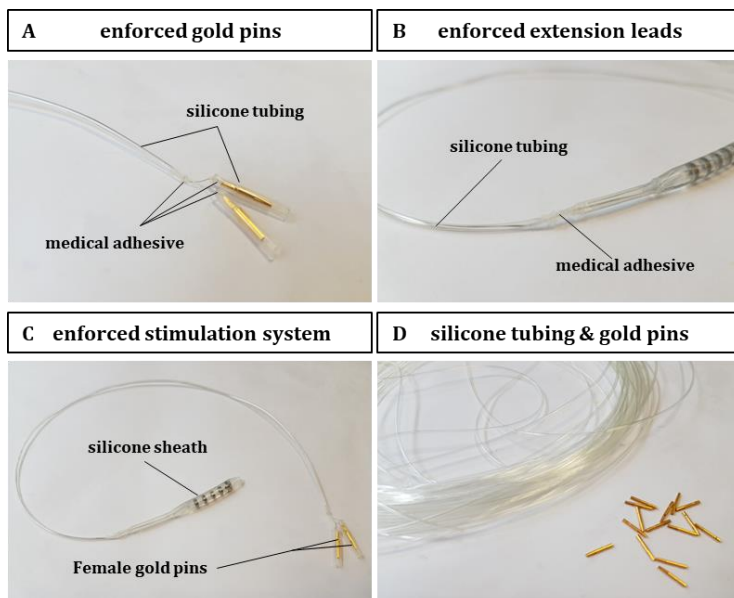


Fig. 9 Enforcement of stimulation system. **A** Female gold pins sheathed with silicone tubing. **B** Extension leads emerging from the stimulator enclosed in silicone tubing to reinforce insulation and sturdiness. **C** Complete reinforced extension lead including the silicone sheath housing the four electrode contacts (see CHAPTER ONE). All connection points between silicone sheath, extension leads and gold pins were sealed with sterile medical adhesive. **D** Silicone tubing and female gold pins used to strengthen the stimulation system for a long-term use inside the rats' bodies.

II.iv Treatment Regimes

Animals were measured under two different DBS treatments: eight animals received acute STN DBS for about 24 h (ON), and four out of those eight continued to receive chronic DBS for a duration of five weeks (ON5W). The remaining four rats lost their electrode caps at different time points after the ON but before the ON5W scan/cylinder test and could therefore not be included in the chronic treatment analyses.

II.iv.i Deep Brain Stimulation

Stimulation was turned on after behavioural testing and [^{18}F]FDG-PET in the OFF condition had been completed. This was at least a day before the [^{18}F]FDG-PET scan in the ON condition took place. It lasted until the end of experiments. For four animals that meant until all acute testing had been done, whereas for the other four rats stimulation lasted until after the tests following five weeks of continuous STN DBS.

Stimulation was set at a frequency of 130 Hz and a pulse width of 60 μ s. The amplitude started at 30 μ A for all animals and was increased in steps of 5 μ A until side effects like jaw clenching, chewing, apathy or gagging occurred. The individual amplitude for each rat was then set at 80 % of the side effect-evoking amplitude. In this study, amplitudes ranged from 125 to 220 μ A.

II.v Cylinder Test

Like in CHAPTER ONE, the cylinder test was used to investigate motor deficits evoked by 6-OHDA lesions by looking specifically at the front paw use of animals. Animals with unilateral 6-OHDA lesions show a strong preference for their healthy, ipsilesional front paw (IF), while preserving the contralesional affected one (CF). The transparent acrylic cylinder used in this study was 30 cm high and had a diameter of 20 cm. It was placed in a dark chamber illuminated with red light, and animals were video-recorded from above during tests for later analysis using the tracking software The Observer® XT (Noldus, Wageningen, Netherlands). Each session lasted ten minutes.

Animals were tested in the cylinder three and four times, respectively: A baseline test was conducted in the naive animal before any surgical intervention (PRE), a second test took place without STN DBS a week after surgeries when animals had sufficiently recovered (OFF), and a third test (ON) was done after DBS had been turned on for at least a day. The four chronically stimulated animals additionally underwent a last one after continuous DBS for five weeks (ON5W). All tests were executed on different days.

II.vi Positron Emission Tomography

PET-scans were performed in the same small-animal-PET scanner used in CHAPTER ONE (Siemens Focus 200, Berlin, Germany). Animals underwent a total of three and four PET scans, respectively: A first [18 F]FDG scan took place for all eight rats around a week after surgeries but before start of therapy (OFF), a second [18 F]FDG scan was conducted a day after stimulation onset (ON). The four rats receiving chronic stimulation also had a third [18 F]FDG PET scan after continuous STN DBS for five weeks (ON5W) to investigate possible differences in metabolic activity between acute and chronic DBS. At least four weeks after 6-OHDA injections, all eight rats received an [18 F]FDOPA scan to verify the dopaminergic lesion and evaluate its extent. Only one scan was performed per day. During each scan, body temperature was maintained by means of a warm air system integrated in the animal holder (Medres® Medical Research GmbH, Cologne, Germany) and breathing rate was monitored.

II.v.i [18 F]FDG

Animals received an i.p. injection of 72.30 ± 13.72 MBq of [18 F]FDG in approximately 0.5 ml saline under brief anaesthesia (< 2 min, see CHAPTER ONE). [18 F]FDG uptake then occurred in the awake and freely moving rat. Sixty minutes after the injection, animals were anaesthetised again for the 30 min emission scan. On each PET day, the last animal measured also underwent a 10 min transmission scan using a ^{57}Co point source used later for attenuation correction. At the end of each scan, blood glucose levels of all rats were measured.

II.v.ii [18 F]FDOPA

One hour before [18 F]FDOPA injections, rats were briefly anaesthetised (< 2 min) and received an i.p. injection of 15 mg/kg benserazide hydrochloride (Sigma Aldrich, St. Louis, USA) to increase brain uptake by blocking peripheral decarboxylation of [18 F]FDOPA. Animals then received 73.13 ± 3.23 MBq [18 F]FDOPA in 0.5 ml saline through a catheter in the lateral tail vein under anaesthesia. Animals were allowed back in the cage for tracer uptake before emission scans started another 30 min later.

II.vii Statistical Analysis

II.vi.i Behaviour

As in CHAPTER ONE, behavioural data was analysed by calculating the percentage of CF and IF use from all recorded wall touches. Percentages were again arcus-sinus-transformed to obtain a normal distribution (see 2.8.1). A two-way repeated measures ANOVA using the software Graphpad Prism version 8 for macOS was then used to test the differences between CF and IF use during PRE, OFF, ON and ON5W tests, respectively, for significance ($p \leq 0.05$). As before, factors were paw (CF and IF) and DBS status (PRE, OFF, ON or ON5W). For post-hoc testing Sidak's multiple comparison test was used. Tests concerning the chronic DBS were only conducted with the data of the four rats that received the continuous stimulation.

II.vi.ii [^{18}F]FDG PET

After full 3D rebinning, summed images (60 – 90 min p.i.) were reconstructed using the iterative OSEM3D/MAP procedure (311) resulting in voxel sizes of $0.38 \times 0.38 \times 0.80$ mm. All further analysis was done with the software VINCI (312). Images were co-registered manually to the Swanson rat brain atlas (313). If necessary, images were mirrored so that the intervention was always displayed on the left. Intensity was normalised to the cerebral global mean ($\text{SUVR}_{\text{wb}} = \text{individual voxel value divided by mean value of the whole brain}$). [^{18}F]FDG uptake in ON/ON5W and OFF conditions were compared voxel-wise using a paired t-test followed by a TFCE procedure with subsequent permutation testing (314), resulting in statistical t-maps corrected for multiple testing (thresholded at $p = 0.05$). Colour bars of TFCE maps are labelled with the original t-values, marked t_{TFCE} , as TFCE values are at random.

To investigate whether STN DBS affected brain network activity, seed-based metabolic analyses (138,329) were conducted separately for ON and OFF conditions in the acutely stimulated rats ($n = 7$). Four seed regions, each four voxels in size, were chosen according to the response pattern seen in Figure 12: one in the hypothalamus, a region with significantly lower [^{18}F]FDG uptake in the ON compared to the OFF condition, one each in the ipsi- and contralesional SN, both also showing significantly reduced glucose metabolism under DBS, and one in the ipsilesional cerebellum which showed significantly increased [^{18}F]FDG uptake in the ON condition. To detect brain regions that were interconnected with the seed regions, identified by associated changes in metabolism, PET images were correlated voxel-wise with the mean SUVR_{wb} of each seed region using the Pearson correlation test. t-maps showing significant R-values were TFCE-corrected as mentioned above. Unfortunately, reliable network analyses were not possible with the chronically stimulated animals due to the small n .

II.vi.iii [^{18}F]FDOPA PET

Other than [^{18}F]FDG images, [^{18}F]FDOPA images were summed over 30 – 60 min p.i. After coregistration and reconstruction (see above) images were smoothed with a Gauss kernel of 1.5 mm FWHM and intensity normalised to the cerebellum (SUVR_{cer}). To illustrate and verify dopaminergic cell loss, VOIs were drawn in [^{18}F]FDOPA images for medial and lateral striatum. Ipsi- versus contralesional mean SUVRs were compared using a paired t-test. Results were considered significant when $p < 0.05$.

III. Results

The behavioural as well as the PET ([^{18}F]FDG and [^{18}F]FDOPA) data of only seven of the eight rats used in this study were examined. One rat showed profound inflammatory signs in the lesioned hemisphere and was therefore left out of all analyses. Rats were scanned and tested in the OFF condition only once. Hence, for acute

stimulation analyses, OFF data of seven animals were included, while OFF data of only the four rats stimulated for five weeks were integrated in the chronic stimulation analyses.

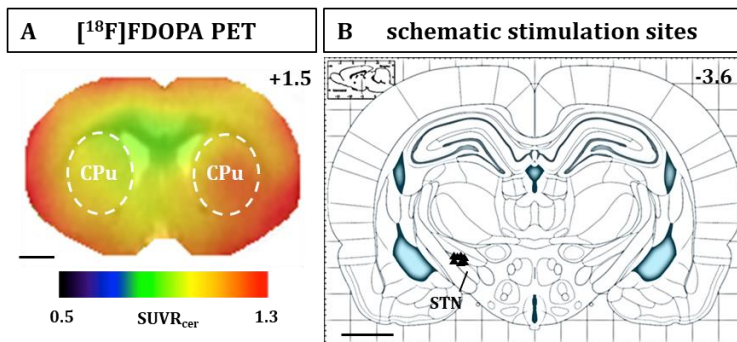


Fig. 10 6-OHDA lesion and stimulation sites. **A** Mean [^{18}F]FDOPA SUVR_{cer} values of animals injected with 6-OHDA in the medial forebrain bundle ($n = 7$), projected onto an MRI template. The dashed lines indicate the striatal areas (caudate putamen, CPu). The left CPu shows a significantly decreased [^{18}F]FDOPA uptake compared to the right CPu. **B** Schematic brain atlas (adapted (315)) showing stimulation sites (black triangles) in the STN of rats implanted with a DBS electrode ($n = 7$). Sites were determined by verifying catheter placements using interoperative MRI. Images of rats lesioned and implanted in the right hemisphere were flipped so that lesions and stimulation sites are always depicted on the left. Scale bars represent 2 mm. Numbers in the upper right corners show the axial distance (in mm) of the respective section level from Bregma.

III.i Dopaminergic Lesion and Electrode Placement

Figure 10 A illustrates the mean [^{18}F]FDOPA SUVR_{cer} values of the seven rats. The right CPu (striatum) clearly shows a more distinct tracer uptake when compared to the left 6-OHDA-lesioned hemisphere. The paired t-test confirmed this impression by identifying a significantly lower [^{18}F]FDOPA uptake in medial and lateral striatum of the ipsilesional compared to the contralesional hemisphere ($p = 0.0002$). A considerable dopaminergic lesion in the basal ganglia of all seven rats after receiving the 6-OHDA injection could therefore be validated.

Figure 10 B shows the position of electrode tips of all rats as verified by the correct placement of guide cannulas during interoperative MRI. In this manner, all eight electrodes could be confirmed to be located in the STN.

Looking at the data of the four rats that continued to receive DBS for five weeks, animals used the later affected front paw slightly more than the non-affected paw during PRE tests, i.e. in 61.05 % of all wall touches. After 6-OHDA lesions, CF use dropped to 3.41 % and could be nearly quintupled to 16.35 % of all wall touches after five weeks of STN DBS (Fig. 11 B). The two-way repeated measures ANOVA revealed a significant cross-over interaction between DBS state and paw ($F(2, 6) = 10.45, p < 0.0111$). The Sidak's multiple comparisons test showed that CF use differed significantly between PRE and OFF ($p = 0.0448$) but not between PRE and ON5W or OFF and ON5W. Hence, chronic DBS was able to improve CF use to a certain degree but failed to restore PRE levels. This result is comparable with that achieved in CHAPTER ONE under acute STN DBS (Fig. 7 B). Unfortunately, some animals did not move at all in the OFF condition or responded to the stimulation while others showed good improvements under DBS. The extremely high intra- and inter-animal variability in paw use in this study might therefore have compromised the data and prevented further significant findings, especially concerning the difference between acute and chronic stimulation.

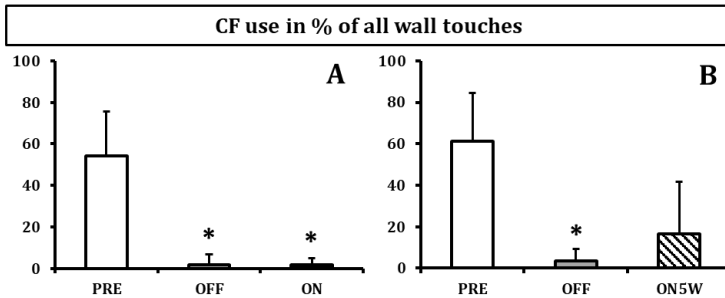


Fig. 11 Behavioural effects of acute and chronic STN DBS. **A** Contralesional front paw (CF) use in percent of all wall touches in acutely stimulated animals ($n = 7$). 6-OHDA injections into the medial forebrain bundle caused a significant decrease of CF use compared to the ipsilesional front paw (IF) in the OFF condition that could not be restored by acute STN DBS. **B** Four rats continued to receive non-stop STN DBS for five weeks. While CF use was also significantly reduced in the OFF compared to the PRE condition, chronic STN DBS was able to restore CF use to a certain degree and abolish the significant difference between paw use during PRE and ON5W. PRE = baseline before surgical interventions, OFF = after 6-OHDA injection but before onset of STN DBS, ON = after one day of STN DBS, ON5W = after five weeks of continuous STN DBS. Asterisks indicate a significant difference between CF and IF use (A) and in CF use compared to PRE (B).

III.iii Effects of Acute and Chronic STN DBS on Cerebral [18 F]FDG Uptake

Stimulation of the STN had activating as well as inhibiting effects on cerebral glucose consumption depending on brain area and duration of DBS (Fig. 12). Acute STN stimulation caused an increase of tracer uptake bilaterally in prelimbic, cingulate and secondary sensory cortices. Contralesionally, increased [18 F]FDG uptake could be observed in primary and secondary motor cortices, thalamus, as well as in primary sensory cortex and CPu. More caudally, contralesional parietal association cortex, secondary visual cortex, superior colliculus and hippocampus showed significantly higher glucose consumption under acute STN DBS when compared to the OFF condition. Ipsilesionally, dorsal endopiriform cortex, presubiculum and crus two of the ansiform cerebellar lobule presented increased tracer uptake in the ON condition (Fig. 12 A).

Significantly decreased tracer uptake in the ON compared to the OFF condition was found in the ipsilesional ventral pallidum, primary sensory cortex, amygdala, subbrachial nucleus and presubiculum. Contralesional areas with significantly lower [18 F]FDG uptake under STN DBS were medial geniculate nucleus, microcellular tegmental nucleus, reticular nucleus and spinal trigeminal nucleus. Hypothalamus, entorhinal cortex, and SN were significantly less active in the ON compared to the OFF condition in both hemispheres (Fig. 12 A).

Only four of the seven animals that underwent [18 F]FDG PET scans after acute STN DBS received a second scan after five weeks of continuous STN stimulation (ON5W). When comparing ON5W and OFF conditions, there were similarities as well as differences in cerebral glucose metabolism compared to the acute treatment (Fig. 12 B). As acute STN DBS, chronic stimulation significantly activated prelimbic and cingulate cortices bilaterally. Beyond that, the chronic treatment also caused a significant bilateral increase in tracer uptake in CPu, primary and secondary motor cortices, primary sensory cortex, orbitofrontal cortex and retrosplenial granular and retrosplenial dysgranular cortices. Both treatments of STN DBS caused significant increases in [18 F]FDG uptake in contralesional parietal association cortex, thalamus and hippocampus. Other than after the short stimulation, five weeks of STN DBS increased tracer uptake in the secondary sensory cortex only contralesionally. On the other hand, contralesional superior colliculus and secondary visual cortex did not show increased tracer accumulation in the ON5W condition. In the ipsilesional hemisphere, both periods of

STN DBS caused significant increases of glucose metabolism in crus two of the cerebellar ansiform lobule when compared to OFF. Chronic treatment additionally increased activity in ipsilesional primary visual cortex, parastriar nucleus and eighth and ninth cerebellar lobule. Differing from the ON condition, ipsilesional dorsal endopiriform cortex did not show increased $[^{18}\text{F}]$ FDG uptake in the ON5W compared to the OFF condition

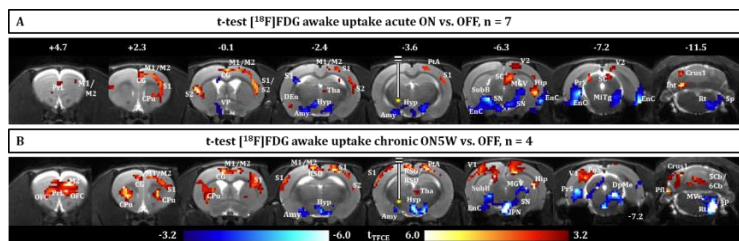


Fig. 12 Effects of acute and chronic DBS on cerebral glucose metabolism. Subtractive t-maps ($p < 0.05$, TFCE-corrected) projected onto an MRI template displaying the $[^{18}\text{F}]$ FDG uptake difference between DBS ON and OFF in **A** acutely (24 h, ON, $n = 7$) and **B** chronically (five weeks, ON5W, $n = 4$) stimulated 6-OHDA rats. Red voxels indicate that $[^{18}\text{F}]$ FDG accumulation was significantly higher during DBS ON, while blue voxels indicate a significantly higher $[^{18}\text{F}]$ FDG uptake during DBS OFF. Abbreviations: 5/6 Cb = 5th/6th cerebellar lobule, Amy = amygdala, CG = cingulate cortex, CPu = caudate putamen, Crus1 = crus one of the ansiform lobule, DEN = dorsal endopiriform cortex, DpMe = deep mesencephalic nucleus, Enc = entorhinal cortex, Hip = hippocampus, Hyp = hypothalamus, Int = interposed cerebellar nucleus, IPN = interpeduncular nucleus, M1/2 = primary/secondary motor cortex, MGV = medial geniculate nucleus, MiTg = microcellular tegmental nucleus, MnR = median raphe nucleus, MVe = medial vestibular nucleus, Pfl = paraflocculus, PrL = prelimbic cortex, PrS = presubiculum, PaS = postsubiculum, PtA = parietal association cortex, RSD = retrosplenial dysgranular cortex, RSG = retrosplenial granular cortex, Rt = reticular nucleus, S1/2 = primary/secondary somatosensory cortex, SC = superior colliculus, SN = substantia nigra, Sp = spinal trigeminal nucleus, SubB = subbrachial nucleus, Tha = thalamus, V1/2 = primary/secondary visual cortex, VP = ventral pallidum. PET images of animals implanted in the right hemisphere were flipped so that all stimulation sites are shown on the left. Colour bars of TFCE maps are labelled with the original suprathreshold t-values. Numbers indicate rostrocaudal coordinates in mm distance to Bregma.

Acute and long-term STN DBS caused a significant bilateral decrease of glucose metabolism in the hypothalamus. However, animals showed a more pronounced decrease contralesionally after chronic stimulation and an additional significant bilateral deactivation of the interpeduncular nucleus. In the contralesional hemisphere, medial geniculate nucleus and spinal trigeminal nucleus had significantly lower glucose consumptions under both DBS conditions when compared to OFF. Other than in the ON condition, in the ON5W condition, animals showed significant decreases of $[^{18}\text{F}]$ FDG uptake only in the contralateral SN. Further caudal were the most differences between acute and chronic STN DBS. Under chronic treatment, microcellular tegmental nucleus and reticular nucleus did not show changes between OFF and ON5W. However, median raphe nucleus, deep mesencephalic nucleus and nucleus of the solitary tract all showed significant reductions of glucose metabolism under chronic STN stimulation when compared to OFF. Significant reductions of tracer accumulation in the ipsilesional hemisphere were seen for both stimulation durations in amygdala, subbrachial nucleus and presubiculum. Chronic STN DBS failed to evoke reductions in the ventral pallidum and only the ipsilesional entorhinal cortex showed decreased glucose metabolism.

III.iv Effects of Acute STN DBS on Brain Networks

To investigate the effects of STN DBS on brain network activity seed-based metabolic analyses were conducted for OFF and ON conditions in acutely stimulated rats. Brain regions can be positively or negatively correlated to a seed. With positive correlations, the connected brain regions will show increased $[^{18}\text{F}]$ FDG uptake if the

seed region exhibits higher uptake and *vice versa*. When a negative correlation exists, connected brain regions will have lower [¹⁸F]FDG uptake while the seed region shows increases in uptake and the other way round. Regarding the wording in this section, ipsi- and contralesional always refers to the side of lesion, *i.e.* the left hemisphere in all figures. Ipsi- and contralateral refers to the respective brain region, *e.g.* the seed, regardless whether it is on the same, or the opposite side of the lesion. Four seeds were placed in regions that showed significantly altered (increased or decreased) [¹⁸F]FDG uptake during acute STN DBS.

Hypothalamus Seed

The ipsilesional hypothalamus showed significantly lower glucose metabolism under STN DBS compared to OFF (Fig. 12 A). In the OFF condition, [¹⁸F]FDG uptake of a seed placed in this region was positively correlated mainly with ipsilateral, and negatively primarily with contralateral structures. More specifically, tracer uptake in contralateral periaqueductal grey, prelimbic cortex (both not shown), bilateral, but predominantly ipsilateral CPu, ipsilateral GPe, bed nucleus of stria terminalis (BNST), reticular thalamic nucleus, retrosplenial granular cortex, temporal association cortex, subiculum, and subiculum transition area were positively correlated to that of the seed (Fig. 13 A, upper row). Negative correlations with glucose metabolism of the ipsilesional hypothalamus appeared in contralateral microcellular tegmental nucleus, spinal trigeminal nucleus, ipsilateral spinal vestibular nucleus, and bilateral gigantocellular reticular nucleus.

DBS in the ipsilesional STN changed these connections while the general trend of positive and negative correlations in the ipsi- and contralesional hemisphere remained (Fig. 13 A, lower row). The positive correlation between [¹⁸F]FDG uptake of the seed and that of contralateral periaqueductal grey, prelimbic cortex, ipsilateral GPe, BNST, subiculum, and temporal association cortex disappeared under STN DBS. The positive correlation between glucose metabolism in seed and ipsilateral reticular thalamic nucleus persisted, while that of retrosplenial granular cortex was reversed from positive ipsilateral, to a negative contralateral correlation. The bilateral positive correlations of CPu shifted to a negative contralateral one, while the negative correlation between seed glucose metabolism and that of contralateral spinal trigeminal nucleus reversed to a positive contralateral correlation. Additional positive correlations under DBS appeared between [¹⁸F]FDG uptake of the seed and that of ipsilateral thalamus, and bilateral medial septal nucleus. None of the remaining negative correlations persisted under STN DBS, but new ones were formed between glucose metabolism of seed and that of ipsilateral fifth to seventh cerebellar lobule, crus two of the ansiform lobule, contralateral primary and secondary somatosensory cortex, and primary visual cortex.

Ipsilesional Substantia nigra Seed

STN DBS caused a significant bilateral decrease of [¹⁸F]FDG uptake in the SN (Fig. 12 A). Hence, seeds were placed in the SN in both hemispheres. In the OFF condition, [¹⁸F]FDG uptake of the seed in the left, ipsilesional SN was positively correlated to that of the contralateral piriform cortex, SN, cortical amygdaloid nucleus, and lateral paragigantocellular nucleus (Fig. 13 B, upper row). Bilateral positive glucose metabolism correlations formed between ipsilesional SN and amygdalohippocampal area, ventral subiculum, spinal trigeminal nucleus, and medullary reticular nucleus. In the ipsilateral hemisphere, the [¹⁸F]FDG uptake of dorsal premammillary nucleus, entorhinal cortex, central nucleus of the inferior colliculus, parvocellular reticular nucleus, and ninth cerebellar lobule were positively correlated with that of the seed. [¹⁸F]FDG uptake of the seed in the ipsilesional SN was negatively correlated ipsilaterally to that of the hippocampus, and contralaterally to tracer uptake of CPu, primary and secondary motor cortex, thalamus, lateral parietal association cortex, primary somatosensory, secondary visual as well as auditory cortex.

STN DBS altered network connections of the ipsilesional SN (Fig. 13 B, lower row). [¹⁸F]FDG uptake of the seed was still positively correlated to that of ipsilateral entorhinal cortex, contralateral SN, cortical

amygdaloid nucleus, and central nucleus of the inferior colliculus. Bilateral positive correlations to the amygdalohippocampal area only remained contralaterally, while additional positive correlations appeared between tracer uptake of the seed and that of ipsilateral caudomedial entorhinal cortex, contralateral amygdala, and bilateral rostral interpeduncular nucleus. All other positive correlations disappeared under DBS. The negative correlations between [¹⁸F]FDG uptake of the seed in the ipsilesional SN and that of contralateral CPU, primary and secondary motor cortex, and parts of the thalamus were not present under DBS. Tracer uptake of ipsilateral hippocampus was no longer negatively correlated with that of the seed, but uptake of its contralateral counterpart. Negative correlations between glucose metabolism of seed and contralateral primary somatosensory, secondary visual and auditory cortex remained unchanged.

Contralesional Substantia nigra Seed

Without stimulation, [¹⁸F]FDG uptake of a seed placed in the right, contralesional SN correlated positively with that of ipsilateral spinal trigeminal nucleus, contralateral amygdalohippocampal area, ventral subiculum, piriform cortex, SN, entorhinal cortex, medullary reticular nucleus, and ninth cerebellar lobule (Fig. 13 C, upper row). Negative correlations existed between glucose metabolism of the seed and that of ipsilateral parts of the thalamus, anterior pretectal nucleus, and medial cerebellar nucleus. In the contralateral hemisphere, tracer uptake of parietal cortex and hippocampus correlated negatively with that of the contralesional seed. Ipsilesional STN DBS had marked effects on the networks of the contralesional SN (Fig. 13 C, lower row). The positive correlation between [¹⁸F]FDG uptake of the seed and ipsilateral SN, spinal trigeminal nucleus and contralateral piriform cortex and amygdalohippocampal area vanished, while that of the contralateral ventral subiculum and entorhinal cortex was now bilateral. The positive correlation between glucose metabolism of the ipsilesional SN and that of contralateral ninth cerebellar lobule increased noticeably. Additional positive correlations appeared between seed and contralateral primary visual, bilateral perirhinal and entorhinal cortex. More pronounced changes could be observed among the negative correlations. None of the correlations observed during OFF remained, while new ones appeared between contralesional seed and ipsilateral CPU, secondary somatosensory cortex, dorsal tegmental nucleus, contralateral ventral and lateral orbital cortex (not shown), and dorsal cortex of the inferior colliculus. Bilaterally, negative correlations were observed for seed and primary somatosensory, auditory, parietal, and retrosplenial granular cortex, thalamus, hippocampus, superior colliculus, medial cerebellar nucleus, and medial vestibular nucleus.

Cerebellum Seed

The fourth seed was placed in the ipsilesional cerebellum, specifically the interposed cerebellar nucleus, which showed significantly higher [¹⁸F]FDG uptake under acute STN DBS (Fig. 12 A). In the OFF condition, tracer uptake of ipsilateral crus one of the cerebellar ansiform lobule, contralateral temporal association cortex, perirhinal cortex, lateral periaqueductal grey, and bilateral hippocampus were positively correlated with that of the seed (Fig. 13 D, upper row). Glucose metabolism of ipsilateral primary and secondary motor cortex, primary somatosensory cortex, CPU, cingulate cortex, and bilateral retrosplenial granular cortex were negatively correlated with that of the ipsilesional cerebellar seed without DBS.

Again, these interconnections were partly changed by stimulation of the STN (Fig. 13 D, lower row). Positive correlations between tracer uptake of the seed and that of ipsilateral crus one of the ansiform cerebellar lobule and contralateral lateral periaqueductal grey remained, while that of contralateral temporal association and perirhinal cortex disappeared. Instead, additional positive correlations appeared between [¹⁸F]FDG uptake of the seed and that of ipsilateral sixth cerebellar lobule, contralateral thalamus, superior colliculus, anterior pretectal nucleus, and bilateral ventral part of the dorsal raphe nucleus.

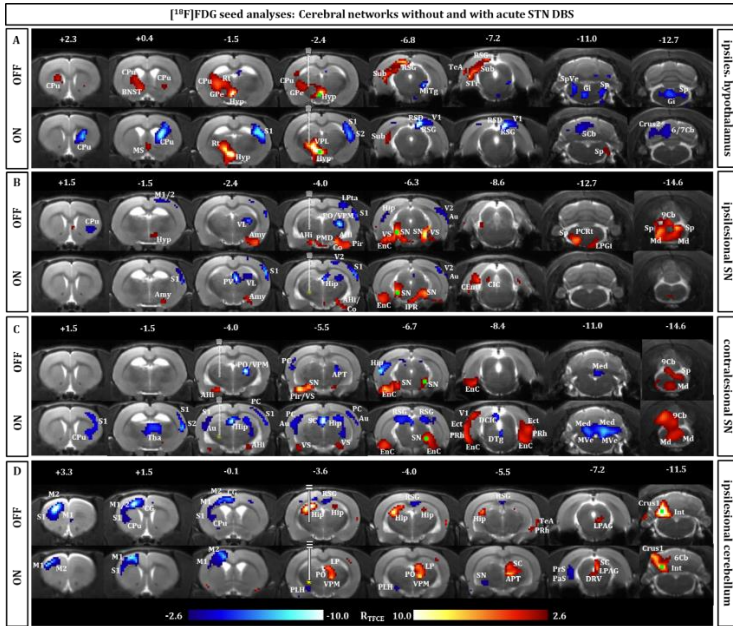


Fig. 13 Brain network connectivity is affected by acute STN DBS. *t*-maps showing significant correlation (*R*)-values of Pearson correlation analyses performed between each seed region and all other voxels of the brain projected onto an MRI template, *n* = 7. Seeds are represented by green squares. **A** The seed was placed in the hypothalamus, a region displaying significantly more [¹⁸F]FDG uptake in the OFF compared to the ON condition. **B** The seed was placed in the ipsilesional substantia nigra, which also showed significantly more [¹⁸F]FDG uptake in the OFF condition. **C** The seed was placed in the contralateral substantia nigra, displaying the same reaction to STN DBS as its ipsilesional counterpart. **D** The seed was placed in the cerebellum, which took up significantly more [¹⁸F]FDG in the ON condition. Red voxels indicate positive correlations, while blue voxels indicate negative correlations. Yellow filled circles at the electrode tip represent ongoing stimulation (ON). Transparent, dashed electrodes are illustrated in slices more rostral or caudal to the actual position. Abbreviations: 5Cb = 5th cerebellar lobule, 6/7Cb = 6th/7th cerebellar lobule, 9Cb = 9th cerebellar lobule, AHI = amygdalohippocampal area, Amy = amygdala, APT = anterior pretecal nucleus, Au = auditory cortex, BNST = bed nucleus of stria terminalis, CEnt = caudomedial entorhinal cortex, CG = cingulate cortex, CIC = central nucleus of the inferior colliculus, Co = cortical amygdaloid nucleus, CPu = caudate putamen, Crus1/2 = crus one/two of the ansiform lobule, DCIC = dorsal cortex of the inferior colliculus, DRV = dorsal raphe nucleus, ventral part, DTg = dorsal tegmental nucleus, Ect = ectorhinal cortex, EnC = entorhinal cortex, Gi = gigantocellular reticular nucleus, GPc = globus pallidus externus, Hip = hippocampus, Hyp = hypothalamus, Int = interposed cerebellar nucleus, IPR = rostral interpeduncular nucleus, LP = lateral posterior thalamic nucleus, LPAG = lateral periaqueductal grey, LPGI = lateral paraventricular nucleus, LPLA = lateral parietal association cortex, M1/2 = primary/secondary motor cortex, Md = medullary reticular nucleus, Med = medial cerebellar nucleus, Mitg = microcellular tegmental nucleus, MS = medial septal nucleus, MVe = medial vestibular nucleus, PLH = peduncular part of lateral hypothalamus, PaS = parasubiculum, PC = parietal cortex, PCRt = parvocellular reticular nucleus, Pir = piriform cortex, PMD = dorsal premammillary nucleus, PO = posterior thalamic nuclear group, PRh = perirhinal cortex, PrS = presubiculum, PV = paraventricular thalamic nucleus, RSD = retrosplenial dysgranular cortex, RSG = retrosplenial granular cortex, Rt = reticular thalamic nucleus, S1/S2 = primary secondary somatosensory cortex, SC = superior colliculus, SN = substantia nigra, Sp = spinal trigeminal nucleus, SpVe = spinal vestibular nucleus, STR = subiculum transition area, Sub = subiculum, TeA = temporal association cortex, Tha = thalamus, V1/V2 = primary secondary visual cortex, VL = ventrolateral thalamic nucleus, VPL = ventral posterolateral thalamic nucleus, VPM = ventral posteromedial thalamic nucleus, VS = ventral subiculum. PET images of animals implanted in the right hemisphere were flipped so that all stimulation sites are shown on the left. Colour bars of TFCE maps are labelled with the original suprathreshold *t*-values. Numbers indicate rostrocaudal coordinates in mm distance to Bregma.

Of the negative [^{18}F]FDG uptake correlations, those between seed and primary and secondary motor cortex, and primary somatosensory cortex remained, while that of ipsilateral cingulate cortex and contralateral CPU were no longer present. Glucose metabolism of ipsilateral peduncular part of lateral hypothalamus, SN, presubiculum, and parasubiculum showed new negative correlations to the tracer uptake of the seed under acute STN DBS.

IV. Discussion

As a first objective, this study ought to compare the effects of acute (~ 24 h) and chronic (5 weeks) STN DBS on brain glucose metabolism and front paw use in rats unilaterally lesioned with 6-OHDA. This was achieved by employing the new, fully implantable stimulation system established in CHAPTER ONE and additionally improving its durability (287). As a result, eight animals were tested under acute stimulation, while four out of those eight remained to be stimulated continuously for five weeks.

Unilateral 6-OHDA lesions lead to significant reductions in ipsilesional [^{18}F]FDOPA uptake in all rats, indicating a successful dopaminergic denervation leading to parkinsonian symptoms. Indeed, while using both front paws nearly equally in the naïve PRE condition, all animals showed a profound and significant reduction in CF use during OFF after 6-OHDA lesions. However, despite the assured, correct placement of electrode tips in the STN, acute STN DBS was not able to recover CF use. This can have several reasons. DBS is a highly sensitive therapeutic technique whose outcome depends on many factors. For example, patients suffering from PD are selected very carefully for the option of DBS by a multidisciplinary team. Type of PD (idiopathic or hereditary), response to L-DOPA therapy, type and severity of motor symptoms, general health status, and cognitive, behavioural and psychiatric condition are some of the factors that need to be thoroughly considered before the implementation of DBS (330–332). While 6-OHDA lesioned rats do not represent the full spectrum of PD complexity, each 6-OHDA lesion is unique in its exact position and degree. Hence, each rat has its own individual parkinsonian syndrome of which some might be better suitable for the treatment with STN DBS than others.

Similarly, the exact position of electrode and contacts is extremely important for an optimal result of DBS. Not only is there a difference in effect between the various targets for DBS, *i.e.* STN, GPi or VIM (209,212), the outcome of DBS also depends on the exact position within the target area (333,334). The unintended stimulation of neighbouring structures like zona incerta or internal capsule can influence the effectiveness of STN DBS (266). Figure 14 shows the stimulation sites of the seven animals included in the analysis. Three out of the seven sites (marked in red) are particularly close to zona incerta and internal capsule. Hence, stimulation effects of these three animals might not have been ideal and compromised the data so that there was no recognisable pattern of increased ipsilesional and decreased contralesional [^{18}F]FDG uptake as has previously been shown, and no effect on paw use (137,138). Although the zona incerta has been discovered as a suitable and potent DBS target for essential tremor, rats do not develop tremor as a symptom of PD after 6-OHDA injections into the MFB (335–337). Hence, the accidental stimulation of this structure is unlikely to have had additive positive effects. To avoid this problem in the clinical use, efforts were made in recent years to improve DBS therapy. New electrodes with split contacts were developed that allow for directional stimulation (338). By steering the current selectively to the target area, side effects caused by the stimulation of neighbouring brain structures can be minimised, while beneficial effects and therapeutic window are optimised (219–222). However, this technique is not available for animal experiments to date.

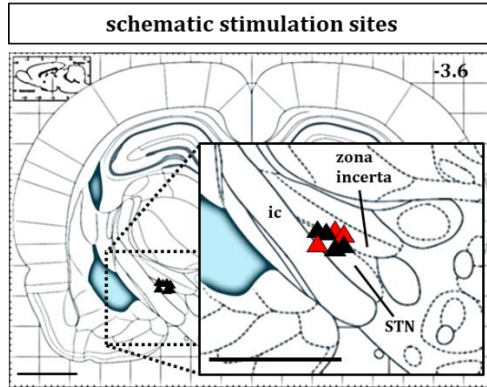


Fig. 14 Stimulation sites. Schematic brain atlas (adapted from (315)) showing stimulation sites (triangles) in the STN of rats implanted with a DBS electrode ($n = 7$) in a whole brain overview and an amplified insert for a more detailed view. Sites were determined by verifying catheter placements using interoperative MRI. Images of rats implanted in the right hemisphere were flipped so that stimulation sites are always depicted on the left. Black triangles represent stimulation sites well in the target area while red triangles represent stimulation sites that could also stimulate neighbouring brain regions like zona incerta and internal capsule (ic). Scale bars represent 2 mm.

A third possible source of error could be the absence of any postoperative adaptation of stimulation settings. In the clinical practice, the care of PD patients after DBS implantation is a highly complex and individual process. Questions regarding the time point of stimulation onset, stimulation parameters, and the addition and dosing of medication are just some of the considerations that need to be taken into account in close consultation with the patient (339). Stimulation settings of the rats in this study were determined as mentioned above following the postoperative recovery period and not changed thereafter in the lack of “patient” feedback. Hence, stimulation settings might not have been ideal for some of the rats and, therefore, not evoked the full therapeutic potential concerning changes of cerebral glucose metabolism and motor performance. This agrees with a more recent finding of Badstuebner *et al.* (2017) who used a backpack-like stimulation system to investigate hemiparkinsonian rats in several behavioural tests under different subchronic (three days) and chronic (three and six weeks) STN DBS conditions. They found a DBS (subchronic and chronic)-induced reduction of locomotor activity in the open field test that was reversible after cessation of stimulation (278). They assumed this unexpected motor impairment to be a direct consequence of harmful stimulation settings, therefore questioning their parameters. One explanation for the immobilising effect of inadequate stimulation settings could be the induction of dyskinesia/akinesia caused by increased levels of glutamate (Glu) in the SNr. A study by Boulet and team (2006) found Glu levels in the SNr of unilaterally 6-OHDA-lesioned rats to be increased under STN DBS of an intensity that induced forelimb dyskinesia, while Glu levels were normal under STN DBS of non-impairing intensity (340). Interestingly, GABA levels showed the opposite: they were significantly higher in SNr of rats stimulated with normal intensities while not being affected by dyskinesia-inducing DBS. The stimulation parameters that induced axial and forelimb dyskinesia in their study are comparable to the ones applied in the present experiments, *i.e.* a frequency of 130 Hz, a pulse width of 60 μ s and an amplitude in the range of about 75 – 275 μ A (125 – 220 μ A in this study). Similarly, another group found striatal Glu and GABA concentrations to be increased after STN DBS, however, motor performance and therapeutic effect was not assessed (341). Glu and GABA levels have also been shown to be

elevated in ipsilesional striatum and SNr of 6-OHDA lesioned non-stimulated rats showing motor impairments. STN DBS that was able to recover motor performance also decreased this transmitter elevation (279). Thus, the right balance between Glu and GABA of the basal ganglia and related network structures is crucial for normal motor output. PD (or DA depletion evoked by 6-OHDA lesion) as well as STN DBS at the wrong intensity or with unsuitable parameters can disturb this balance, manifesting in increased Glu levels in SNr and/or striatum and deteriorated motor performance. STN DBS applied at the right intensity and with the right parameters is able to normalise neurotransmitter levels and, as a consequence, improve motor performance. It is therefore possible that the stimulation settings used during the acute STN DBS treatment in this study were of inadequate intensity and induced dyskinesia/akinesia by disturbing the balance of Glu and GABA in the basal ganglia rather than improving paw use. In conclusion, stimulation settings in animal studies employing long-term DBS should be reassessed regularly after the initial adjustment by means of a volt- or amperemeter if possible to minimise the risk of inappropriate settings and the accompanying negative impact on behaviour.

PD patients that first receive DBS after implantation need to be made aware that microlesioning effects resulting from the surgical intervention may influence and compromise DBS efficacy during the first few months (339). Hence, it is possible that STN DBS results improve after full resolution of these effects and the therapy unfolds its full impact with a certain delay. Comparing the motor performance of the four animals that received continuous STN DBS for five weeks with that after acute stimulation could provide an indication for this phenomenon. As before, both front paws were nearly equally used in the PRE condition (CF use in 61 % of all wall touches). After 6-OHDA lesion, rats then exhibited a significant reduction in CF use during OFF. However, different to the acute stimulation, chronic DBS for five weeks was able to recover CF use to a certain degree, eliminating the significant reduction towards PRE levels. Nevertheless, chronic DBS failed to produce a significant increase of CF use compared to OFF as could also be observed with acute STN DBS in CHAPTER ONE. This may be due to the high standard deviation of the data, *i.e.* the noticeable difference in response to (chronic) DBS between animals. While one animal in particular was akinetic regardless of the stimulation condition, two animals showed good results under DBS. This could partly be explained by the occurrence of issues like those discussed above. For example, in animals with less effective DBS, the electrode might not have been located ideally or stimulation settings could have been suboptimally adjusted. Indeed, the stimulation site of the akinetic animal was one of those close to the zona incerta. An excessively profound dopaminergic lesion could also be the cause for bad motoric results despite DBS. However, all animals received the same amount of 6-OHDA and [¹⁸F]FDOPA images did not endorse this assumption.

The results with chronic STN DBS for five weeks obtained in this study are comparable to those obtained by Forni and colleagues (2012) who compared healthy, sham implanted rats with two 6-OHDA-lesioned groups, one with chronic (two and five weeks) and one without DBS (280). They could show that chronic STN DBS improves CF use (here expressed as the percentage of wall touches using both front paws) in 6-OHDA-lesioned animals compared to OFF and to unstimulated lesioned animals. However, similar to the present results, neither two, nor five weeks of STN DBS was able to recover CF use in 6-OHDA-lesioned rats to the level of sham-implanted animals manifesting in a persisting significantly lower amount of double contacts. Hence, despite the different study design (inter- vs. intra-animal comparisons, external stimulation system fixed on the rats' heads vs. fully implanted system, no direct comparison to acute stimulation) both studies could show that chronic STN DBS is able to improve but not normalise front paw motor performance in 6-OHDA-lesioned rats. Chassain *et al.* (2016), employing the same stimulation system as Forni, used a different behavioural test, namely the staircase test, in which unilaterally 6-OHDA-lesioned rats reach for pellets with either the affected or non-affected front paw. They compared two and five weeks of chronic STN DBS with OFF and were able to

show a significant unilateral improvement of front paw use after two, and an even greater, bilateral improvement after five weeks of STN DBS (279) agreeing with the findings of this study. As a potential cause for the continuing improvement over time, Chassain and colleagues propose the normalisation of striatal and SN neurotransmitters and their metabolites, as well as the restoration of long-term potentiation and depression as a sign of intact synaptic plasticity. Comparing acute, subchronic and chronic STN DBS, they conclude that the long-term benefits of DBS rely on acute as well as delayed effects in the basal ganglia and according involved networks (279,327). This theory agrees with the imbalance of neurotransmitters in the parkinsonian brain and the accompanying motor deficits mentioned earlier that can be normalised by adequate DBS. Alternatively or additionally, the compensatory mechanisms that take effect after 6-OHDA lesions could slowly adapt to chronic STN DBS, thereby improving its efficacy. For example, Hefti and colleagues (1985) found that dopaminergic neurons that survived the 6-OHDA lesion of the striato-nigral pathway synthesise and release DA at a several fold rate compared to neurons in the non-lesioned hemisphere (342). This increase in DA could initially interfere with the impact of STN DBS on transmitter levels, preventing the development of full therapeutic effects. After a certain adaptation phase, such compensatory mechanisms might slowly degenerate under the influence of STN DBS and neurotransmitter levels and neuronal activity come to a more cooperating balance. Hence, the resolution of microlesioning effects, the adaptation of compensatory mechanisms, and acute and long-term synaptic and network changes could be responsible for the full impact of STN DBS over time. Unfortunately, the time course of the mechanisms of action of DBS is not well studied to date. Human studies rather focus on the ideal time point for implantation, immediate effects of DBS, or the duration of effectiveness and the time point when disease progression interferes with therapeutic outcome after several years (261,263,323,343–345). Animal studies looking at the changes evoked by DBS on a behavioural, cellular, and/or molecular level have long been limited by short stimulation times and or external and confining stimulation systems (275,305,346–349). Thus, the continuing analysis and comparison of acute and chronic (STN) DBS and the timeline of its impact on behaviour, brain networks, as well as neuronal and synaptic changes in studies using implantable DBS systems in freely moving animals is crucial to further understand and improve this therapeutic strategy.

Hence, to shed some light on the effects of STN DBS on brain activity and networks, we also compared the changes in cerebral glucose consumption evoked by acute and chronic STN DBS by employing [¹⁸F]FDG PET imaging. Cell uptake of [¹⁸F]FDG is considered to be a surrogate for cell glucose consumption and, more specifically, synaptic activity (318,319). Therefore, in the following, cerebral activity will be used synonymously to tracer uptake. Since the acute effects of STN DBS on glucose metabolism in the rat hemiparkinsonian brain have been extensively discussed in CHAPTER ONE, in this chapter, the differences of acute and chronic DBS shall be in focus. Chronic STN DBS did not change the general picture of [¹⁸F]FDG uptake but reinforced some of the effects seen with acute stimulation. For example, while under acute stimulation, increased tracer uptake could only be observed in the contralesional CPu, cingulate cortex and small parts of ipsilesional cerebellum, chronic DBS caused significant enhancements of glucose metabolism in bilateral CPu, cingulate cortex, orbitofrontal cortex, and larger areas of ipsilesional cerebellum. Greater parts of the ipsilesional somatosensory, motor and visual cortex were also only activated under chronic stimulation. Similarly, the reduced uptake of hypothalamus, contralesional mesencephalon and cerebellar nuclei during acute STN DBS further decreased under chronic treatment. In contrast, significant reductions in bilateral entorhinal cortex and ipsilesional SN disappeared after five weeks of STN DBS. In general, chronic STN DBS for five weeks resulted in more activation in the ipsilesional and less activity in the contralesional hemisphere. Although this effect was not very distinctive in this study, it generally agrees with the findings of CHAPTER ONE and previous studies showing that therapeutic acute STN DBS counteracts the imbalance of brain

metabolic activity induced by unilateral 6-OHDA lesion by increasing ipsi- and decreasing contralesional glucose consumption (132,137,154). Furthermore, the increased recruitment of cerebellar nuclei seen with chronic stimulation agrees with a study that found STN DBS-induced activation of cerebellar structures to be involved in the improvement of parkinsonian motor symptoms (350). In this study, acute STN DBS had no therapeutic effect on behaviour as discussed above. Consistently, brain metabolic activity was not changed as expected, *i.e.* ipsilesional up- and contralesional downregulation of synaptic activity. This picture only formed after five weeks of continuous STN DBS, with according behavioural results: ipsilesional orbitofrontal and cingulate cortex, CPu, SN, and somatosensory and motor cortical areas increased activity, while contralesional mesencephalic and cerebellar areas decreased metabolism. Thus, due to suboptimal stimulation settings, changes evoked by DBS and compensatory and pathological mechanisms might have taken longer to attune to/counteract one another to induce behavioural improvements.

To further analyse the effects of STN DBS on brain networks, seed-based metabolic analyses were conducted for four seeds, each four voxels in size, chosen according to the response pattern seen with STN DBS. The first seed was placed in the ipsilesional hypothalamus which showed significantly reduced [¹⁸F]FDG uptake under STN stimulation. The hypothalamus is involved in numerous functions including somatic activities, autonomic nervous system processes, water balance, metabolism, body weight and temperature, reproductive issues, (neuro)endocrine functions, emotion, reaction to stress, and behaviour (351). It is known to receive input from cerebellum and brainstem. More precisely, Cavdar and colleagues (2001) could show connections between posterior/dorsomedial hypothalamus and contralateral spinal trigeminal nucleus, ipsilateral spinal vestibular nucleus, and bilateral gigantocellular reticular nucleus, all areas that negatively correlated with the hypothalamic seed during OFF in this study (352,353). They proposed that these connections contribute to an involvement of the cerebellum in autonomic activity (352). Other studies found hypothalamic connections to parts of the periaqueductal grey, positively correlating with the seed in this study, and assumed a potential role in thermoregulation (354–356). Since PD patients suffer from various autonomic dysfunctions such as excessive sweating, weight loss, or erectile dysfunction (66), the activation of this network could indicate that 6-OHDA lesioned rats also develop some form of autonomic disturbances caused by DA depletion. STN DBS slightly altered these networks, for example by reversing correlations from negative to positive or vice versa (contralateral spinal trigeminal nucleus), or eliminating and adding correlations (LPAG, microcellular tegmental, gigantocellular reticular nucleus). These alterations may point to a potential improvement or at least alteration of these autonomic dysfunctions and the underlying pathological brain networks. Unfortunately, the 6-OHDA rat model is not suitable to estimate potential changes in (pathologic) autonomic functions evoked by STN DBS. Hence, this explanation can only remain speculative to date.

Glucose consumption of the ipsilateral BNST positively correlated with that of the hypothalamic seed in the OFF but not in the ON condition. Choi *et al.* (2007) found the paraventricular nucleus of the hypothalamus to be innervated by the BNST and suggest the latter to act as a relay station for limbic information influencing the hypothalamic-pituitary-adrenal axis response to stress (357). They found that subdomains of the BNST play different roles in the stress response by either inhibiting or exciting the hypothalamic-pituitary-adrenal axis depending on the limbic input. Feldman and colleagues (1983) investigated the role of MFB catecholaminergic fibers in the modulation of the hypothalamic stress response (358). They discovered that bilaterally 6-OHDA lesioned rats display significantly lower serum levels of corticosterone compared to controls when pre-treated with a glucocorticoid (dexamethasone) and exposed to ether stress. They conclude that MFB noradrenergic neurons take part in the MFB-mediated modulation of hypothalamic sensitivity to glucocorticoids or stress, respectively (358). Hence, BNST, hypothalamus, and 6-OHDA-lesioned MFB may all play a role in the potentially pathological stress network that was activated due to the handling and short

isoflurane anaesthesia leading up to tracer injections in this study. The fact that glucose uptake of the hypothalamus correlated positively with that of the BNST only in the OFF condition may indicate that this (pathologic) network was altered by STN stimulation.

[¹⁸F]FDG uptake of the hypothalamic seed correlated with that of cortical areas, like prelimbic (positive during OFF only, not shown), somatosensory, visual, temporal association, and retrosplenial granular cortex, in the OFF and the ON condition. Tracer uptake of the CPU also showed correlations with that of the seed, *i.e.* positive bilateral connections in the OFF and negative contralateral correlations during ON. These areas have all been shown to be part of two networks found in rat and macaque, namely the medial and orbital prefrontal network connecting (limbic) cortical areas, striatum, PAG, thalamus, and hypothalamus (359–361). Floyd and colleagues (2001) suggested these networks to be involved in “emotional motor” circuits and emotional coping strategies with stress, while the retrosplenial granular cortex is known to play a role in navigation and spatial cognition (359,361). These networks were clearly affected by STN DBS as seen by the changes evoked in connectivity patterns during ON and OFF. Functional PET imaging using more suitable behavioural tests regarding spatial cognition and navigation (*e.g.* Barnes maze), or active and passive emotional coping strategies (*e.g.* resident-intruder test) directly after [¹⁸F]FDG injection could be useful to shed more light on the exact impairments of these functions after 6-OHDA lesions and potential improvements elicited by STN DBS.

Ipsi- and contralesional SN showed significantly lower activity under STN DBS when compared to OFF. Tracer uptake of a seed placed in the ipsilesional SN showed strong positive correlations with that of contralateral SN, and negative correlations with that of contralateral motor and sensorimotor cortex and contralateral CPU in the OFF condition. These correlations were weakened (SN) or abolished (motor cortex, CPU) under STN DBS. That goes partly in line with findings of Perlberg *et al.* (2018) who found increased functional connectivity in bilateral cortico-basal ganglia network pathways including motor cortex, globus pallidus and striatum of unilaterally 6-OHDA lesioned rats (362). Even though a pallidal involvement could not be shown in this study and correlations for motor cortex and CPU were mainly contralateral, the fact that parts of this motor network showed strong connectivity after 6-OHDA injections that weakened under STN DBS could indicate that the stimulation counteracted or superseded the pathological and/or compensatory increase of functional connectivity. Similarly, positive correlations between glucose consumption of the nigral seed and that of ipsilateral parvocellular reticular nucleus, and bilateral medullary reticular and spinal trigeminal nucleus were only present during OFF. Under DBS, positive correlations in cerebellar or medullary structures were found merely for the ipsilateral ventral medullary reticular nucleus (not shown). SN, parvocellular reticular, medullary reticular, and spinal trigeminal nucleus are all interconnected either by direct fibre projections or via complex interconnections also including striatum, thalamus, hypothalamus, amygdala, superior colliculus, dorsal tegmental nucleus, and cerebellum, all shown to correlate with tracer uptake in the SN differently during OFF and ON in this study (363–368). Pontine and medullary nuclei of the reticular formation play a major role in the upper motor neuron extrapyramidal control of weight support and the generation of gait, while the parvocellular reticular nucleus is thought to play a role in orofacial motor control (367,369). It has been previously shown that unilaterally 6-OHDA lesioned rats develop pathological and compensatory weight shifting and gait patterns (154). Hence, the different networks (nigro-striatal, medullary/pontine) responsible for the various motor aspects and activated during free movement of animals after tracer injection seem to display pathologic/compensatory activity patterns during OFF that are normalised and/or superseded by STN DBS, indicated by the varying correlation patterns.

Parts of the hippocampal formation, *i.e.* hippocampus, ventral subiculum and entorhinal cortex, also showed [¹⁸F]FDG uptake that correlated with that of the seed, as did several contralateral sensory cortical areas,

including visual, parietal, and auditory cortex, amygdalohippocampal area, thalamus, and hypothalamus. Together with the hippocampal formation, these brain areas belong to a network responsible for episodic memory formation and spatial navigation (370–372). The ventral subiculum in particular is involved in anxiety, stress, emotion, and episodic recollection (370,373). While hippocampal formation and SN have no direct fibre connections, a correlating activation could have been mediated through common thalamic relay areas. The fact that the hippocampus has strong connections to the ipsilateral thalamus and that in this study glucose metabolism of contralateral thalamic nuclei and contralateral hippocampus strongly negatively correlated with that of ipsilesional SN under STN DBS support this assumption (374). Alternatively, the hippocampus could have communicated with the SN via the CPU with which it shares an anatomical link with the orbitofrontal cortex (375). However, the fact that tracer uptake of the seed correlated with that of contralateral CPU during OFF and with that of contralateral hippocampus during ON indicates otherwise. PD patients can suffer from visuospatial memory impairments accompanied by hallucinations. Yao and colleagues (2016) found a link between those hallucinations and changes in hippocampal functional connectivity. In a multimodal MRI study including PD patients with and without hallucinations as well as healthy controls, they showed that hippocampal connectivity to visual cortices was lower in PD patients with hallucinations compared to the other two groups (376). While rats are unlikely to develop hallucinations, the hemiparkinsonian rats in this study might still have had problems with visuospatial recognition while moving around after tracer injection in the OFF condition. This could be indicated by the absence of tracer uptake correlations between seed and hippocampus, and the small involvement of the visual cortex in the employed network during OFF. Under STN DBS however, a correlation to the hippocampus appeared and more areas of the visual cortices were employed. Hence, STN DBS could have improved hippocampal functional connectivity and, therefore, visuospatial memory. Studies in PD patients have been inconclusive regarding the effect of STN DBS on visuospatial memory functions so far as positive as well as negative effects have been observed (377–380).

[¹⁸F]FDG uptake of the seed placed in the contralesional hemisphere showed similar correlations to its ipsilesional counterpart. Three major differences could be observed, however. First, the correlation between tracer uptake in both SN's was not as pronounced as compared to when the seed was ipsilesional and disappeared completely during ON. This could be explained by a compensatory recruitment of the contralateral SN by the ipsilateral, lesioned one. While there is no direct fibre connection between left and right SN, it has been shown that the one SN is connected to its contralateral counterpart via multisynaptical crossed connections involving hypothalamus, thalamus, superior colliculus and other brain regions (365). For the present data, where correlations between left and right SN was weakened or absent under STN DBS regardless of the side of the seed, this could mean that STN DBS makes part of the contralesional compensatory activity obsolete. Additionally, the fact that tracer uptake of the healthy SN correlated more with that of the lesioned one than *vice versa*, explains that the intact SN compensates the lacking activity of the impaired one but that the lesioned SN is not influenced by the activity of its contralateral counterpart to the same extend.

The second difference is a strong positive correlation between [¹⁸F]FDG uptake in nigral seed and that in bilateral entorhinal, ectorhinal, perirhinal and contralateral primary visual cortex during STN DBS that was, except for the ipsilateral entorhinal cortex, absent for the ipsilesional seed. This can have two reasons. For once, it is possible that the healthy, contralesional networks for motor control and visuospatial functions that involve the SN, peri- ecto- and entorhinal cortex, *i.e.* basal ganglia and hippocampal formation as mentioned above, stepped in to compensate for the insufficient activity of the networks including the ipsilesional, impaired SN, and that this phenomenon was especially present under DBS. Secondly, the networks as seen

with the contralesional seed during OFF represent the healthy system that is overstimulated by STN DBS, and the connectivity pattern seen with the ipsilesional SN represents a pathological state with potential compensatory aspects.

The last big difference between ipsi- and contralesional seed was present in cerebellar and medullary structures. [¹⁸F]FDG uptake between ipsilesional SN and medullary structures, such as parvocellular reticular, medullary reticular and spinal trigeminal nucleus, had strong positive correlations during OFF that nearly vanished during STN stimulation. Tracer uptake of the contralesional SN, however, correlated only moderately positively with that of contralateral medullary reticular and ipsilateral spinal trigeminal nucleus during OFF, while showing a negative correlation to tracer uptake in the ipsilateral medial cerebellar nucleus. The correlation to the spinal trigeminal nucleus vanished while others increased in the ON condition. STN DBS lead to additional negative correlations between uptake in contralesional SN and that in contralateral medial cerebellar and bilateral medial vestibular nucleus, and additional positive correlations in ipsilateral medullary reticular nucleus and ninth cerebellar lobule. This underlines the assumption made earlier, that the lesioned nigro-striatal and medullary networks display pathologic/compensatory activity patterns during OFF that are normalised and/or superseded by STN DBS. Since the contralesional SN is not impaired, the networks do not display the same degree of pathological or compensatory activity during OFF but a moderate, healthy level. During ON however, the networks might either be overstimulated leading to the additional recruitment of auxiliary motor and balance related cerebellar regions, or simply display the normal state of the upper motor neuron extrapyramidal network controlling weight support and gait that was slightly underactive during OFF. Interestingly, in a recent DBS study using seed based analysis in hemiparkinsonian rats, it was shown that negative metabolic connections existed between ipsilesional SN and contralesional CPu only during OFF, and between contralesional SN and bilateral CPu during STN DBS (138). This hemispherical shift of connection between CPu and SN could be largely replicated in this study. Without stimulation, the ipsilesional SN was negatively metabolically connected to the contralesional CPu, whereas the contralesional SN was metabolically connected to the contralesional CPu under STN DBS. The slight discrepancy of the lack of connection between contralesional SN and ipsilesional CPu during ON could be due to the different placing of the seed, *i.e.* in the SN in this study versus in the CPu in the other study. Similar findings, if not completely comparable due to the unilateral nature of the 6-OHDA Parkinson model of this study, were also made for PD patients. In an fMRI study Hacker and colleagues (2012) found a shift towards weaker (negative) correlations between striatal seeds and the “extended brainstem” including midbrain structures (381). The previous animal study explained the negative correlation by synaptic activity within a bilateral basal ganglia network comprising a connection between ipsilesional midbrain and contralesional CPu via the medial thalamic nucleus and orbitofrontal cortex (138). In this study, there was no metabolic connection between SN and orbitofrontal cortex for the ipsilesional but only a negative one for the contralesional nigral seed during ON. Again, the different placement of seeds may have caused these differences. However, the interhemispheric connection, the metabolic connectivity between ipsi- and contralesional SN and CPu and the shift induced by STN DBS seem to be stable and reproducible phenomenon. Nevertheless, more imaging studies utilising seed based analyses are needed to establish the exact pathways and nature of information transmission.

The last seed was placed in the ipsilesional cerebellum, more specifically in the interposed cerebellar nucleus, which showed significantly higher [¹⁸F]FDG uptake in the ON condition. In the OFF condition, glucose uptake of the seed negatively correlated with that of ipsilateral motor and somatosensory cortices and CPu, while positively correlating with that of bilateral hippocampus. Under STN DBS, correlations to cingulate cortex, CPu, and hippocampus disappeared, and positive correlations to several contralateral thalamic nuclei emerged. The cerebellum and the basal ganglia are subcortical structures crucial for numerous motoric

functions. The interposed cerebellar nucleus in particular has been shown to be involved, among other motor aspects, in the coordination of limb movements (382). Therefore, both cerebellum and basal ganglia communicate with cortical areas via separate thalamo-cortical loops and olivo-cortico nuclear circuits, respectively (382-384). However, there are also bisynaptic connections from cerebellum to basal ganglia (striatum/CPu), and from basal ganglia (STN) to cerebellar cortex that are independent of the cortex (385,386). Additionally, cerebellum and hippocampus have been shown to share bidirectional functional connections involved in spatial navigation (387). Hence, in the pathological state of the 6-OHDA lesioned brain, all possible networks, *i.e.* cerebello-cortical, cerebello-basal ganglia, and cerebello-hippocampal networks, may have been recruited to support normal motor functioning. Stimulation of the STN could then have reduced this compensatory recruitment of hippocampus and CPu through its bisynaptic input to the cerebellum indicated by an additional positive correlation to the cerebellar cortex (crus one of the ansiform lobule). The seed could have instead increasingly communicated with the ipsilesional cortex via thalamic relays like ventral posterior thalamic nucleus (388).

In conclusion, seed based network analysis is a strong tool to investigate brain network changes in the healthy and diseased state and the impact of therapeutic interventions. However, data concerning the network changes in PD and their modulation by (STN) DBS and other therapies are still scarce. Hence, the reproducibility and, therefore, reliability of the findings of this study need to be confirmed in future studies. Additionally, more specific functional PET studies correlating network activities with behavioural findings are needed to analyse the true nature of these network changes and distinguish pathological from compensatory phenomena.

CHAPTER THREE: Comparing the effects of DBS of the subthalamic nucleus and systemic L-DOPA treatment on brain (network) activity and motor performance in hemiparkinsonian rats

A. Introduction

L-DOPA and its chemical structure were isolated and established in the early 20th century (389,390). The discovery of AADC about 15 years later then identified it as a precursor of DA, giving the two a (rather small) role in the biosynthetic way of catecholamines in the body (391). Found to exist in the human brain in 1957, the excitatory central effects of L-DOPA were soon attributed to DA as its active metabolite (392,393). The major localisation of DA in the striatum then led to the assumption of its involvement in motor function and PD (394,395). And indeed, Ehringer and Hornykiewicz (1960) found striatal DA levels to be significantly decreased in PD patients (396). Since then, research has successfully focused on the potential of L-DOPA to enhance striatal dopaminergic transmission as a pharmacological "dopamine replacement therapy" (397–399). It has been shown to alleviate all cardinal symptoms of the disease for several years and is still considered as the gold standard therapy to date (163,398).

However, chronic L-DOPA treatment does not come without challenges. After four to six years, about 40 % of PD patients suffer from L-DOPA-induced dyskinesia and motor fluctuations (400). While dyskinesia comprises different forms of abnormal involuntary movements (401), motor fluctuations describe the reduced duration of action of L-DOPA (wearing off phenomenon) as well as unpredictable, sudden changes in response to the drug irrespective of medication timing (ON-OFF phenomenon) (402,403). As dosing of L-DOPA needs to be increased with the progression of PD to have the same positive effect on symptoms, the biggest challenge with time is to find the dosage delivering the best compromise between anti-parkinsonian effect and dyskinesia (171,404).

Several attempts have been made to prolong the action of each L-DOPA dose to stabilise plasma concentrations and minimise OFF phases. For example, L-DOPA is mostly given in combination with peripheral AADC inhibitors like carbidopa or benserazide (405,406), COMT inhibitors like entacapone or tolcapone (407,408), or MAOB inhibitors like rasagiline or selegiline (409,410) to maximise brain L-DOPA levels. Since continuous administration of L-DOPA was found to be superior to the intermittent oral dosing the development of controlled release formulations tried to eliminate the problem of instable L-DOPA plasma levels, with moderate success (411–413). Intraintestinal or intravenous pumps target the same outcome by steadily releasing L-DOPA (414–416). However, not only dosage, formulation, or route of administration are responsible for the problems arising from chronic L-DOPA treatment. The drug itself is far more than a precursor for DA. It might, for instance, interact with compensatory mechanisms within the nigro-striatal pathway that change over time, or potentially cause the death of dopaminergic neurons by converting into the excitotoxin 2,4,5-trihydroxyphenylalanine quinone (342,417,418).

Interestingly, besides the involvement of dopaminergic depletion in the pathology of PD, the serotonergic system has also been shown to play a role in non-motor symptoms and treatment-related complications (419). For example, studies suggest that DA release by serotonergic neurons is associated with L-DOPA- and cell graft-induced dyskinesia (420,421). Consistently, studies found that serotonergic neurons are able to convert exogenously administered L-DOPA into DA via AADC (422), and that L-DOPA induces ectopic DA release in brain regions innervated by serotonergic neurons like striatum, hippocampus, or SN (423). Noteworthy, serotonergic neurons increase DA levels predominantly in the extracellular space (422). Consequently, future

therapies addressing the serotonergic system could yield a remedy for side effects resulting from long-term L-DOPA administration.

DBS of the STN allows for the reduction of dopaminergic medication and is therefore also able to reduce motor complications associated with chronic L-DOPA treatment while improving symptoms of PD (215,291,323,424). Nevertheless, the exact commonalities and differences as well as the interplay of the two forms of therapy are not fully understood today (425,426). While there are many imaging studies looking at the effects of L-DOPA and DBS on brain glucose metabolism individually, the exact differences and especially combined effects have not been investigated sufficiently (97,133,135,136,427). Hence, the current study aimed at investigating the effects of single doses of L-DOPA and STN DBS separately and in combination on behaviour, brain glucose metabolism, and network activity in the rat 6-OHDA model of PD using functional [¹⁸F]FDG PET imaging.

B. Material and Methods

B.a Animals

The same eight rats as in CHAPTER TWO were used in this study. They were housed in groups of two to four in individually ventilated cages. Rodent chow and water were given *ad libitum*. The day-night-cycle was reversed with lights on at 8:30 pm, the ambient temperature was 22 ± 1 °C and relative humidity set at 55 ± 5 %.

All eight rats received unilateral 6-OHDA lesions in the medial forebrain bundle and ipsilesional DBS electrode implantation as described in CHAPTERS ONE and TWO. After sufficient recovery, OFF testing, and testing following a single dose of L-DOPA, stimulation was turned on for the tests under STN DBS and the combination of DBS and L-DOPA. Stimulation then lasted until the end of experiments with the exception of one day on which [¹⁸F]FDG PET imaging took place under L-DOPA only. A schematic overview of all experiments can be seen in Figure 15.

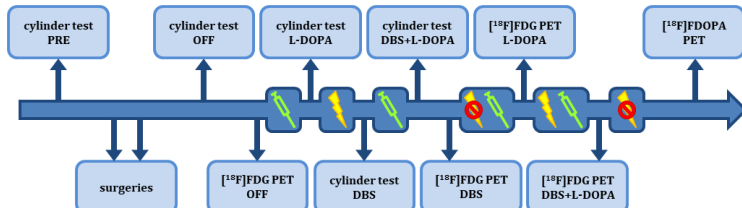


Fig. 15 Timeline of surgeries, tests and treatments. Before any intervention, naïve animals were tested in the cylinder for baseline values. Then, two days of surgeries followed in which the medial forebrain bundle was lesioned unilaterally with 6-OHDA and electrode and stimulator were implanted. Before any treatment started, animals were then tested in the OFF condition in cylinder and measured with [¹⁸F]FDG PET. The cylinder test was then performed following a single dose of L-DOPA before STN DBS was turned on. Approx. one day later, the cylinder test was then conducted under DBS alone and, on a different day, after a single dose of L-DOPA while DBS was still on. The [¹⁸F]FDG PET followed before stimulation was then turned off for one day to measure [¹⁸F]FDG PET after a single dose of L-DOPA only. After that, DBS was turned back on one a last time for [¹⁸F]FDG PET under DBS and after a single dose of L-DOPA. Stimulation was then turned off and [¹⁸F]FDOPA PET scans were conducted two to three months post surgeries. Experiments were performed on different days. Green syringe = i.p. L-DOPA injection, flash = DBS is turned on, cancelled flash = DBS is turned off. Timeline is schematic and spaces between procedures are not true to scale.

All experiments were executed in the dark (active) phase of the rats at roughly the same time each day to avoid changes caused by their circadian rhythm. Experiments were carried out in accordance with the EU directive 2010/63/EU for animal experiments and the German Animal Welfare Act (TierSchG, 2006) and were approved by regional authorities (LANUV NRW; application number 84-02.04.2012.A304).

B.b Stimulation System and Surgical Procedures

Stimulation system and surgical procedures of this study corresponded to those used and practised in CHAPTER TWO. In short, in a first surgery, the medial forebrain bundle (-4.4 mm posterior, ± 1.2 mm lateral) was lesioned with 14 μg of 6-OHDA free base (21 μg of 6-Hydroxydopamine hydrobromide containing ascorbic acid as stabiliser, Sigma Aldrich®, St. Louis, USA) in 3 μl of NaCl, and the guide cannula for the stimulation electrode was implanted (-3.6 mm posterior, ± 2.8 mm lateral). In a second surgery, the concentric bipolar platinum/iridium electrode (Science Products GmbH, Hofheim, Germany) was inserted into the catheter until reaching the STN and connected to the stimulation system (Medtronic) reinforced with silicone tubing and sterile medical adhesive silicone type A (Silastic®, Dow Corning Corp., Midland, MI, USA), that was implanted subcutaneously on the rats' backs. The side of the lesion for each animal, and therefore the DBS electrode, was randomised between animals.

B.c Treatment Regimes

Animals received three different treatments: L-DOPA alone, STN DBS alone, and a combination of the two. Cylinder test as well as [^{18}F]FDG PET imaging were performed under all three conditions.

B.c.a Deep Brain Stimulation

Stimulation was turned on after animals had recovered sufficiently, in this case six to eleven days after surgeries, and at least a day before the first test in the ON stimulation condition. Rats were then stimulated until after the last [^{18}F]FDG PET scan. Stimulation settings were the same as in CHAPTERS ONE and TWO, *i.e.* a pulse width of 60 μs and a frequency of 130 Hz. The amplitude was initially set at 30 μA for all rats. It was then increased in steps of 5 μA until side effects occurred. The final amplitude was then 80 % of the side effect evoking amplitude. Final amplitudes varied from 125 – 220 μA .

B.c.b L-DOPA Injections

Rats received intraperitoneal injections of L-DOPA (Sigma Aldrich, St. Louis, USA) in combination with 15 mg/kg of the peripheral decarboxylase inhibitor benserazide hydrochloride (Sigma Aldrich, St. Louis, USA) one hour before experiments started. Before PET imaging, the L-DOPA+benserazide mix was injected at the same time as [^{18}F]FDG. Dosages varied between PET and behavioural testing. Before PET imaging, animals were injected with 25 mg/kg L-DOPA adapted from Trugman *et al.* (1996), while the dose before behavioural tests was 5 mg/kg as was determined through pre-tests (428).

B.d Cylinder Test

To investigate the effectiveness of both treatment options on a behavioural level, all rats performed the cylinder test. It serves as an indicator of unilateral front paw impairment as caused by, for example, unilateral 6-OHDA lesions.

All animals underwent a baseline test before any surgical intervention (PRE) and one test in the OFF condition after surgeries and a recovery period of at least four days but before onset of therapy (OFF). The L-DOPA test then started 60 min after the injection of 5 mg/kg L-DOPA and 15 mg/kg benserazide (L-DOPA). The DBS test

took place a day after STN DBS onset (DBS), and the DBS/ L-DOPA test 60 min after the injection of L-DOPA and benserazide while DBS was ON (DBS+ L-DOPA). All tests were conducted on different days.

B.e Positron Emission Tomography

PET-scans took place in the same small-animal-PET scanner used in CHAPTERS ONE and TWO (Siemens Focus 200, Berlin, Germany). Animals underwent five PET scans: One [¹⁸F]FDG scan after surgeries but without any treatment (PRE), one [¹⁸F]FDG scan each, 60 min after tracer and L-DOPA+benserazide injection (L-DOPA) and a day after DBS onset (DBS), a last [¹⁸F]FDG scan 60 min after tracer and L-DOPA+benserazide injection while DBS was still ON (DBS+L-DOPA), and one [¹⁸F]FDOPA scan to verify striatal dopaminergic lesions at least five weeks after surgeries. [¹⁸F]FDG was injected 60 min before each scan so that [¹⁸F]FDG uptake occurred simultaneously to L-DOPA uptake and/or while DBS was ON. Rats were only scanned once per day, *i.e.* different conditions were measured on different days. Heart rate was monitored during each scan and body temperature kept at 37 °C using a warm air system integrated in the animal holder (Medres® Medical Research GmbH, Cologne, Germany).

B.e.a [¹⁸F]FDG PET

For the PET scans in this study, animals received *i.p.* injections of 69.93 ± 12.88 MBq of [¹⁸F]FDG in approximately 0.5 ml saline under brief anaesthesia (see CHAPTER ONE). Tracer uptake then occurred under active DBS and/or simultaneously to L-DOPA uptake in the awake and freely moving animal for 60 min before start of a 30 min emission scan. The last animal on each PET day also underwent a 10 min transmission scan for later attenuation correction as mentioned in CHAPTERS ONE and TWO. Blood glucose levels were measured at the end of each scan.

B.e.b [¹⁸F]FDOPA PET

Rats were briefly anaesthetised and received an *i.p.* injection of 15 mg/kg benserazide hydrochloride (Sigma Aldrich, St. Louis, USA). Sixty minutes later and again under anaesthesia, animals were then given 73.13 ± 3.23 MBq [¹⁸F]FDOPA in 0.5 ml saline via a catheter in the lateral tail vein. After 30 min back in the home cage, animals were anaesthetised again and 30 min emission scans started.

B.f Statistical Analysis

B.f.a Behaviour

As in CHAPTERS ONE and TWO, the percentage of CF and IF use was calculated from all wall touches recorded during the cylinder tests. After arcus-sinus transformation, significant ($p \leq 0.05$) deviations from a 50 % usage of CF and IF during PRE, OFF, L-DOPA, DBS and DBS+L-DOPA were analysed with the software Graphpad Prism version 8 for macOS using one-sample t-tests and a theoretical mean of 0.5.

B.f.b [¹⁸F]FDG PET

Images were summed (60 – 90 min *p.i.*), full 3D-rebinned and reconstructed as mentioned earlier (see 2.8.2). Manual coregistration to the Swanson rat brain Atlas (313) and all further analyses were done using the software VINCI (312). $SUVR_{wb}$ was obtained by normalising the intensity to the cerebral global mean ($SUVR_{wb}$ = individual voxel value divided by mean value of the whole brain). To have lesion and electrode always displayed on the left, images of animals with interventions on the right were flipped. Voxel-wise comparisons of [¹⁸F]FDG uptake using a paired t-test followed by a TFCE procedure with subsequent permutation testing

(314) were executed between DBS and OFF, L-DOPA and OFF, and DBS+L-DOPA and OFF. This resulted in t-maps corrected for multiple testing (thresholded at $p = 0.05$). As TFCE values are random, like in CHAPTERS ONE and TWO, colour bars of TFCE maps are labelled with the original t-values, marked as t_{TFCE} .

To point out potential variability in effects of the different treatments on brain networks, seed-based metabolic analyses (138,329) were calculated separately for the different treatment (DBS, L-DOPA, DBS+L-DOPA) and OFF conditions. Two seed regions of four voxels each were chosen according to a recent paper (138), namely one in the ventral ipsilesional CPu and one in the dorsal contralesional CPu. Again, PET images were correlated voxel-wise with the mean $SUVR_{wb}$ of each seed using the Pearson correlation test to identify connected brain regions. Displayed t-maps showing significant R-values were TFCE-corrected as mentioned earlier.

B.fc [18F]FDOPA PET

Since in this study the same animals were used as in CHAPTER TWO, the procedures to illustrate and verify the dopaminergic lesion can be read in *Il.vi.iii*. In short, VOIs were drawn for medial and lateral striatum and ipsi- and contralesional mean SUVRs were compared using a paired t-test. Results were considered significant when $p \leq 0.05$.

C. Results

Only the data of seven animals were included in behavioural and PET ([18F]FDG and [18F]FDOPA) image evaluation as one animal showed profound cerebral inflammation in the lesioned hemisphere and had therefore to be excluded to prevent tampering of results.

C.a Dopaminergic Lesion and Electrode Placement

A profound dopaminergic lesion could be confirmed by a paired t-test comparing ipsi- and contralesional [18F]FDOPA uptake in medial and lateral striatum ($p = 0.0002$) (see III.i and Fig. 10 A). All electrode tips were proven to be located in the STN by interoperative MRI (Fig. 10 B).

C.b Effects of DBS and L-DOPA on Behaviour

The data of seven of the twelve rats were used to analyse paw use under the five different treatment conditions, namely PRE, OFF, L-DOPA, DBS, and DBS+L-DOPA. Data exhibited high standard deviations as a result of the rats' differing quality of response to the various treatment conditions. For example, three rats did not present any wall touches under L-DOPA, DBS, and/or DBS+L-DOPA treatment during the ten-minute tests. Hence, percentages of CF and IF do not always add up to 100 % and one-sample t-tests against the theoretical mean of 0.5 were calculated for CF and IF to get a clear picture of the relation between the two paws.

During the baseline test ahead of any surgical interventions, rats used both paws nearly equally, *i.e.* the prospective contralesional, affected front paw was used in 54.35 % and the future ipsilesional, healthy front paw in 45.65 % of all wall touches (Fig. 16). The one-sample t-tests against a theoretical mean of 0.5, *i.e.* 50 % usage of a paw, revealed significant deviations of CF and IF from that mean in the OFF ($p_{CF} < 0.0001$; $mean_{CF} = 0.038$; $p_{IF} = 0.0193$; $mean_{IF} = 1.197$) and the DBS condition ($p_{CF} < 0.0001$; $mean_{CF} = 0.018$; $p_{IF} = 0.0143$; $mean_{IF} = 1.24$), but not during PRE, L-DOPA, or DBS+L-DOPA (Fig. 16). In other words, 6-OHDA lesions strongly reduced CF (3.79 %) and increased IF use (81.92 %) during OFF when compared to PRE, and this state was not changed by STN DBS (CF = 1.94 %; IF = 83.77 %). Intraperitoneal injections of 5 mg/kg L-DOPA reversed the 6-OHDA-induced change in paw use. Animals now used CF in nearly 50 % of all wall touches (43.45 %)

again, but IF use was reduced below PRE levels (13.69%). Only L-DOPA in combination with STN DBS lead to a near normalisation of paw use compared to PRE levels, i.e. a usage of CF in 47.57% and IF in 38.14% of all wall touches.

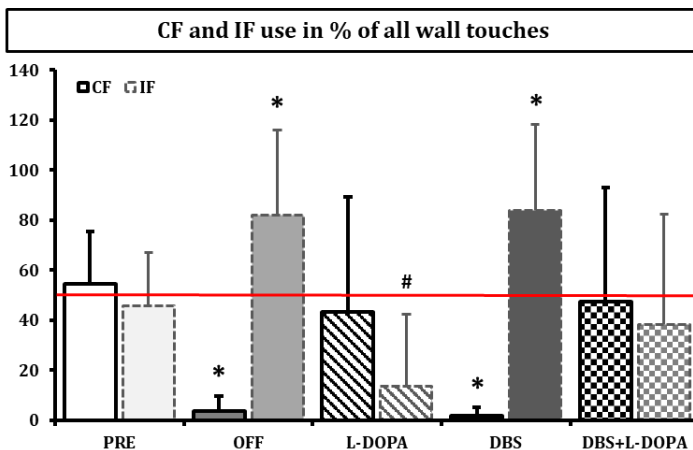


Fig. 16 Cylinder test. Percentage of wall touches with the contralesional, affected front paw (CF) and the ipsilesional healthy front paw (IF) during a 10-min cylinder test ($n = 7$) before surgery (PRE), after surgery but before treatment onset (OFF), after 5 mg/kg L-DOPA (L-DOPA), under STN DBS (DBS), and after a combination of the two (DBS+L-DOPA). There was a significant deviation from a 50% use in wall touches of CF and IF after 6-OHDA lesion (OFF), which could not be recovered under DBS, but after L-DOPA injection and a combination of L-DOPA and DBS. Asterisks indicate significant deviations from a theoretical mean of 0.5 (50% usage, red line). Values do not always add up to 100% because three animals used neither paw in some conditions.

C.c Effects of DBS and L-DOPA on Cerebral [18 F]FDG Uptake

DBS and L-DOPA had different effects on brain glucose metabolism, while the combination of the two treatments caused a metabolic picture containing features of both treatments alone (Fig. 17). Intraperitoneal injections of 25 mg/kg of L-DOPA administered at the same time as the tracer caused mainly contralesional increases of [18 F]FDG uptake, namely in somatosensory and motor cortices, thalamus, parietal cortices, lateral periaqueductal grey, anterior pretectal nucleus, second cerebellar lobule, peritrigeminal zone and parafoveus when compared to the OFF condition (Fig. 17 A). Ipsilesional increases in tracer uptake could just be observed in postsubiculum and central inferior colliculus. Superior colliculus, reticulotegmental nucleus, crus one of the cerebellar ansiform lobule, fifth and sixth cerebellar lobule and gigantocellular reticular nucleus expressed an increased glucose consumption in both hemispheres.

Decreases in glucose metabolism under L-DOPA compared to OFF were more widespread. They were found in ipsilesional primary and secondary somatosensory, insular, and temporal association cortex. Contralesional decreases in tracer uptake were present in preoptic area, amygdalopiriform transition area, inferior colliculus, microcellular tegmental nucleus, and perirhinal cortex. Caudate putamen, amygdala, hypothalamus, and ecto- and endorhinal cortex showed decreases in glucose consumption bilaterally.

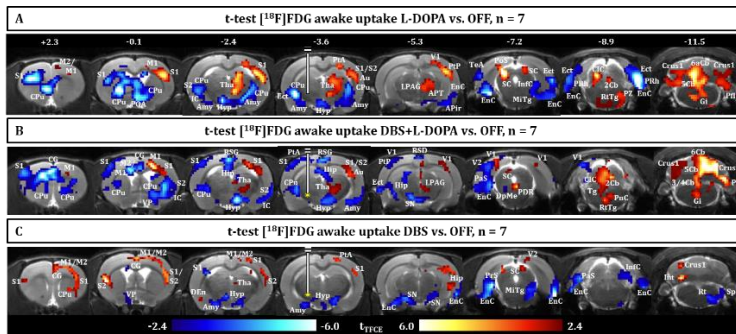


Fig. 17 Effects of systemic L-DOPA and acute STN DBS on cerebral glucose metabolism. Subtractive *t*-maps ($p < 0.05$, TFCE-corrected) projected onto an MRI template displaying the [^{18}F]FDG uptake difference between **A** L-DOPA and OFF, **B** DBS additive to L-DOPA and OFF, and **C** DBS and OFF in 6-OHDA rats ($n = 7$). Red voxels indicate that [^{18}F]FDG accumulation was significantly higher during L-DOPA or DBS, while blue voxels indicate a significantly higher [^{18}F]FDG uptake during OFF conditions. Abbreviations: 2Cb = 2nd cerebellar lobule, 3/4Cb = 3rd and 4th cerebellar lobule, 5Cb = 5th cerebellar lobule, 6Cb = 6th cerebellar lobule, Amy = amygdala, APr = amygdalopiriform transition area, APT = anterior pretectal nucleus, Au = auditory cortex, CIC = central nucleus of inferior colliculus, CG = cingulate cortex, CPu = caudate putamen, Crus1 = crus one of the ansiform lobule, DeN = dorsal endopiriform cortex, DeMe = deep mesencephalic nucleus, Ect = ectorhinal cortex, EnC = entorhinal cortex, Gi = gigantocellular reticular nucleus, Hip = hippocampus, Hyp = hypothalamus, IC = insular cortex, InfC = inferior colliculus, Int = interposed cerebellar nucleus, LPAG = lateral periaqueductal grey, M1/2 = primary/secondary motor cortex, MiTg = microcellular tegmental nucleus, PaS = parasubiculum, PDR = postdorsal raphe nucleus, Pfl = paraflocculus, PnC = caudal pontine reticular nucleus, POA = preoptic area, PoS = postsubiculum, PRh = perirhinal cortex, PrS = presubiculum, PtA = parietal association cortex, PTP = posterior parietal cortex, PZ = peritrigeminal zone, RSD = retrosplenial dysgranular cortex, RSG = retrosplenial granular cortex, Rt = reticular nucleus, RtTg = reticulotegmental nucleus, S1/2 = primary/secondary somatosensory cortex, SC = superior colliculus, SN = substantia nigra, Sp = spinal trigeminal nucleus, Tg = tegmental nucleus, TeA = temporal association cortex, Tha = thalamus, V1/2 = primary/secondary visual cortex, VP = ventral pallidum. PET images of animals implanted in the right hemisphere were flipped so that all stimulation sites are shown on the left. Colour bars of TFCE maps are labelled with the original suprathreshold *t*-values. Numbers indicate rostracaudal coordinates in mm distance to Bregma.

As already explicated in CHAPTER TWO, acute STN DBS caused bilateral increases of [^{18}F]FDG uptake in cingulate cortex, prelimbic and somatosensory cortices. Ipsilaterally, tracer uptake increased significantly in dorsal endopiriform cortex, and crus two of the ansiform cerebellar lobule. In the contralesional hemisphere, motor cortices, thalamus, CPu, parietal association cortex, secondary visual cortex, superior colliculus and hippocampus exhibited increased glucose consumption under STN DBS (Fig. 17 C).

Ipsilesional ventral pallidum, primary somatosensory cortex, amygdala, subrachial nucleus and pre- and parasubiculum showed significantly decreased glucose metabolism, as well as contralesional medial geniculate nucleus, microcellular tegmental nucleus, inferior colliculus, reticular nucleus and spinal trigeminal nucleus. Bilateral decreases were found in hypothalamus, entorhinal cortex, and SN under STN DBS compared to OFF.

The combination of 25 mg/kg L-DOPA and STN stimulation evoked some of the metabolic effects seen with sole L-DOPA treatment, some that were seen under STN DBS, some of these effects were altered, and some changes appeared that could not be attributed to either treatment alone (Fig. 17 B). As seen under L-DOPA treatment alone, the simultaneous administration of L-DOPA and DBS lead to an increase of [^{18}F]FDG uptake in ipsilesional central nucleus of the inferior colliculus, in contralesional somatosensory and auditory cortices, lateral periaqueductal grey, and paraflocculus, and in bilateral reticulotegmental nucleus, crus one of the ansiform cerebellar lobule, fifth and sixth cerebellar lobule, and gigantocellular reticular nucleus. In

accordance with the effects of STN DBS and L-DOPA alone, contralesional primary motor cortex (M1) and thalamus also show increased tracer uptake under the simultaneous administration. Additional significant increases in glucose metabolism were found in ipsilesional tegmental nucleus and superior colliculus that showed bilateral increases under L-DOPA alone. Furthermore, increases occurred in contralesional caudal pontine reticular nucleus, and bilateral primary visual cortex, postdorsal raphe nucleus, as well as second cerebellar lobule and crus one of the cerebellar ansiform lobule, which showed increases only contra- and ipsilesionally, respectively, in solely L-DOPA and DBS treated animals.

Significant decreases in glucose metabolism under DBS+L-DOPA showed less commonalities with the two treatments alone. Ipsilesional decreases were found in motor, parietal, and visual cortices, as well as deep mesencephalic nucleus. In accordance with both treatments alone and DBS alone, respectively, ipsilesional primary somatosensory cortex (both) and parasubiculum (DBS) also exhibited decreased tracer uptake. Contrary to the bilateral decreases of glucose consumption seen in SN and entorhinal cortex under DBS, the combined treatment evoked decreases of [18 F]FDG uptake only ipsilesionally. Similarly, L-DOPA alone induced bilateral decreases in ento- and ectorhinal cortices, while DBS+L-DOPA caused reductions only ipsilesionally. The contralesional decrease of glucose metabolism in ventral pallidum, hypothalamus, and amygdala found with DBS+L-DOPA are in contrast to the ipsilesional (ventral pallidum, amygdala) and bilateral (hypothalamus) decreases found under DBS alone. Similarly, the combined treatment caused decreased tracer uptake in contralateral insular and secondary somatosensory cortices, while L-DOPA alone evoked ipsilesional decreases of glucose metabolism. Bilateral decreases of tracer uptake could be found in hippocampus and retrosplenial dysgranular and granular cortices under DBS+L-DOPA. As seen with L-DOPA alone, but contrary to DBS alone, the combined treatment also caused bilateral decreases in the CPu. Lastly, while DBS alone caused bilateral increases in glucose consumption of the cingulate cortex, a combination of DBS and L-DOPA evoked bilateral decreases in that area.

C.d Effects of DBS and L-DOPA on Brain Networks

To further analyse the effects of the different treatments on brain network activity seed-based metabolic correlation analyses were conducted for two seeds of four voxels each, one in the ipsilesional ventral and one in the contralesional dorsal CPu, according to a previous study (138).

Ipsilesional Striatum Seed

During OFF, [18 F]FDG uptake of the seed placed in the ipsilesional affected ventral striatum only moderately correlated positively with the striatal tissue in its immediate vicinity (Fig. 18 A, top row). The only other positive correlations were found between glucose metabolism of the seed and that of bilateral prelimbic cortex and ipsilateral secondary motor cortex. Negative correlations existed between tracer uptake of the seed and that of ipsilateral ventral tegmental area (VTA), dorsal nucleus of the lateral lemniscus, dorsomedial tegmental area, spinal trigeminal nucleus, and spinal vestibular nucleus (latter two not shown).

Intraperitoneal administration of 25 mg/kg L-DOPA injected concurrently to the tracer increased the positive correlation between glucose consumption of the seed and that of its surrounding striatal tissue (Fig. 18 A, second row). Tracer uptake of ipsilateral M1, cingulate cortex, amygdala, contralateral periaqueductal grey, and bilateral GPe, thalamus, and ventral periaqueductal grey also correlated positively with that of the seed under L-DOPA. Negative correlations could only be observed contralaterally to the seed, *i.e.* in cingulate cortex, hippocampus, substantia nigra, ventral lateral geniculate nucleus, superior colliculus, microcellular tegmental nucleus, pedunculopontine tegmental nucleus (PPTg), VTA, A7 noradrenaline cells, caudomedial entorhinal cortex, lateral parabrachial nucleus, ventral nucleus of the lateral lemniscus, and facial nucleus (latter not shown).

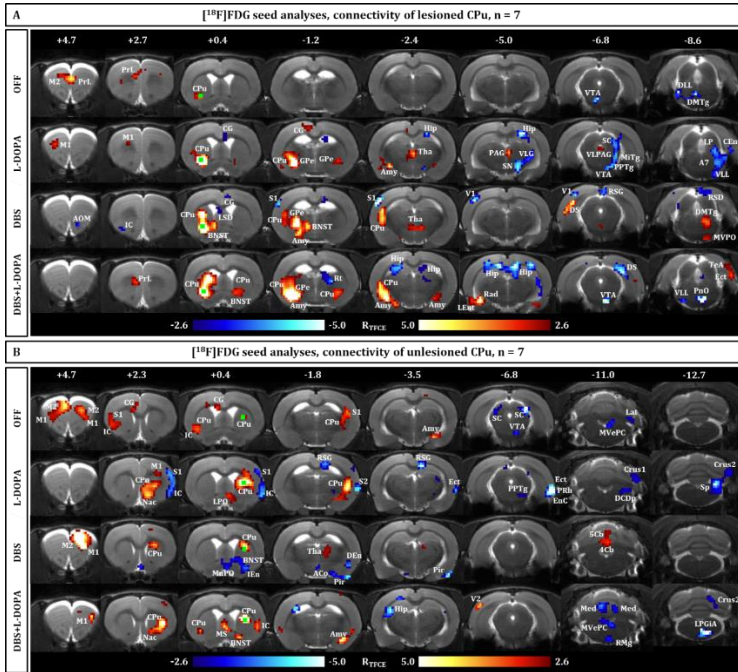


Fig. 18 Striatal (CPU) connectivity is affected differently by L-DOPA, STN DBS, and a combination of the two. *t*-maps showing significant correlation (*R*)-values of Pearson correlation analyses performed between each seed region (green squares) and all other voxels of the brain projected onto an MRI template, *n* = 7. Seeds were placed in the **A** ipsilesional ventral and **B** contralateral dorsal CPU. Red voxels indicate positive correlations, while blue voxels indicate negative correlations. Abbreviations: 3Cb/4Cb/5Cb/6Cb = 3rd/4th/5th/6th cerebellar lobule, A7 = A7 noradrenergic cells, AGo = anterior cortical amygdaloid nucleus, Amy = amygdala, AOM = medial anterior olfactory nucleus, CEnt = caudomedial entorhinal cortex, CG = cingulate cortex, CPu = caudate putamen, Crus1/2 = crus one/two of the ansiform lobule, DCDp = deep core of the dorsal cochlear nucleus, DEN = dorsal endopiriform cortex, DLL = dorsal nucleus of the lateral lemniscus, RSD = retrosplenial dysgranular cortex, DS = dorsal subiculum, Ect = entorhinal cortex, ENc = entorhinal cortex, FN = facial nucleus, GPe = globus pallidus externus, Hip = hippocampus, IC = insular cortex, INtp = posterior interposed cerebellar nucleus, IEN = intermediate endopiriform nucleus, Lat = lateral cerebellar nucleus, LEnt = lateral entorhinal cortex, LP = lateral parabrachial nucleus, LPGIA = lateral paragigantocellular nucleus alpha part, LPO = lateral preoptic area, LSD = dorsal lateral septal nucleus, M1/2 = primary/secondary motor cortex, Med = medial cerebellar nucleus, RSG = retrosplenial granular nucleus, MnPO = median preoptic nucleus, MS = medial septal nucleus, MvPeC = parvicellular medial vestibular nucleus, MVPO = medioventral periolivary nucleus, Nac = nucleus accumbens, PAG = periaqueductal grey, Pfl = paraflocculus, Pir = piriform cortex, PnO = oral pontine reticular nucleus, PPTg = pedunculopontine tegmental nucleus, PRh = perirhinal cortex, PrL = prelimbic cortex, Rad = radiatum layer, RMg = raphe magnus nucleus, RSD = retrosplenial dysgranular cortex, RSG = retrosplenial granular nucleus, Rt = reticular nucleus, S1/2 = primary/secondary somatosensory cortex, SC = superior colliculus, SN = substantia nigra, Sp = spinal trigeminal nucleus, SpVe = spinal vestibular nucleus, TeA = temporal association cortex, Tha = thalamus, V1/2 = primary/secondary visual cortex, VLg = ventral lateral geniculate nucleus, VLL = ventral nucleus of the lateral lemniscus, VLPAG = ventrolateral periaqueductal grey, VS = ventral subiculum, VTA = ventral tegmental area. PET images of animals implanted in the right hemisphere were flipped so that all stimulation sites are shown on the left. Colour bars of TFCCE maps are labelled with the original suprathreshold *t*-values. Numbers indicate rostrocaudal coordinates in mm distance to Bregma.

Acute stimulation of the STN shared some, but not all effects of L-DOPA on striatal connectivity (Fig. 18 A, third row). The positive correlation between [¹⁸F]FDG uptake of the seed and that of the surrounding striatal tissue was even more pronounced under STN DBS and also extended to more dorsal parts of the ipsilesional CPU. Similarly to L-DOPA, STN DBS also evoked positive correlations between tracer uptake of ipsilateral amygdala and bilateral thalamus and that of the seed, while that of the GPe only correlated positively in the ipsilateral hemisphere. Additional positive correlations occurred in ipsilateral BNST, dorsal subiculum, contralateral dorsomedial tegmental area, and medioventral periolivary nucleus. Different to the picture seen with L-DOPA, where negative correlations only occurred contralaterally, stimulation of the STN caused negative correlations in both hemispheres. Glucose metabolism of ipsilateral insular cortex, dorsal lateral septal nucleus, primary somatosensory and visual cortex, crus one of the ansiform cerebellar lobule, and third and sixth cerebellar lobule (latter three not shown), as well as contralateral medial anterior olfactory nucleus, cingulate cortex, and retrosplenial granular and dysgranular cortex correlated negatively with that of the seed. The combination of STN DBS and L-DOPA had the most prominent effects on network activity (Fig. 18 A, bottom row). [¹⁸F]FDG uptake of ipsilateral prelimbic cortex, GPe, posterior interposed cerebellar nucleus, lateral entorhinal cortex, and radiatum layer positively correlated with that of the ipsilesional seed. Positive correlations were also found between glucose consumption of the seed and that of large areas of the complete ipsilateral as well as ventral contralateral CPU and bilateral amygdala, while contralaterally, tracer uptake of BNST, temporal association cortex, and entorhinal cortex correlated positively with that of the seed. The combination of DBS and L-DOPA lead to negative correlations between glucose metabolism of the seed and that of ipsilateral ventral nucleus of the lateral lemniscus, contralateral reticular nucleus, VTA, dorsal subiculum, oral pontine reticular nucleus, parafoveus (not shown), and bilateral hippocampus and second cerebellar lobule (not shown).

Contralesional Striatum Seed

The second seed was placed in the contralesional, healthy dorsal CPU. In the OFF condition, its [¹⁸F]FDG uptake correlated positively with that of the contralateral CPU as well as slightly with that of striatal tissue directly surrounding the seed, comparable to the ipsilesional seed in the OFF condition (Fig. 18 B, top row). Other bilateral positive correlations could be observed for primary and secondary motor and primary somatosensory cortex. Tracer uptake of ipsilateral amygdala and contralateral cingulate cortex and insular cortex also positively correlated with that of the seed. Glucose metabolism of ipsilateral VTA, lateral cerebellar nucleus, parvocellular medial vestibular nucleus, and bilateral superior colliculus correlated negatively with that of the contralesional seed during OFF.

L-DOPA treatment had different effects on network activity of the contralesional striatal seed compared to its ipsilesional counterpart (Fig. 18 B, second row). All correlations found in this condition were ipsilateral to the seed. Positive correlations existed between [¹⁸F]FDG uptake of the seed and that of larger areas of surrounding striatal tissue, Nac, M1, and lateral preoptic area. Negative correlations were found between tracer uptake of the seed and that of ipsilateral primary and secondary somatosensory, insular, retrosplenial granular, entorhinal, entorhinal, and perirhinal cortex, PPTg, crus one and two of the ansiform cerebellar lobule, deep core of the dorsal cochlear nucleus, and spinal trigeminal nucleus.

During STN DBS, correlations with the seed could be seen in both hemispheres, *i.e.* either ipsilateral or bilateral (Fig. 18 B, third row). Glucose metabolism of ipsilateral primary and secondary motor cortex, striatal tissue surrounding the seed, and thalamus, as well as bilateral fourth and fifth cerebellar lobule correlated positively with that of the seed. Negative correlations could be observed between tracer uptake of the seed and that of ipsilateral BNST, intermediate endopiriform nucleus, anterior cortical amygdaloid nucleus, piriform and dorsal endopiriform cortex, and bilateral median preoptic nucleus.

Again, the most widespread network activity, including ipsi-, contra-, and bilateral brain areas, could be observed when L-DOPA injection and STN DBS were combined (Fig. 18 B, bottom row). Ipsilaterally, [¹⁸F]FDG uptake of M1, striatal tissue surrounding the seed, Nac, BNST, insular cortex, and amygdala correlated positively with that of the seed, contralaterally that of secondary visual and dorsal endopiriform cortex, and bilaterally that of medial septal nucleus. Negative correlations were present between glucose consumption of the seed and that of ipsilateral alpha part of the lateral paragigantocellular nucleus, crus two of the ansiform cerebellar lobule, contralateral hippocampus, parvocellular medial vestibular nucleus, central nucleus of inferior colliculus, and bilateral medial cerebellar nucleus, and raphe magnus nucleus.

D. Discussion

In the first two chapters of this work, a new, fully implantable stimulation system for rodents was established, and its applicability for DBS in hemiparkinsonian rats was tested. Thus, the effects of acute and chronic STN DBS on paw use, brain metabolic and network activity have been investigated. As a last step, this study ought to compare the effects seen with DBS to those evoked by acute doses of L-DOPA. To this end, in addition to STN DBS, animals received 5 mg/kg L-DOPA one hour before cylinder tests, and 25 mg/kg L-DOPA at the same time as [¹⁸F]FDG either alone, or in combination with DBS. Since the rats employed in this study were the same as in CHAPTER TWO, a significant unilateral reduction in striatal dopaminergic uptake was confirmed by [¹⁸F]FDOPA PET imaging as mentioned in III.i. The position of all electrode tips was also proven to be located in the STN as shown in III. and discussed in IV.

On the behavioural level, animals used both front paws to a similar extent during PRE cylinder tests. During OFF, they showed a strong reduction of CF and an increase of IF use, manifested by the significant deviation from using each paw in 50 % of all wall touches, as expected. Intraperitoneal injections of 5 mg/kg L-DOPA (in combination with the peripheral decarboxylase inhibitor benserazide) were able to restore CF use to an extent that even exceeded IF usage in that condition. Similar results were obtained by Lundblad *et al.* (2004) in mice unilaterally lesioned with 6-OHDA in the MFB that received 6 mg/kg L-DOPA (429). Additionally, they found that not only the dosing of L-DOPA affects its efficacy, but also the site of 6-OHDA lesion. While a daily dose of 2 mg/kg had no effect in hemiparkinsonian mice, 6 mg/kg improved cylinder test performance regardless of the site of lesion, but caused dyskinetic behaviours, including forelimb dyskinesia, only in MFB- but not in intrastrially lesioned mice (429). An earlier study by Winkler and colleagues (2002) confirms these findings. They found the 6-OHDA rat model with lesions in the MFB to be more vulnerable to abnormal involuntary movements than that with intrastriatal lesions (430). Animals of the present study were lesioned in the MFB and cylinder tests were conducted within the time window known for peak severity of abnormal involuntary movements, *i.e.* 60 to 90 min post injection (429,430). Hence, it cannot be excluded that rats exhibited a certain degree of L-DOPA-induced involuntary dyskinetic CF movement that lead to the higher percentage of CF compared to IF use. On the other hand, similar to PD patients, animal models of PD typically develop L-DOPA-induced dyskinesias under chronic treatment rather than after single doses (430–432). However, mice and rats can show a certain handedness (433,434), making it more likely that the preference for CF over IF after L-DOPA injections observed here is simply the result of paw preference. Especially as CF was already used slightly more often than IF during PRE tests.

Similar to the results in CHAPTER TWO, acute STN DBS did not improve CF use which again showed a significant deviation from being used half of the time to support body weight while rearing against the cylinder wall under STN stimulation. Possible reasons for this were extensively discussed in IV. Interestingly, a combination of L-DOPA and STN DBS lead to the best results concerning equal use of both front paws. While

the percentage of CF use was comparable to that in the L-DOPA only condition, the percentage of IF use was increased, so that paw use resembled PRE levels. The exact interactions between STN DBS and L-DOPA treatment are not fully understood to date. Nutt and colleagues (2001) found that DBS does neither affect peak response nor duration of response to L-DOPA but rather reduces motor fluctuations by diminishing off drug disability in PD patients (426). This is likely due to the amplification of the L-DOPA-induced increase of striatal DA levels, as STN DBS intensifies the responsiveness of striatal cells to L-DOPA (274,435). As animals of this study only received a single dose of L-DOPA leading up to the cylinder test, it is unlikely that they experienced motor fluctuations, which were improved by DBS. Hence, the equalisation of paw use has to have other reasons. In the unilaterally 6-OHDA lesioned rat, there is an ipsilesional decrease and contralesional increase of brain metabolism (154). Effective STN DBS is able to partly abolish this imbalance by augmenting brain activity in ipsilesional structures including the striatum, and decreasing it in contralesional ones leading to the increased use of CF at the cost of IF (137). Since the action of L-DOPA is pervasive and does not originate in one hemisphere as DBS does, it could counteract the DBS-induced contralesional metabolic reduction by activating striatal dopaminergic cells, thus leading to an additional activation of IF. However, STN DBS was, by itself, not effective in this study. It can therefore not be excluded that the positive effects seen under the combined treatment are, to a high degree, L-DOPA mediated. The additional small improvement of paw use could then be the result of an interplay between L-DOPA and atypical STN stimulation, which is probably not applicable for effective STN DBS. However, this theory needs to remain speculative until future imaging studies further broaden the understanding of the metabolic effects of STN DBS and L-DOPA in PD.

To better understand the differences of and the interaction between L-DOPA and STN DBS, animals were measured with [¹⁸F]FDG PET one hour after simultaneous administration of tracer and 25 mg/kg L-DOPA, under acute STN DBS, and with a combination of the two treatments. Imaging studies in PD patients have detected the PDRP, a specific metabolic pattern that is characterised by activity increases in GPI, thalamus, pons, cerebellum, and sensorimotor cortex, and decreases in posterior parietal, supplementary, and premotor cortices (156,436,437). Treatment with L-DOPA attenuates this pattern by normalising metabolic activity of these brain areas (133,427,438). The unilateral 6-OHDA hemiparkinsonian rat has been shown to exhibit a metabolic imbalance manifested by contralesional hypermetabolism, especially in the CPU, and ipsilesional hypometabolism (131,137). This imbalance could be seen as the rat equivalent of the human PDRP. While many animal imaging studies investigate dopaminergic integrity, DA receptor occupation or function in models of PD (421,439,440), only very few studies engaged in brain glucose metabolism under different treatments so far. Studies looking at the dissociation of metabolic and hemodynamic responses to L-DOPA (also seen in PD patients) in 6-OHDA lesioned rats found that L-DOPA therapy causes further metabolic reductions in the ipsilesional basal ganglia in 6-OHDA lesioned rats (441), and increases in glucose metabolism of ipsilesional basal ganglia output nuclei, *i.e.* entopeduncular nucleus and SNr, respectively (442). A human study investigating the network modulatory effects of L-DOPA and STN DBS independently found that both treatments lead to metabolic reductions in putamen/globus pallidus, sensorimotor cortex and cerebellum (134). These findings could partly be replicated in this study, as profound reductions of [¹⁸F]FDG uptake were seen especially in ipsilateral CPU and sensorimotor cortex. Nevertheless, these results are also in contrast to the fact that the PDRP is weakened in PD patients after L-DOPA administration, whereas the metabolic imbalance induced by unilateral 6-OHDA lesion in hemiparkinsonian rats seems to be further strengthened by L-DOPA. The additional significant increase of glucose consumption in contralesional (motor and somatosensory) cortical and thalamic areas found in this study underline this assumption. The unilateral nature of the 6-OHDA animal model of PD could be responsible for the difference in metabolic response to L-DOPA. The omnipresent effect of the drug could have lowered metabolism not only in the contralesional

striatum, as expected, but also in the already inactive ipsilesional one. Additionally, activity in the already overactive contralateral hemisphere was further enhanced as seen in the significant increase in contralesional cortical and thalamic activity. The vast bilateral activation of cerebellar, midbrain, and pontine structures could be a compensatory mechanism ultimately leading to the normalisation of CF use. In favour of this hypothesis is the fact that fMRI studies investigating the effects of L-DOPA on blood oxygenation level-dependent signal changes in early-stage (hemiparkinsonian) patients have also produced confounding results concerning the activation or deactivation of M1 OFF and ON L-DOPA (438,443). Here, the difference in motor task employed and the duration of L-DOPA therapy (naïve vs. chronically treated) are additional potential causes for conflicting results. Hence, there is a great need for imaging studies elucidating the exact way in which L-DOPA influences the basal ganglia-thalamo-cortical network during rest and motor tasks.

As mentioned in CHAPTER TWO, unfortunately acute STN DBS had no therapeutic effect on motor behaviour in this cohort of rats. The possible reasons are discussed extensively in IV. Accordingly, the metabolic picture seen with [¹⁸F]FDG PET did not show the expected ipsilesional increases and contralesional decreases of tracer uptake. Instead, similar to the effects seen with L-DOPA, contralesional cortical areas showed increases in glucose metabolism. Only chronic stimulation was able to counteract the metabolic imbalance by activating more ipsilesional and deactivating contralesional brain areas (see III.iii). Similarly, in this study the combination of L-DOPA and acute STN DBS, despite being sub-therapeutic, seemed to have an additional beneficial effect as this treatment led to the best behavioural result. Compared to the L-DOPA only condition, the combined treatment resulted in less activation of contralesional cortical and thalamic areas, and additional decreases in ipsilesional motor cortex, while ipsilesional CPU and contralesional cerebellar structures showed slightly more activity. These findings agree with the combined results of Müller *et al.* (2018) and Berding and colleagues (2001). While the former found STN DBS to cause increased connectivity between bilateral motor cortices, thalamus, and cerebellum compared to L-DOPA treatment, the latter showed further reductions of glucose consumption in orbitofrontal cortex and thalamus after L-DOPA administration (133,265). Hence, STN DBS and L-DOPA in combination have an effect on networks that exceeds the simple combination of both treatments alone, probably also comprising entirely additive effects. In this case, L-DOPA might have also compensated for or improved the (partly) insufficient DBS. The sole reversion of pathological metabolic imbalances does therefore not seem to be sufficient to improve motor deficits. It is more likely that a complex recruitment of alternative networks depending on treatment strategy compensates pathology (444).

For a better understanding of the differences in brain networks elicited by the two treatments, seed-based metabolic analyses were conducted with two seeds, one in the ipsi- and one in the contralesional CPU, for baseline and all three treatment conditions. In the healthy animal, basal ganglia, including striatum and Nac, of both hemispheres show a strong connectivity which is potentially mediated by cortical interhemispheric projections (138). During OFF, tracer uptake of the seed in the ventral ipsilesional CPU only slightly correlated positively with that of ipsilateral secondary motor and prelimbic cortex, while showing no connections to the contralateral CPU. This agrees with previous findings showing a reduction of the striatal interhemispheric connections after 6-OHDA lesions (138). These network impairments are likely due to a pathological modification of the firing rates of (motor) cortical pyramidal tract neurons projecting to the striatum, caused by dopaminergic loss (445,446).

A similar picture was found for the seed in the dorsal contralesional, healthy CPU, although additional positive correlations were present for contralateral CPU, cingulate cortex, ipsilateral amygdala, and bilateral motor cortices, all belonging to the above mentioned basal ganglia-cortical functional network. Since the contralesional striatum does not suffer the direct physiological consequences of dopaminergic loss (447,448), its connectivity is less affected by the unilateral 6-OHDA lesion compared to the lesioned hemisphere. This

could explain the more intact connections seen between the seed in the contralesional striatum and bilateral motor cortices. The impairment of the striato-cortical motor network in the hemiparkinsonian rat agrees with a study by Hacker and team (2012) who also showed altered striatal correlations in PD patients (381). Injections of 25 mg/kg L-DOPA slightly expanded the basal ganglia network involving the ipsilesional seed. In addition to connections to the ipsilateral motor cortex, it showed stronger positive intrahemispheric striatal correlations as well as correlations to the cingulate cortex, amygdala, thalamus, bilateral GPe and contralateral dorsal hippocampus. This improvement of the cortico-striato-thalamo-cortical motor network elicited by L-DOPA agrees with other studies that also found an L-DOPA-induced enhancement of the functional connectivity of motor networks in PD patients (449,450). The hippocampus is involved in spatial navigation and, therefore, in motor behaviour. Here, the contralateral hippocampus showed negative correlations to the ipsilesional striatal seed. It is known that the hippocampus connects to the striatum via the orbitofrontal cortex (375). However, the orbitofrontal cortex was not part of the network seen under L-DOPA treatment in this study. Alternatively, the hippocampus could be involved through its connections to the ipsilateral thalamus (374). The positive correlations between ipsilesional seed and contralateral thalamus favour this theory. Negative correlations were found between ipsilesional seed and contralateral SN as previously shown under STN DBS (138). Thus, the communication between ipsilesional striatum and contralesional SN, which could be mediated via the thalamus (365,451), seems to be a stable effect of parkinsonian therapy as it occurred with DBS as well as L-DOPA. Further negative correlations existed between ipsilesional seed and contralesional pontine and medullary nuclei including the PPTg and the VTA. The PPTg is part of the mesencephalic locomotor region and known to send ascending fibres to thalamus, SN, and globus pallidus while receiving input from striatum and SN (452,453). The VTA is involved in reward-related behaviour and connects to striatum, thalamus, amygdala, and entorhinal cortex (454,455). As both structures play a role in locomotion and behaviour, and the VTA contains dopaminergic neurons (456–458), they could have been additionally recruited/activated by the L-DOPA-induced increase of extracellular dopamine in striatum, SN, or hippocampus (423).

The contralesional striatal seed showed a similar expansion of connectivity under L-DOPA, especially to ipsilateral CPu and Nac. Interestingly, glucose metabolism of the ipsilateral lateral preoptic area of the hypothalamus also positively correlated with that of the contralesional seed. The lateral preoptic area plays a role in locomotion and is connected to the PPTg of the mesencephalic locomotor region as well as to the VTA (459–461). Since the ipsilateral PPTg, but not the VTA, is part of the functional network around the contralesional striatal seed activated by L-DOPA, it is possible that a further connection between PPTg and lateral preoptic area has been recruited to improve motor functioning. Another aspect distinguishing the connections of the contralesional striatal seed from its ipsilesional counterpart is a distinct negative correlation between glucose consumption of the seed and that of ipsilateral somatosensory, insular, entorhinal, and perirhinal cortices, as well as spinal trigeminal nucleus. The somatosensory cortex is connected to motor cortex, striatum, perirhinal cortex, spinal trigeminal nuclei and insular cortex (462), while the latter also receives input from rhinal cortices (463,464). Hence, they could all be part of the network aiding in normal motor functioning. This suggests that L-DOPA does not reinstate the interhemispheric functional basal ganglia network, but rather seems to improve motor symptoms by recruiting additional auxiliary structures that are inactive in the untreated (hemi)parkinsonian motor networks and differ between lesioned and unaffected hemisphere.

Since STN DBS was not effective on the behavioural level in this study, caution needs to be exercised when interpreting the connectivity analysis data. As is known from other animal studies, DBS (in STN and thalamus) is able to increase striatal interhemispheric connectivity in rats (138,465). More specifically, STN DBS in

hemiparkinsonian rats strengthens an interhemispheric functional unit involving M1, orbitofrontal cortex, bilateral striatum, and SN (138). Only very recently, human studies also started to increasingly look at DBS-induced changes in functional connectivity (466,467). One study found that STN DBS modulates two distinct neuronal circuits in PD. It activates a circuit including GPi, thalamus, and deep cerebellar nuclei resulting in motor improvements, and deactivates one comprising M1, putamen, and cerebellum leading to reduced bradykinesia (468). In this study, STN DBS only strengthened intrahemispheric basal ganglia connectivity for both seeds. The ipsilesional striatal seed showed additional correlations to amygdala, BNST, thalamus, somatosensory and visual cortices, dorsal subiculum, retrosplenial cortex, and brainstem nuclei. The contralesional seed showed connections to motor cortex, BNST, hypothalamus, piriform cortex, and cerebellum. Therefore, although some of the network elements found to be involved in motor improvement under effective STN DBS, *i.e.* motor cortex, thalamus, CPu, and cerebellum, were activated in this study, the pathological network impairments still prevailed, preventing a positive behavioural effect of the stimulation. Possible reasons, as previously discussed, could be imprecise stimulation sites, suboptimal stimulation parameters, excessive dopaminergic lesions, or even faulty stimulation systems.

The combined therapy with STN DBS and L-DOPA lead to activation of the most complex network. It was the only condition in which [¹⁸F]FDG uptake of the ipsilesional seed correlated not only profoundly with that of ipsilateral basal ganglia, but also with that of contralesional CPu, potentially mediated through the prefrontal cortex that sends bilateral projections to the striatum (469). Therefore, the interhemispheric basal ganglia functional network was partly re-established, making it clear that the interaction of L-DOPA and STN DBS leads to more complex effects than just the sum of effects of both treatments alone. Glucose consumption of the dorsal hippocampus correlated negatively with that of the seed. While the dorsal hippocampus has been shown to be part of the network in healthy animals, opposite to the present findings, the correlation was positive in the previous study (138). Since front paw use of animals treated with both, L-DOPA and STN DBS, simultaneously closely resembled that of the pre-lesion condition, it is likely that the hippocampus plays a role in the improvement of motor behaviour. The exact nature of this role, however, still needs to be determined. Tracer uptake of VTA and amygdala also correlated negatively and positively, respectively, with that of the ipsilesional seed. Both structures are connected with each other as well as to the striatum (454,470). The involvement of the VTA could be L-DOPA mediated as it showed connections to the seed during L-DOPA but not DBS treatment. Connections to the ipsilateral amygdala were present during both treatments, making it a stable part of the network. However, the simultaneous treatment also engaged the contralateral amygdala. Together with the behavioural data, this suggests that the bilateral involvement of the amygdala may add to the positive outcome and confirms once again that the interplay of L-DOPA and STN DBS provokes effects exceeding those of each treatment on their own. Similarly, Mondillon and colleagues (2012) showed that the combined effect of STN DBS and L-DOPA therapy on emotion recognition in PD patients was greater than that of both treatments alone. They concluded that both therapies have common, complementary, and opposing effects on the activity of certain brain areas (471).

Interestingly, the combined treatment of L-DOPA and STN DBS was the only treatment condition, apart from the OFF state when looking at the contralesional seed, that evoked a bilateral striatal connection, albeit weak. STN DBS alone has been shown to increase the interhemispheric striatal network strength (138), and also L-DOPA is known to normalise pathological networks (427,438). Nevertheless, in this study neither treatment alone could restore the interhemispheric striatal functional connectivity as seen in healthy rats. Grafton *et al.* (2006) found unilateral subtherapeutic (ineffective) STN DBS to influence brain activation patterns differently compared to therapeutic DBS that normalised the pathological changes (472). Since in this study, STN DBS was not effective on the behavioural level, it does not surprise that its brain metabolic effects were different

from what was expected with effective stimulation. L-DOPA treatment alone caused several additional negative mesencephalic, pontine, and cerebellar correlations with both seeds. Gopinath and colleagues (2015) suggest negative correlations to represent regulatory mechanisms including reciprocal modulations, suppression, inhibition, and neurofeedback (473). Another study suggests the abnormal connectivity in brain regions like M1 or cerebellum to be compensatory (450). Hence, instead of simply reversing the pathological (striatal) network changes, L-DOPA could have additionally recruited compensatory brain structures like M1, and mesencephalic, pontine, and cerebellar structures to improve motor performance. Regarding the contralesional seed, the simultaneous treatment could now have combined these compensatory mechanisms, visible in positive correlations to M1 and negative correlations to pons and cerebellum, and interacted with STN DBS in a way that re-established an interhemispheric striatal connection, therefore leading to the best behavioural result.

Although the identification of the exact mechanisms, differences, and interactions of L-DOPA and STN DBS was beyond the scope of this study, it became clear that both therapeutic approaches have specific, partly overlapping, effects on brain metabolic activity, functional connectivity, and consequently on behaviour. Most importantly, the combination of both therapies seems to exceed the mere sum of the effects of each treatment alone and cause its own complex brain activity pattern. While the specific metabolic and connectivity profile of L-DOPA as well as DBS need to be further characterised in the future, one should also continue to look into the interactions between the two. The vast majority of PD patients eligible for STN DBS is on dopaminergic medication (331) and continues to be so after DBS surgeries, even though doses can initially be reduced in many cases (291). Hence, to improve the interplay of both therapies and therefore the outcome for the patient, more clarity is needed about how the different treatments affect each other and the effects on pathological features.

Conclusion

The present work successfully introduced a new, fully implantable stimulation system suitable for acute and chronic DBS in freely moving and behaving rats, and tested its application range. To this end, animals were unilaterally lesioned with 6-OHDA in the MFB to generate a hemiparkinsonian state including behavioural impairments and pathological brain metabolic and network changes. The cylinder test was used to reveal lesion-induced motor deficits in front paw use, while [^{18}F]FDOPA and [^{18}F]FDG PET were applied to illustrate dopaminergic integrity, changes in brain glucose consumption, and altered functional connectivity. Animals were tested in the naïve state, the postoperative OFF condition, and four different ON conditions, depending on the treatment group, *i.e.* acute DBS, chronic DBS, L-DOPA, and L-DOPA in addition to acute DBS. The stimulation system was well tolerated by the animals and allowed for the collection of acute and chronic stimulation data. 6-OHDA lesions in the MFB led to a significantly decreased [^{18}F]FDOPA uptake in the ipsilesional striatum, the reduced use of the contralesional front paw, and an imbalance of brain metabolism. Therapeutic acute stimulation of the STN caused improvements in front paw use, increased tracer uptake in ipsilesional brain areas, and decreased it contralesionally. Chronic STN DBS strengthened these effects. L-DOPA also restored front paw use while evoking a different metabolic pattern compared to DBS. The simultaneous treatment with both therapeutic strategies led to the best behavioural result and a metabolic pattern including features of both treatments alone as well as some distinct characteristics. Similarly, acute DBS, L-DOPA and the combination of both each had distinct effects on cortico-striato-thalamo-cerebellar networks, including the reversion of pathological changes as well as compensatory mechanisms.

DBS, like dopaminergic therapy, is a chronic treatment applied for years to decades. Accordingly, many clinical studies investigate the long-term effects, problems, and changes in efficacy of these therapies over years (261,345,411,474,475). However, while animal models of PD keep getting more realistic in mimicking distinct pathological features of the disease (17), the simulation of treatments, and DBS in particular, still lack behind in modelling the clinical (chronic) use. To date, most preclinical studies look at stimulation times of minutes to days and stimulation systems can be restricting (270,272,275,280,305–307). Different imaging techniques like fMRI or PET imaging offer valuable possibilities to better understand the complex mechanisms responsible for the disease as well as the effectiveness of treatments. Hence, they have been extensively used to study pathological brain activity patterns and networks in PD (132,153,156,450,476), and the specific effects of STN DBS or L-DOPA on these pathologies (135,136,443,477,478). Here, the modulation of brain networks and functional connectivity is an important aspect that is only recently increasingly focused on (134,479). For example, it has been shown that the pathological network changes in PD differ depending on the dominant symptoms, like freezing of gait or L-DOPA-induced dyskinesia, or the type of PD (476,478). Another group found that specific resting state functional connectivity patterns were associated with the degree of responsiveness to, and therefore effectiveness of L-DOPA in PD patients (480). Similar results might also be obtained for DBS in the near future, making characteristic functional connectivity patterns a potential prerequisite for patient selection and the success of DBS outcome. Hence, studies investigating the pathological mechanisms and exclusive actions of single therapies are still required for a better understanding of the disease and further development of therapeutic approaches. However, while STN DBS allows for the reduction of dopaminergic drugs (215,291), the two therapies are usually applied simultaneously to get the best possible outcome for the patient. Imaging studies looking at the combined effects of DBS and L-DOPA, especially on a brain metabolic or network level, are scarce (426,471). Hence, prospective studies should also investigate the simultaneous impact of DBS and dopaminergic treatments on the parkinsonian brain to best

mimic and understand the situation in the patient. Thereby, reliable and transferable animal models will continue to play a crucial role.

In this study, [^{18}F]FDOPA and [^{18}F]FDG PET were used to illustrate pathological cerebral changes as well as therapeutic effects and interactions in freely moving hemiparkinsonian animals receiving L-DOPA and DBS treatment. These effects could then be interpreted in relation to motor performance. The stimulation system used avoids previous compromises like short stimulation times and restriction of the animals by being fully implantable and rechargeable for continuous use up to several weeks. This is a first step towards more realistic preclinical simulation of the situation in PD patients. Nevertheless, for the long-term use, great caution should be exercised as failures in system integrity and functionality, imprecise electrode placement, and post-surgical infections can compromise results (334,339). In conclusion, the introduced stimulation system, in combination with imaging techniques, is a suitable tool yielding great potential to add to the knowledge concerning PD symptoms, different therapies, and the underlying brain metabolic and network mechanisms.

References

1. Lang AE, Lozano AM. Parkinson's disease. First of two parts. *N Engl J Med*. 1998 Oct 8;339(15):1044–53.
2. WHO. WHO | Neurological Disorders: Public Health Challenges [Internet]. WHO. World Health Organization; [cited 2020 Nov 10]. Available from: https://www.who.int/mental_health/neurology/neurodiso/en/
3. de Lau LM, Breteler MM. Epidemiology of Parkinson's disease. *Lancet Neurol*. 2006 Jun 1;5(6):525–35.
4. Bennett DA, Beckett LA, Murray AM, Shannon KM, Goetz CG, Pilgrim DM, et al. Prevalence of parkinsonian signs and associated mortality in a community population of older people [Internet]. Vol. 334, *The New England journal of medicine*. *N Engl J Med*; 1996 [cited 2020 Nov 18]. Available from: <https://pubmed.ncbi.nlm.nih.gov/8531961/>
5. Pringsheim T, Jette N, Frolkis A, Steeves TDL. The prevalence of Parkinson's disease: A systematic review and meta-analysis. *Mov Disord*. 2014 Nov;29(13):1583–90.
6. Van Den Eeden SK, Tanner CM, Bernstein AL, Fross RD, Leimpeter A, Bloch DA, et al. Incidence of Parkinson's Disease: Variation by Age, Gender, and Race/Ethnicity. *Am J Epidemiol*. 2003 Jun 1;157(11):1015–22.
7. Singleton AB, Farrer M, Johnson J, Singleton A, Hague S, Kachergus J, et al. α -Synuclein locus triplication causes Parkinson's disease. *Science*. 2003 Oct 31;302(5646):841–841.
8. Gibb WR, Lees AJ. The relevance of the Lewy body to the pathogenesis of idiopathic Parkinson's disease. *J Neurol Neurosurg Psychiatry*. 1988 Jan 6;51(6):745–52.
9. Toulorge D, Schapira AHV, Hajj R. Molecular changes in the postmortem parkinsonian brain. *J Neurochem*. 2016 Jul 5;
10. Valente EM, Abou-Sleiman PM, Caputo V, Muqit MMK, Harvey K, Gispert S, et al. Hereditary early-onset Parkinson's disease caused by mutations in pink1. *Science*. 2004 May 21;304(5674):1158–60.
11. Betarbet R, Sherer TB, MacKenzie G, Garcia-Osuna M, Panov AV, Greenamyre JT. Chronic systemic pesticide exposure reproduces features of Parkinson's disease. *Nat Neurosci*. 2000 Dec;3(12):1301–6.
12. Langston WJ, Ballard P, Tetrud JW, Irwin I. Chronic Parkinsonism in Humans Due to a Product of Meperidine-Analog Synthesis [Internet]. [cited 2021 Sep 6]. Available from: <https://www.science.org/doi/epdf/10.1126/science.6823561>
13. Davis GC, Williams AC, Markey SP, Ebert MH, Caine ED, Reichert CM, et al. Chronic parkinsonism secondary to intravenous injection of meperidine analogues. *Psychiatry Res*. 1979 Dec 1;1(3):249–54.
14. Emborg ME. Nonhuman primate models of Parkinson's disease. *ILAR J*. 2007 Jan 1;48(4):339–55.
15. Bellou V, Belbasis L, Tzoulaki I, Evangelou E, Ioannidis JPA. Environmental risk factors and Parkinson's disease: An umbrella review of meta-analyses [Internet]. Vol. 23, *Parkinsonism & related disorders*. *Parkinsonism Relat Disord*; 2016 [cited 2020 Nov 18]. Available from: <https://pubmed.ncbi.nlm.nih.gov/26739246/>
16. Chade AR, Kastan M, Tanner CM. Nongenetic causes of Parkinson's disease. In: Riederer P, Reichmann H, Youdim MBH, Gerlach M, editors. *Parkinson's Disease and Related Disorders*. Vienna: Springer; 2006. p. 147–51. (Journal of Neural Transmission. Supplementa).
17. Konnova EA, Swanberg M. Animal Models of Parkinson's Disease. In: Stoker TB, Greenland JC, editors. *Parkinson's Disease: Pathogenesis and Clinical Aspects* [Internet]. Brisbane (AU): Codon Publications; 2018 [cited 2021 Sep 13]. Available from: <http://www.ncbi.nlm.nih.gov/books/NBK536725/>
18. Krüger R. Genes in familial parkinsonism and their role in sporadic Parkinson's disease. *J Neurol*. 2004 Sep 1;251(6):vi2–6.

19. Dawson TM, Dawson VL. The role of parkin in familial and sporadic Parkinson's disease: The Role of Parkin in Familial and Sporadic PD. *Mov Disord*. 2010;25(S1):S32–9.
20. Puschmann A. New Genes Causing Hereditary Parkinson's Disease or Parkinsonism [Internet]. Vol. 17, *Current neurology and neuroscience reports*. Curr Neurol Neurosci Rep; 2017 [cited 2020 Nov 18]. Available from: <https://pubmed.ncbi.nlm.nih.gov/28733970/>
21. Park JS, Davis RL, Sue CM. Mitochondrial Dysfunction in Parkinson's Disease: New Mechanistic Insights and Therapeutic Perspectives. *Curr Neurol Neurosci Rep*. 2018 May;18(5):21.
22. Polito L, Greco A, Seripa D. Genetic Profile, Environmental Exposure, and Their Interaction in Parkinson's Disease. *Park Dis*. 2016 Jan 31;2016:e6465793.
23. Michel PP, Hirsch EC, Hunot S. Understanding Dopaminergic Cell Death Pathways in Parkinson Disease. *Neuron*. 2016 May 18;90(4):675–91.
24. Burré J, Sharma M, Tsetsenis T, Buchman V, Etherton MR, Südhof TC. α -Synuclein Promotes SNARE-Complex Assembly in Vivo and in Vitro. *Science* [Internet]. 2010 Sep 24 [cited 2021 Sep 6]; Available from: <https://www.science.org/doi/abs/10.1126/science.1195227>
25. Polymeropoulos MH, Lavedan C, Leroy E, Ide SE, Dehejia A, Dutra A, et al. Mutation in the α -Synuclein Gene Identified in Families with Parkinson's Disease. *Science* [Internet]. 1997 Jun 27 [cited 2021 Sep 6]; Available from: <https://www.science.org/doi/abs/10.1126/science.276.5321.2045>
26. Chartier-Harlin MC, Kachergus J, Roumier C, Mouroux V, Douay X, Lincoln S, et al. α -synuclein locus duplication as a cause of familial Parkinson's disease. *The Lancet*. 2004 Sep 25;364(9440):1167–9.
27. Lashuel HA, Overk CR, Oueslati A, Masliah E. The many faces of α -synuclein: from structure and toxicity to therapeutic target. *Nat Rev Neurosci*. 2013 Jan;14(1):38–48.
28. Spillantini MG, Schmidt ML, Lee VMY, Trojanowski JQ, Jakes R, Goedert M. α -Synuclein in Lewy bodies. *Nature*. 1997 Aug;388(6645):839–40.
29. Baba M, Nakajo S, Tu PH, Tomita T, Nakaya K, Lee VM, et al. Aggregation of alpha-synuclein in Lewy bodies of sporadic Parkinson's disease and dementia with Lewy bodies. *Am J Pathol*. 1998 Apr;152(4):879–84.
30. Wakabayashi K, Tanji K, Odagiri S, Miki Y, Mori F, Takahashi H. The Lewy Body in Parkinson's Disease and Related Neurodegenerative Disorders. *Mol Neurobiol*. 2013 Apr 1;47(2):495–508.
31. Pollanen MS, Dickson DW, Bergeron C. Pathology and Biology of the Lewy Body. *J Neuropathol Exp Neurol*. 1993 May 1;52(3):183–91.
32. Olanow CW, Perl DP, DeMartino GN, McNaught KSP. Lewy-body formation is an aggresome-related process: a hypothesis. *Lancet Neurol*. 2004 Aug 1;3(8):496–503.
33. Dickson DW, Fujishiro H, DelleDonne A, Menke J, Ahmed Z, Klos KJ, et al. Evidence that incidental Lewy body disease is pre-symptomatic Parkinson's disease. *Acta Neuropathol (Berl)*. 2008 Apr 1;115(4):437–44.
34. Tanaka M, Kim YM, Lee G, Junn E, Iwatsubo T, Mouradian MM. Aggresomes Formed by α -Synuclein and Synphilin-1 Are Cytoprotective*. *J Biol Chem*. 2004 Feb 6;279(6):4625–31.
35. Chen L, Feany MB. α -Synuclein phosphorylation controls neurotoxicity and inclusion formation in a Drosophila model of Parkinson disease. *Nat Neurosci*. 2005 May;8(5):657–63.
36. Ding TT, Lee SJ, Rochet JC, Lansbury PT. Annular α -Synuclein Protofibrils Are Produced When Spherical Protofibrils Are Incubated in Solution or Bound to Brain-Derived Membranes. *Biochemistry*. 2002 Aug 1;41(32):10209–17.
37. Lashuel HA, Petre BM, Wall J, Simon M, Nowak RJ, Walz T, et al. α -Synuclein, Especially the Parkinson's Disease-associated Mutants, Forms Pore-like Annular and Tubular Protofibrils. *J Mol Biol*. 2002 Oct 4;322(5):1089–102.
38. Fedorow H, Tribi F, Halliday G, Gerlach M, Riederer P, Double KL. Neuromelanin in human dopamine neurons: Comparison with peripheral melanins and relevance to Parkinson's disease. *Prog Neurobiol*. 2005 Feb 1;75(2):109–24.

39. Mann DMA, Yates PO. Possible role of neuromelanin in the pathogenesis of Parkinson's disease. *Mech Ageing Dev.* 1983 Feb 1;21(2):193–203.
40. Vila M. Neuromelanin, aging, and neuronal vulnerability in Parkinson's disease. *Mov Disord.* 2019;34(10):1440–51.
41. Isaias IU, Trujillo P, Summers P, Marotta G, Mainardi L, Pezzoli G, et al. Neuromelanin Imaging and Dopaminergic Loss in Parkinson's Disease. *Front Aging Neurosci* [Internet]. 2016 [cited 2022 Feb 21];8. Available from: <https://www.frontiersin.org/article/10.3389/fnagi.2016.00196>
42. Zucca FA, Segura-Aguilar J, Ferrari E, Muñoz P, Paris I, Sulzer D, et al. Interactions of iron, dopamine and neuromelanin pathways in brain aging and Parkinson's disease. *Prog Neurobiol.* 2017 Aug 1;155:96–119.
43. Halliday GM, Ophof A, Broe M, Jensen PH, Kettle E, Fedorow H, et al. Alpha-synuclein redistributes to neuromelanin lipid in the substantia nigra early in Parkinson's disease. *Brain J Neurol.* 2005 Nov;128(Pt 11):2654–64.
44. Albin RL, Young AB, Penney JB. The functional anatomy of basal ganglia disorders. *Trends Neurosci.* 1989 Jan 1;12(10):366–75.
45. Surmeier DJ, Ding J, Day M, Wang Z, Shen W. D1 and D2 dopamine-receptor modulation of striatal glutamatergic signaling in striatal medium spiny neurons. *Trends Neurosci.* 2007 May 1;30(5):228–35.
46. Lang AE, Lozano AM. Parkinson's disease. Second of two parts. *N Engl J Med.* 1998 Oct 15;339(16):1130–43.
47. Vallone D, Picetti R, Borrelli E. Structure and function of dopamine receptors. *Neurosci Biobehav Rev.* 2000 Jan 1;24(1):125–69.
48. Gingrich JA, Caron MG. Recent Advances in the Molecular Biology of Dopamine Receptors. *Annu Rev Neurosci.* 1993 Mar 1;16(1):299–321.
49. Tritsch NX, Sabatini BL. Dopaminergic Modulation of Synaptic Transmission in Cortex and Striatum. *Neuron.* 2012 Oct 4;76(1):33–50.
50. Yao WD, Speelman RD, Zhang J. Dopaminergic Signaling in Dendritic Spines. *Biochem Pharmacol.* 2008 Jun 1;75(11):2055–69.
51. Perreault M, Hasbi A, O'Dowd B, George S. The Dopamine D1–D2 Receptor Heteromer in Striatal Medium Spiny Neurons: Evidence for a Third Distinct Neuronal Pathway in Basal Ganglia. *Front Neuroanat* [Internet]. 2011 [cited 2022 Feb 18];5. Available from: <https://www.frontiersin.org/article/10.3389/fnana.2011.00031>
52. Monakow KH, Akert K, Künzle H. Projections of the precentral motor cortex and other cortical areas of the frontal lobe to the subthalamic nucleus in the monkey. *Exp Brain Res.* 1978 Nov 15;33(3–4):395–403.
53. Nambu A, Tokuno H, Hamada I, Kita H, Imanishi M, Akazawa T, et al. Excitatory Cortical Inputs to Pallidal Neurons Via the Subthalamic Nucleus in the Monkey. *J Neurophysiol.* 2000 Jul 1;84(1):289–300.
54. Petersen MV, Lund TE, Sunde N, Frandsen J, Rosendal F, Juul N, et al. Probabilistic versus deterministic tractography for delineation of the cortico-subthalamic hyperdirect pathway in patients with Parkinson disease selected for deep brain stimulation. *J Neurosurg.* 2017 May 1;126(5):1657–68.
55. Chen W, de Hemptinne C, Miller AM, Leibbrand M, Little SJ, Lim DA, et al. Prefrontal-Subthalamic Hyperdirect Pathway Modulates Movement Inhibition in Humans. *Neuron.* 2020 May 20;106(4):579–588.e3.
56. Temiz G, Sébille SB, Francois C, Bardinet E, Karachi C. The anatomo-functional organization of the hyperdirect cortical pathway to the subthalamic area using in vivo structural connectivity imaging in humans. *Brain Struct Funct.* 2020 Mar 1;225(2):551–65.
57. Nambu A. A new approach to understand the pathophysiology of Parkinson's disease. *J Neurol.* 2005 Oct 1;252(4):iv1–4.

58. Hikosaka O, Takikawa Y, Kawagoe R. Role of the Basal Ganglia in the Control of Purposive Saccadic Eye Movements. *Physiol Rev.* 2000 Jul;80(3):953–78.
59. Deniau JM, Chevalier G. Disinhibition as a basic process in the expression of striatal functions. II. The striato-nigral influence on thalamocortical cells of the ventromedial thalamic nucleus. *Brain Res.* 1985 May 20;334(2):227–33.
60. Chu HY, McIver EL, Kovaleski RF, Atherton JF, Bevan MD. Loss of Hyperdirect Pathway Cortico-Subthalamic Inputs Following Degeneration of Midbrain Dopamine Neurons. *Neuron.* 2017 Sep 13;95(6):1306–1318.e5.
61. Oswal A, Yeh CH, Neumann WJ, Gratwicke J, Akram H, Horn A, et al. Neural signatures of pathological hyperdirect pathway activity in Parkinson's disease [Internet]. *Neuroscience*; 2020 Jun [cited 2021 Sep 24]. Available from: <http://biorxiv.org/lookup/doi/10.1101/2020.06.11.146886>
62. Blandini F, Nappi G, Tassorelli C, Martignoni E. Functional changes of the basal ganglia circuitry in Parkinson's disease. *Prog Neurobiol.* 2000 Sep 1;62(1):63–88.
63. Wichmann T, DeLong MR. Pathophysiology of Parkinson's Disease: The MPTP Primate Model of the Human Disorder. *Ann N Y Acad Sci.* 2003;991(1):199–213.
64. Calabresi P, Picconi B, Tozzi A, Ghiglieri V, Di Filippo M. Direct and indirect pathways of basal ganglia: a critical reappraisal. *Nat Neurosci.* 2014 Aug;17(8):1022–30.
65. Zhai S, Shen W, Graves SM, Surmeier DJ. Dopaminergic modulation of striatal function and Parkinson's disease. *J Neural Transm.* 2019 Apr 1;126(4):411–22.
66. Jankovic J. Parkinson's disease: clinical features and diagnosis. *J Neurol Neurosurg Psychiatry.* 2008 Jan 4;79(4):368–76.
67. Sveinbjornsdottir S. The clinical symptoms of Parkinson's disease. *J Neurochem.* 2016 Jul 1;n/a-n/a.
68. Don C. Parkinson's disease. Diagnosis and treatment. *West J Med.* 1996 Oct;165(4):234–40.
69. Hayes MT. Parkinson's Disease and Parkinsonism. *Am J Med.* 2019 Jul 1;132(7):802–7.
70. Porter B, Macfarlane R, Walker R. The frequency and nature of sleep disorders in a community-based population of patients with Parkinson's disease. *Eur J Neurol.* 2008;15(1):50–4.
71. Lees AJ, Blackburn NA, Campbell VL. The nighttime problems of Parkinson's disease. *Clin Neuropharmacol.* 1988 Dec 1;11(6):512–9.
72. Mehta SH, Morgan JC, Sethi KD. Sleep Disorders Associated with Parkinson's Disease: Role of Dopamine, Epidemiology, and Clinical Scales of Assessment. *CNS Spectr.* 2008 Mar;13(54):6–11.
73. Monderer R, Thorpy M. Sleep disorders and daytime sleepiness in Parkinson's disease. *Curr Neurol Neurosci Rep.* 2009 Mar;9(2):173–80.
74. Doty RL, Deems DA, Stellar S. Olfactory dysfunction in parkinsonism: a general deficit unrelated to neurologic signs, disease stage, or disease duration. *Neurology.* 1988 Aug;38(8):1237–44.
75. Bayulkem K, Lopez G. Clinical approach to nonmotor sensory fluctuations in Parkinson's disease. *J Neurol Sci.* 2011 Nov 15;310(1):82–5.
76. Bayulkem K, Lopez G. Nonmotor fluctuations in Parkinson's disease: Clinical spectrum and classification. *J Neurol Sci.* 2010 Feb 15;289(1):89–92.
77. Broen MPG, Braaksma MM, Patijn J, Weber WEJ. Prevalence of pain in Parkinson's disease: A systematic review using the modified QUADAS tool. *Mov Disord.* 2012;27(4):480–4.
78. Tolosa E, Wenning G, Poewe W. The diagnosis of Parkinson's disease. *Lancet Neurol.* 2006 Jan 1;5(1):75–86.
79. Rao G, Fisch L, Srinivasan S, D'Amico F, Okada T, Eaton C, et al. Does This Patient Have Parkinson Disease? *JAMA.* 2003 Jan 15;289(3):347–53.
80. Gelb DJ, Oliver E, Gilman S. Diagnostic Criteria for Parkinson Disease. *Arch Neurol.* 1999 Jan 1;56(1):33–9.

81. Li T, Le W. Biomarkers for Parkinson's Disease: How Good Are They? *Neurosci Bull.* 2019 Oct 23;36(2):183–94.
82. Strafella AP, Bohnen NI, Perlmutter JS, Eidelberg D, Pavese N, Eimeren TV, et al. Molecular imaging to track Parkinson's disease and atypical parkinsonisms: New imaging frontiers. *Mov Disord.* 2017;32(2):181–92.
83. Pagano G, Nicolini F, Politis M. Imaging in Parkinson's disease. *Clin Med.* 2016 Aug;16(4):371–5.
84. Brooks DJ. Imaging Approaches to Parkinson Disease. *J Nucl Med.* 2010 Apr 1;51(4):596–609.
85. Lotankar S, Prabhavalkar KS, Bhatt LK. Biomarkers for Parkinson's Disease: Recent Advancement [Internet]. Vol. 33, Neuroscience bulletin. *Neurosci Bull*; 2017 [cited 2020 Nov 18]. Available from: <https://pubmed.ncbi.nlm.nih.gov/28936761/>
86. Satue M, Obis J, Rodrigo MJ, Otin S, Fuertes MI, Vilades E, et al. Optical Coherence Tomography as a Biomarker for Diagnosis, Progression, and Prognosis of Neurodegenerative Diseases. *J Ophthalmol.* 2016 Oct 20;2016:e8503859.
87. Inzelberg R, Ramirez JA, Nisipeanu P, Ophir A. Retinal nerve fiber layer thinning in Parkinson disease. *Vision Res.* 2004 Nov 1;44(24):2793–7.
88. Altıntaş Ö, Işeri P, Özkan B, Çağlar Y. Correlation between retinal morphological and functional findings and clinical severity in Parkinson's disease. *Doc Ophthalmol.* 2008 Mar 1;116(2):137–46.
89. Bouwmans AEP, Vlaar AMM, Mess WH, Kessels A, Weber WEJ. Specificity and sensitivity of transcranial sonography of the substantia nigra in the diagnosis of Parkinson's disease: prospective cohort study in 196 patients. *BMJ Open.* 2013 Jan 1;3(4):e002613.
90. Pykett IL, Newhouse JH, Buonanno FS, Brady TJ, Goldman MR, Kistler JP, et al. Principles of nuclear magnetic resonance imaging. *Radiology.* 1982 Apr 1;143(1):157–68.
91. Heim B, Krismer F, De Marzi R, Seppi K. Magnetic resonance imaging for the diagnosis of Parkinson's disease. *J Neural Transm.* 2017 Aug 1;124(8):915–64.
92. Miyoshi F, Ogawa T, Kitao S i., Kitayama M, Shinohara Y, Takasugi M, et al. Evaluation of Parkinson Disease and Alzheimer Disease with the Use of Neuromelanin MR Imaging and 123I-Metaiodobenzylguanidine Scintigraphy. *AJNR Am J Neuroradiol.* 2013 Nov;34(11):2113–8.
93. Stefurak T, Mikulis D, Mayberg H, Lang AE, Hevenor S, Pahapill P, et al. Deep brain stimulation for Parkinson's disease dissociates mood and motor circuits: A functional MRI case study. *Mov Disord.* 2003 Dec 1;18(12):1508–16.
94. Knight EJ, Testini P, Min HK, Gibson WS, Gorny KR, Favazza CP, et al. Motor and non-motor circuitry activation induced by subthalamic nucleus deep brain stimulation (STN DBS) in Parkinson's disease patients: Intraoperative fMRI for DBS. *Mayo Clin Proc.* 2015 Jun;90(6):773–85.
95. Manza P, Zhang S, Li CSR, Leung HC. Resting-state functional connectivity of the striatum in early-stage Parkinson's disease: Cognitive decline and motor symptomatology. *Hum Brain Mapp.* 2016 Feb;37(2):648–62.
96. Hou Y, Yang J, Luo C, Ou R, Song W, Liu W, et al. Patterns of striatal functional connectivity differ in early and late onset Parkinson's disease. *J Neurol.* 2016 Oct;263(10):1993–2003.
97. Jubault T, Monetta L, Strafella AP, Lafontaine AL, Monchi O. L-Dopa Medication in Parkinson's Disease Restores Activity in the Motor Cortico-Striatal Loop but Does Not Modify the Cognitive Network. *PLoS ONE.* 2009 Jul 7;4(7):e6154.
98. Herz DM, Siebner HR, Hulme OJ, Florin E, Christensen MS, Timmermann L. Levodopa reinstates connectivity from prefrontal to premotor cortex during externally paced movement in Parkinson's disease. *NeuroImage.* 2014 Apr 15;90:15–23.
99. Kuhl DE, Edwards RQ. Image Separation Radioisotope Scanning. *Radiology.* 1963 Apr;80(4):653–62.
100. Ter-Pogossian MM, Phelps ME, Hoffman EJ, Mullani NA. A Positron-Emission Transaxial Tomograph for Nuclear Imaging (PETT). *Radiology.* 1975 Jan 1;114(1):89–98.

101. Phelps ME, Hoffman EJ, Mullani NA, Higgins CS, Ter Pogossian MM. Design considerations for a positron emission transaxial tomograph (PETT III). *IEEE Trans Nucl Sci.* 1976;NS-23(1):516–22.
102. Kharfi F. Principles and Applications of Nuclear Medical Imaging: A Survey on Recent Developments [Internet]. *Imaging and Radioanalytical Techniques in Interdisciplinary Research - Fundamentals and Cutting Edge Applications.* IntechOpen; 2013 [cited 2022 Feb 21]. Available from: <https://www.intechopen.com/chapters/43519>
103. Welsh JS. Beta Decay in Science and Medicine. *Am J Clin Oncol.* 2007 Aug;30(4):437–9.
104. Khalil MM, Tremoleda JL, Bayomy TB, Gsell W. Molecular SPECT Imaging: An Overview. *Int J Mol Imaging.* 2011 Apr 5;2011:1–15.
105. Melcher CL. Scintillation Crystals for PET. *J Nucl Med.* 2000;41:1051–5.
106. Del Guerra A, Belcari N. State-of-the-art of PET, SPECT and CT for small animal imaging. *Nucl Instrum Methods Phys Res Sect Accel Spectrometers Detect Assoc Equip.* 2007 Dec 11;583(1):119–24.
107. Deleye S, Van Holen R, Verhaeghe J, Vandenberghe S, Stroobants S, Staelens S. Performance evaluation of small-animal multipinhole μ SPECT scanners for mouse imaging. *Eur J Nucl Med Mol Imaging.* 2013 May 1;40(5):744–58.
108. España S, Marcinkowski R, Keereman V, Vandenberghe S, Holen RV. DigiPET: sub-millimeter spatial resolution small-animal PET imaging using thin monolithic scintillators. *Phys Med Biol.* 2014 Jun;59(13):3405–20.
109. Pimlott SL, Sutherland A. Molecular tracers for the PET and SPECT imaging of disease. *Chem Soc Rev.* 2011;40(1):149–62.
110. Booi J, Knol RJ. SPECT imaging of the dopaminergic system in (premotor) Parkinson's disease. *Parkinsonism Relat Disord.* 2007 Jan 1;13:S425–8.
111. Fuente-Fernández R de la. Role of DaTSCAN and clinical diagnosis in Parkinson disease. *Neurology.* 2012 Mar 6;78(10):696–701.
112. Gayed I, Joseph U, Fanous M, Wan D, Schiess M, Ondo W, et al. The Impact of DaTscan in the Diagnosis of Parkinson Disease. *Clin Nucl Med.* 2015 May;40(5):390–3.
113. Bega D, Gonzalez-Latapi P, Zadikoff C, Spies W, Simuni T. Is There a Role for DAT-SPECT Imaging in a Specialty Movement Disorders Practice? *Neurodegener Dis.* 2015;15(2):81–6.
114. Oravivattanakul S, Benchaya L, Wu G, Ahmed A, Itin I, Cooper S, et al. Dopamine Transporter (DaT) Scan Utilization in a Movement Disorder Center. *Mov Disord Clin Pract.* 2016;3(1):31–5.
115. Tolosa E, Borghet TV, Moreno E. Accuracy of DaTSCAN (123I-ioflupane) SPECT in diagnosis of patients with clinically uncertain parkinsonism: 2-Year follow-up of an open-label study. *Mov Disord.* 2007;22(16):2346–51.
116. Lameka K, Farwell MD, Ichise M. Chapter 11 - Positron Emission Tomography. In: Masdeu JC, González RG, editors. *Handbook of Clinical Neurology* [Internet]. Elsevier; 2016 [cited 2021 Sep 22]. p. 209–27. (Neuroimaging Part I; vol. 135). Available from: <https://www.sciencedirect.com/science/article/pii/B9780444534859000118>
117. Moses WW. Trends in PET imaging. *Nucl Instrum Methods Phys Res Sect Accel Spectrometers Detect Assoc Equip.* 2001 Sep 21;471(1):209–14.
118. Fahey FH. Data Acquisition in PET Imaging. *J Nucl Med Technol.* 2002 Jun 1;30(2):39–49.
119. Workman RB, Coleman RE. 1. Fundamentals of PET and PET/CT Imaging. *CT Imaging.* :22.
120. Moghbel M, Newberg A, Alavi A. Positron emission tomography. In: *Handbook of Clinical Neurology* [Internet]. Elsevier; 2016 [cited 2017 Apr 11]. p. 229–40. Available from: <http://linkinghub.elsevier.com/retrieve/pii/B978044453485900012X>
121. Ido T, Wan CN, Casella V, Fowler JS, Wolf AP, Reivich M, et al. Labeled 2-deoxy-D-glucose analogs. 18F-labeled 2-deoxy-2-fluoro-D-glucose, 2-deoxy-2-fluoro-D-mannose and 14C-2-deoxy-2-fluoro-D-glucose. *J Label Compd Radiopharm.* 1978;14(2):175–83.

122. Mazière B, Mazière M. Positron emission tomography studies of brain receptors. *Fundam Clin Pharmacol*. 1991;5(1):61–91.
123. Gatley SJ, DeGrado TR, Kornguth ML, Holden JE. Radiopharmaceuticals for positron emission tomography. Development of new, innovative tracers for measuring the rates of physiologic and biochemical processes. *Acta Radiol Suppl*. 1990 Jan 1;374:7–11.
124. Kopin IJ. In-vivo quantitative imaging of catecholaminergic nerve terminals in brain and peripheral organs using positron emission tomography (PET). In: Riederer P, Youdim MBH, editors. *Amine Oxidases and Their Impact on Neurobiology*. Vienna: Springer; 1990. p. 19–27. (Journal of Neural Transmission).
125. Sadzot B, Mayberg H, Frost J. Detection and quantification of opiate receptors in Man by positron emission tomography. Potential applications to the study of pain. *Neurophysiol Clin Neurophysiol*. 1990 Jan 1;20(5):323–34.
126. Sokoloff L, Reivich M, Kennedy C, Rosiers MHD, Patlak CS, Pettigrew KD, et al. The [14C]deoxyglucose Method for the Measurement of Local Cerebral Glucose Utilization: Theory, Procedure, and Normal Values in the Conscious and Anesthetized Albino Rat 1. *J Neurochem*. 1977;28(5):897–916.
127. Reivich M, Kuhl D, Wolf A, Greenberg J, Phelps M, Ido T, et al. The [18F]fluorodeoxyglucose method for the measurement of local cerebral glucose utilization in man. *Circ Res*. 1979 Jan 1;44(1):127–37.
128. Wienhard K. Measurement of glucose consumption using [18F]fluorodeoxyglucose. *Methods*. 2002 Jul;27(3):218–25.
129. Eckert T, Barnes A, Dhawan V, Frucht S, Gordon MF, Feigin AS, et al. FDG PET in the differential diagnosis of parkinsonian disorders. *NeuroImage*. 2005 Jul 1;26(3):912–21.
130. Lozza C, Baron JC, Eidelberg D, Mentis MJ, Carbon M, Marié RM. Executive processes in Parkinson's disease: FDG-PET and network analysis. *Hum Brain Mapp*. 2004 Jul;22(3):236–45.
131. Jang DP, Min HK, Lee SY, Kim IY, Park HW, Im YH, et al. Functional neuroimaging of the 6-OHDA lesion rat model of Parkinson's disease. *Neurosci Lett*. 2012 Apr;513(2):187–92.
132. Casteels C, Lauwers E, Bormans G, Baekelandt V, Van Laere K. Metabolic–dopaminergic mapping of the 6-hydroxydopamine rat model for Parkinson's disease. *Eur J Nucl Med Mol Imaging*. 2008 Jan;35(1):124–34.
133. Berding G, Odin P, Brooks DJ, Nikkhah G, Matthies C, Peschel T, et al. Resting regional cerebral glucose metabolism in advanced Parkinson's disease studied in the off and on conditions with [18F]FDG-PET. *Mov Disord*. 2001 Nov 1;16(6):1014–22.
134. Asanuma K, Tang C, Ma Y, Dhawan V, Mattis P, Edwards C, et al. Network modulation in the treatment of Parkinson's disease. *Brain J Neurol*. 2006 Oct;129(0 10):2667–78.
135. Cao C, Zhang H, Li D, Zhan S, Zhang J, Zhang X, et al. Modified fluorodeoxyglucose metabolism in motor circuitry by subthalamic deep brain stimulation. *Stereotact Funct Neurosurg*. 2017;95(2):93–101.
136. Geday J, Østergaard K, Johnsen E, Gjedde A. STN-stimulation in Parkinson's disease restores striatal inhibition of thalamocortical projection. *Hum Brain Mapp*. 2009 Jan 1;30(1):112–21.
137. Kordys E, Apetz N, Neumaier B, Drzezga A, Timmermann L, Endepols H. Functional connectivity during deep brain stimulation in the subthalamic nucleus of hemiparkinson rats measured with FDG-PET. *J Nucl Med*. 2016 Jan 5;57(supplement 2):217–217.
138. Apetz N, Kordys E, Simon M, Mang B, Aswendt M, Wiedermann D, et al. Effects of subthalamic deep brain stimulation on striatal metabolic connectivity in a rat hemiparkinsonian model. *Dis Model Mech* [Internet]. 2019 May 1 [cited 2019 Jul 11];12(5). Available from: <https://dmm.biologists.org/content/12/5/dmm039065>
139. Le Jeune F, Péron J, Grandjean D, Drapier S, Haegelen C, Garin E, et al. Subthalamic nucleus stimulation affects limbic and associative circuits: a PET study. *Eur J Nucl Med Mol Imaging*. 2010 Aug 1;37(8):1512–20.
140. Snow BJ, Tooyama I, McGeer EG, Yamada T, Calne DB, Takahashi H, et al. Human positron emission tomographic [18F]Fluorodopa studies correlate with dopamine cell counts and levels. *Ann Neurol*. 1993;34(3):324–30.

141. Heiss WD, Hilker R. The sensitivity of 18-fluorodopa positron emission tomography and magnetic resonance imaging in Parkinson's disease. *Eur J Neurol.* 2004;11(1):5–12.
142. Brown CA, Karimi MK, Tian L, Flores H, Su Y, Tabbal SD, et al. Validation of midbrain positron emission tomography measures for nigrostriatal neurons in macaques. *Ann Neurol.* 2013;74(4):602–10.
143. Yee R e., Irwin I, Milonas C, Stout D b., Huang SC, Shoghi-Jadid K, et al. Novel observations with FDOPA-PET imaging after early nigrostriatal damage. *Mov Disord.* 2001;16(5):838–48.
144. Brück A, Aalto S, Nurmi E, Bergman J, Rinne JO. Cortical 6-[18F]fluoro-l-dopa uptake and frontal cognitive functions in early Parkinson's disease. *Neurobiol Aging.* 2005 Jun 1;26(6):891–8.
145. Pikstra ARA, van der Hoorn A, Leenders KL, de Jong BM. Relation of 18-F-Dopa PET with hypokinesia-rigidity, tremor and freezing in Parkinson's disease. *NeuroImage Clin.* 2016 Jan 1;11:68–72.
146. Vingerhoets FJG, Schulzer M, Calne DB, Snow BJ. Which clinical sign of Parkinson's disease best reflects the nigrostriatal lesion? *Ann Neurol.* 1997;41(1):58–64.
147. Otsuka M, Kuwabara Y, Ichiya Y, Hosokawa S, Sasaki M, Yoshida T, et al. Differentiating between multiple system atrophy and Parkinson's disease by positron emission tomography with 18F-dopa and 18F-FDG. *Ann Nucl Med.* 1997 Sep 1;11(3):251–7.
148. Brooks DJ, Ibanez V, Sawle GV, Quinn N, Lees AJ, Mathias CJ, et al. Differing patterns of striatal 18F-dopa uptake in Parkinson's disease, multiple system atrophy, and progressive supranuclear palsy. *Ann Neurol.* 1990;28(4):547–55.
149. Nurmi E, Ruottinen HM, Bergman J, Haaparanta M, Solin O, Sonninen P, et al. Rate of progression in Parkinson's disease: A 6-[18F]fluoro-L-dopa PET study. *Mov Disord.* 2001 Jul 1;16(4):608–15.
150. Morrish PK, Sawle GV, Brooks DJ. An [18F]dopa-PET and clinical study of the rate of progression in Parkinson's disease. *Brain.* 1996 Apr 1;119(2):585–91.
151. Morrish PK, Rakshi JS, Bailey DL, Sawle GV, Brooks DJ. Measuring the rate of progression and estimating the preclinical period of Parkinson's disease with [18F]dopa PET. *J Neurol Neurosurg Psychiatry.* 1998 Jan 3;64(3):314–9.
152. Rakshi JS, Uema T, Ito K, Bailey DL, Morrish PK, Ashburner J, et al. Frontal, midbrain and striatal dopaminergic function in early and advanced Parkinson's disease A 3D [18F]dopa-PET study. *Brain.* 1999 Sep 1;122(9):1637–50.
153. Eidelberg D, Moeller JR, Dhawan V, Sidtis JJ, Ginos JZ, Strother SC, et al. The metabolic anatomy of Parkinson's disease: Complementary [18F]fluorodeoxyglucose and [18F]fluorodopa positron emission tomographic studies. *Mov Disord.* 1990 Jan 1;5(3):203–13.
154. Kordys E, Apetz N, Schneider K, Duncan E, Büschbell B, Rohleder C, et al. Motor impairment and compensation in a hemiparkinsonian rat model: correlation between dopamine depletion severity, cerebral metabolism and gait patterns. *EJNMMI Res [Internet].* 2017 Dec [cited 2019 Jul 30];7(1). Available from: <http://ejnmires.springeropen.com/articles/10.1186/s13550-017-0317-9>
155. Nagano-Saito A, Kato T, Arahata Y, Washimi Y, Nakamura A, Abe Y, et al. Cognitive- and motor-related regions in Parkinson's disease: FDOPA and FDG PET studies. *NeuroImage.* 2004 Jun;22(2):553–61.
156. Holtbernd F, Ma Y, Peng S, Schwartz F, Timmermann L, Kracht L, et al. Dopaminergic correlates of metabolic network activity in Parkinson's disease: Brain Networks in Parkinson's Disease. *Hum Brain Mapp.* 2015 Sep;36(9):3575–85.
157. Emsen B, Villafane G, David JP, Evangelista E, Chalaye J, Lerman L, et al. Clinical impact of dual-tracer FDOPA and FDG PET/CT for the evaluation of patients with parkinsonian syndromes. *Medicine (Baltimore).* 2020 Nov 6;99(45):e23060.
158. Connolly BS, Lang AE. Pharmacological treatment of Parkinson disease: A review. *JAMA.* 2014 Apr 23;311(16):1670.
159. AlDakheel A, Kalia LV, Lang AE. Pathogenesis-targeted, disease-modifying therapies in Parkinson disease. *Neurotherapeutics.* 2013 Oct 2;11(1):6–23.

160. Olanow CW, Rascol O, Hauser R, Feigin PD, Jankovic J, Lang A, et al. A double-blind, delayed-start trial of rasagiline in Parkinson's disease. *N Engl J Med.* 2009 Sep 24;361(13):1268–78.
161. Katzenschlager R, Sampaio C, Costa J, Lees A. Anticholinergics for symptomatic management of Parkinson's disease. In: *Cochrane Database of Systematic Reviews* [Internet]. John Wiley & Sons, Ltd; 2002 [cited 2016 Jul 27]. Available from: <http://onlinelibrary.wiley.com/doi/10.1002/14651858.CD003735/abstract>
162. Schulzer M, Mak E, Calne DB. The antiparkinson efficacy of deprenyl derives from transient improvement that is likely to be symptomatic. *Ann Neurol.* 1992 Dec 1;32(6):795–8.
163. Rinne UK, Sonninen V, Siirtola T. L-dopa treatment in Parkinson's disease. *Eur Neurol.* 1970 Jul 1;4(6):348–69.
164. Poewe W. Chapter 2 - Drug Therapy: Dopamine Agonists. In: Schapira AHV, Olanow CW, editors. *Principles of Treatment in Parkinson's Disease* [Internet]. Philadelphia: Butterworth-Heinemann; 2005 [cited 2021 Sep 9]. p. 25–47. Available from: <https://www.sciencedirect.com/science/article/pii/B9780750654289500068>
165. Calne DB. Diagnosis and treatment of Parkinson's disease. *Hosp Pract.* 1995 Jan 15;30(1):83–9.
166. Hauser RA, Rascol O, Korczyn AD, Jon Stoessl A, Watts RL, Poewe W, et al. Ten-year follow-up of Parkinson's disease patients randomized to initial therapy with ropinirole or levodopa. *Mov Disord.* 2007 Dec 15;22(16):2409–17.
167. Holloway RG, Shoulson I, Fahn S, Kieburtz K, Lang A, Marek K, et al. Pramipexole vs levodopa as initial treatment for Parkinson disease: a 4-year randomized controlled trial. *Arch Neurol.* 2004 Jul;61(7):1044–53.
168. Sprenger F, Poewe W. Management of motor and non-motor symptoms in Parkinson's disease. *CNS Drugs.* 2013 Mar 21;27(4):259–72.
169. Mouradian MM, Junecos JL, Fabbrini G, Schlegel J, Bartko JJ, Chase TN. Motor fluctuations in Parkinson's disease: Central pathophysiological mechanisms, part II. *Ann Neurol.* 1988 Sep 1;24(3):372–8.
170. Goetz CG, Tanner CM, Gilley DW, Klawans HL. Development and progression of motor fluctuations and side effects in Parkinson's disease: comparison of Sinemet CR versus carbidopa/levodopa. *Neurology.* 1989 Nov;39(11 Suppl 2):63–6; discussion 72–73.
171. Obeso JA, Olanow CW, Nutt JG. Levodopa motor complications in Parkinson's disease. *Trends Neurosci.* 2000 Oct;23, Supplement 1:S2–7.
172. Fabbrini G, Mouradian MM, Junecos JL, Schlegel J, Mohr E, Chase TN. Motor fluctuations in Parkinson's disease: Central pathophysiological mechanisms, Part I. *Ann Neurol.* 1988 Sep 1;24(3):366–71.
173. Olanow CW, Obeso JA, Stocchi F. Continuous dopamine-receptor treatment of Parkinson's disease: scientific rationale and clinical implications. *Lancet Neurol.* 2006 Aug;5(8):677–87.
174. Van Gerpen JA, Kumar N, Bower JH, Weigand S, Ahlskog JE. Levodopa-associated dyskinesia risk among Parkinson disease patients in Olmsted County, Minnesota, 1976–1990. *Arch Neurol.* 2006 Feb 1;63(2):205.
175. Cummings JL. Behavioral complications of drug treatment of Parkinson's disease. *J Am Geriatr Soc.* 1991 Jul 1;39(7):708–16.
176. Ryback RS, Schwab RS. Manic response to levodopa therapy. *N Engl J Med.* 1971 Sep 30;285(14):788–9.
177. Fahn S. Adverse effects of levodopa in Parkinson's disease. In: *F.R.C.P.C DBCPDM FRCP*, editor. *Drugs for the Treatment of Parkinson's Disease* [Internet]. Springer Berlin Heidelberg; 1989 [cited 2016 Jul 27]. p. 385–409. (Handbook of Experimental Pharmacology). Available from: http://link.springer.com/chapter/10.1007/978-3-642-73899-9_14
178. Goetz CG, Tanner CM, Klawans HL. Pharmacology of hallucinations induced by long-term drug therapy. *Am J Psychiatry.* 1982 Apr;139(4):494–7.

179. Amro MS, Teoh SL, Norzana AG. The potential role of herbal products in the treatment of Parkinson's disease. *Clin Ter.* 2018 Feb 28;1(1):23–33.
180. Rabeie Z, Solati K, Amini-Khoei H. Phytotherapy in treatment of Parkinson's disease: a review [Internet]. Vol. 57, *Pharmaceutical biology. Pharm Biol*; 2019 [cited 2020 Nov 18]. Available from: <https://pubmed.ncbi.nlm.nih.gov/31141426/>
181. Oertel W, Schulz JB. Current and experimental treatments of Parkinson disease: A guide for neuroscientists [Internet]. Vol. 139 Suppl 1, *Journal of neurochemistry. J Neurochem*; 2016 [cited 2020 Nov 18]. Available from: <https://pubmed.ncbi.nlm.nih.gov/27577098/>
182. Schapira AHV, Bezard E, Brotchie J, Calon F, Collingridge GL, Ferger B, et al. Novel pharmacological targets for the treatment of Parkinson's disease. *Nat Rev Drug Discov.* 2006 Oct;5(10):845–54.
183. Björklund A, Stenevi U. Reconstruction of the nigrostriatal dopamine pathway by intracerebral nigral transplants. *Brain Res.* 1979 Nov 30;177(3):555–60.
184. Björklund A, Stenevi U, Schmidt RH, Dunnett SB, Gage FH. Intracerebral grafting of neuronal cell suspensions. II. Survival and growth of nigral cell suspensions implanted in different brain sites. *Acta Physiol Scand Suppl.* 1983;522:9–18.
185. Perlow MJ, Freed WJ, Hoffer BJ, Seiger A, Olson L, Wyatt RJ. Brain grafts reduce motor abnormalities produced by destruction of nigrostriatal dopamine system. *Science.* 1979 May 11;204(4393):643–7.
186. Freed WJ, Perlow MJ, Karoum F, Seiger A, Olson L, Hoffer BJ, et al. Restoration of dopaminergic function by grafting of fetal rat substantia nigra to the caudate nucleus: Long-term behavioral, biochemical, and histochemical studies. *Ann Neurol.* 1980;8(5):510–9.
187. Parmar M. Towards stem cell based therapies for Parkinson's disease [Internet]. Vol. 145, *Development (Cambridge, England). Development*; 2018 [cited 2020 Nov 18]. Available from: <https://pubmed.ncbi.nlm.nih.gov/29311261/>
188. Peschanski M, Defer G, N'Guyen JP, Ricolfi F, Monfort JC, Remy P, et al. Bilateral motor improvement and alteration of L-dopa effect in two patients with Parkinson's disease following intrastriatal transplantation of foetal ventral mesencephalon. *Brain.* 1994 Jun 1;117(3):487–99.
189. Hitchcock ER, Kenny BG, Henderson BTH, Clough CG, Hughes RC, Detta A. A Series of Experimental Surgery for Advanced Parkinson's Disease by Foetal Mesencephalic Transplantation. In: Hitchcock ER, Broggi G, Burzaco J, Martin-Rodriguez J, Meyerson BA, Tóth S, editors. *Advances in Stereotactic and Functional Neurosurgery 9.* Vienna: Springer; 1991. p. 54–7. (*Acta Neurochirurgica Supplementum*).
190. Thomson JA, Itskovitz-Eldor J, Shapiro SS, Waknitz MA, Swiergiel JJ, Marshall VS, et al. Embryonic stem cell lines derived from human blastocysts. *Science.* 1998 Nov 6;282(5391):1145–7.
191. Kirkeby A, Parmar M, Barker RA. Chapter 7 - Strategies for bringing stem cell-derived dopamine neurons to the clinic: A European approach (STEM-PD). In: Dunnett SB, Björklund A, editors. *Progress in Brain Research* [Internet]. Elsevier; 2017 [cited 2021 Sep 9]. p. 165–90. (*Functional Neural Transplantation IV*; vol. 230). Available from: <https://www.sciencedirect.com/science/article/pii/S0079612316301698>
192. Kirkeby A, Grealish S, Wolf DA, Nelander J, Wood J, Lundblad M, et al. Generation of Regionally Specified Neural Progenitors and Functional Neurons from Human Embryonic Stem Cells under Defined Conditions. *Cell Rep.* 2012 Jun 28;1(6):703–14.
193. Cisbani G, Maxan A, Kordower JH, Planel E, Freeman TB, Cicchetti F. Presence of tau pathology within foetal neural allografts in patients with Huntington's and Parkinson's disease. *Brain.* 2017 Nov 1;140(11):2982–92.
194. Olanow CW, Savolainen M, Chu Y, Halliday GM, Kordower JH. Temporal evolution of microglia and α -synuclein accumulation following foetal grafting in Parkinson's disease. *Brain.* 2019 Jun 1;142(6):1690–700.
195. Christine CW, Starr PA, Larson PS, Eberling JL, Jagust WJ, Hawkins RA, et al. Safety and tolerability of putaminal AADC gene therapy for Parkinson disease. *Neurology.* 2009 Nov 17;73(20):1662–9.

196. Mittermeyer G, Christine CW, Rosenbluth KH, Baker SL, Starr P, Larson P, et al. Long-Term Evaluation of a Phase 1 Study of AADC Gene Therapy for Parkinson's Disease. *Hum Gene Ther.* 2012 Apr 1;23(4):377–81.
197. Kaplitt MG, Feigin A, Tang C, Fitzsimons HL, Mattis P, Lawlor PA, et al. Safety and tolerability of gene therapy with an adeno-associated virus (AAV) borne GAD gene for Parkinson's disease: an open label, phase I trial. *The Lancet.* 2007 Jun 23;369(9579):2097–105.
198. LeWitt PA, Rezaei AR, Leehey MA, Ojemann SG, Flaherty AW, Eskandar EN, et al. AAV2-GAD gene therapy for advanced Parkinson's disease: a double-blind, sham-surgery controlled, randomised trial. *Lancet Neurol.* 2011 Apr 1;10(4):309–19.
199. Axelsen TM, Woldbye DPD. Gene Therapy for Parkinson's Disease, An Update [Internet]. Vol. 8, *Journal of Parkinson's disease.* J Parkinsons Dis; 2018 [cited 2020 Nov 18]. Available from: <https://pubmed.ncbi.nlm.nih.gov/29710735/>
200. Stoddard-Bennett T, Reijo Pera R. Treatment of Parkinson's Disease through Personalized Medicine and Induced Pluripotent Stem Cells. *Cells.* 2019 Jan 7;8(1):26.
201. Walter BL, Vitek JL. Surgical treatment for Parkinson's disease. *Lancet Neurol.* 2004 Dec 1;3(12):719–28.
202. Kelly PJ, Ahlskog JE, Goerss SJ, Daube JR, Duffy JR, Kall BA. Computer-Assisted Stereotactic Ventralis Lateralis Thalamotomy With Microelectrode Recording Control in Patients With Parkinson's Disease. *Mayo Clin Proc.* 1987 Aug 1;62(8):655–64.
203. Vitek JL, Bakay RAE, Freeman A, Evatt M, Green J, McDonald W, et al. Randomized trial of pallidotomy versus medical therapy for Parkinson's disease. *Ann Neurol.* 2003 May;53(5):558–69.
204. Su PC, Tseng HM, Liu HM, Yen RF, Liou HH. Treatment of advanced Parkinson's disease by subthalamotomy: One-year results. *Mov Disord.* 2003;18(5):531–8.
205. Spindola B, Leite MA, Orsini M, Fonoff E, Landeiro JA, Pessoa BL. Ablative surgery for Parkinson's disease: Is there still a role for pallidotomy in the deep brain stimulation era? *Clin Neurol Neurosurg.* 2017 Jul 1;158:33–9.
206. Jourdain VA, Schechtmann G, Paolo TD. Subthalamotomy in the treatment of Parkinson's disease: clinical aspects and mechanisms of action: A review. *J Neurosurg.* 2014 Jan 1;120(1):140–51.
207. Wen Z, Zhang J, Li J, Dai J, Lin F, Wu G. Altered Activation in Cerebellum Contralateral to Unilateral Thalamotomy May Mediate Tremor Suppression in Parkinson's Disease: A Short-Term Regional Homogeneity fMRI Study. *PLoS ONE.* 2016 Jun 16;11(6):e0157562.
208. Hemptinac C, Wang DD, Miocinovic S, Chen W, Ostrem JL, Starr PA. Pallidal thermolesion unleashes gamma oscillations in the motor cortex in Parkinson's disease. *Mov Disord.* 2019 Jun;34(6):903–11.
209. Benabid AL, Pollak P, Hoffmann D, Gervason C, Hommel M, Perret JE, et al. Long-term suppression of tremor by chronic stimulation of the ventral intermediate thalamic nucleus. *The Lancet.* 1991 Feb 16;337(8738):403–6.
210. Benabid AL, Pollak P, Gao D, Hoffmann D, Limousin P, Gay E, et al. Chronic electrical stimulation of the ventralis intermedius nucleus of the thalamus as a treatment of movement disorders. *J Neurosurg.* 1996 Feb 1;84(2):203–14.
211. Siegfried J, Lippitz B. Bilateral Chronic Electrostimulation of Ventroposterolateral Pallidum: A New Therapeutic Approach for Alleviating All Parkinsonian Symptoms. *Neurosurgery.* 1994 Dec 1;35(6):1126–30.
212. The Deep-Brain Stimulation for Parkinson's Disease Study Group. Deep-Brain Stimulation of the Subthalamic Nucleus or the Pars Interna of the Globus Pallidus in Parkinson's Disease [Internet]. <http://dx.doi.org/10.1056/NEJMoa000827>. Massachusetts Medical Society; 2009 [cited 2021 Sep 9]. Available from: <https://www.nejm.org/doi/10.1056/NEJMoa000827>
213. Limousin P, Krack P, Pollak P, Benazzouz A, Ardouin C, Hoffmann D, et al. Electrical stimulation of the subthalamic nucleus in advanced Parkinson's disease. *N Engl J Med.* 1998 Oct 15;339(16):1105–11.

214. Limousin P, Pollak P, Benazzouz A, Hoffmann D, Le Bas JF, Perret JE, et al. Effect on parkinsonian signs and symptoms of bilateral subthalamic nucleus stimulation. *The Lancet*. 1995 Jan 14;345(8942):91–5.
215. Romito LM, Contarino MF, Vanacore N, Bentivoglio AR, Scerrati M, Albanese A. Replacement of dopaminergic medication with subthalamic nucleus stimulation in Parkinson's disease: Long-term observation. *Mov Disord*. 2009 Mar 15;24(4):555–61.
216. Faggiani E, Benazzouz A. Deep brain stimulation of the subthalamic nucleus in Parkinson's disease: From history to the interaction with the monoaminergic systems. *Prog Neurobiol*. 2016 Jul 10;151:139–56.
217. Benabid AL, Chabardes S, Mitrofanis J, Pollak P. Deep brain stimulation of the subthalamic nucleus for the treatment of Parkinson's disease. *Lancet Neurol*. 2009 Jan;8(1):67–81.
218. Benabid AL, Pollak P, Gross C, Hoffmann D, Benazzouz A, Gao DM, et al. Acute and long-term effects of subthalamic nucleus stimulation in Parkinson's disease. *Stereotact Funct Neurosurg*. 1995 Apr 11;62(1–4):76–84.
219. Timmermann L, Jain R, Chen L, Maarouf M, Barbe MT, Allert N, et al. Multiple-source current steering in subthalamic nucleus deep brain stimulation for Parkinson's disease (the VANTAGE study): a non-randomised, prospective, multicentre, open-label study. *Lancet Neurol*. 2015 Jul;14(7):693–701.
220. Chaturvedi A, Foutz TJ, McIntyre CC. Current steering to activate targeted neural pathways during deep brain stimulation of the subthalamic region. *Brain Stimulat*. 2012 Jul 1;5(3):369–77.
221. Contarino MF, Bour LJ, Verhagen R, Lourens MAJ, Bie RMA de, Munchhof P van den, et al. Directional steering: A novel approach to deep brain stimulation. *Neurology*. 2014 Sep 23;83(13):1163–9.
222. Steigerwald F, Müller L, Johannes S, Matthies C, Volkman J. Directional deep brain stimulation of the subthalamic nucleus: A pilot study using a novel neurostimulation device. *Mov Disord*. 2016;31(8):1240–3.
223. Habets JGV, Heijmans M, Kuijf ML, Janssen MLF, Temel Y, Kubben PL. An update on adaptive deep brain stimulation in Parkinson's disease: Update On Adaptive DBS in Parkinson's Disease. *Mov Disord*. 2018 Dec;33(12):1834–43.
224. Betarbet R, Sherer TB, Greenamyre JT. Animal models of Parkinson's disease. *BioEssays*. 2002 Apr 1;24(4):308–18.
225. Blandini F, Armentero MT. Animal models of Parkinson's disease. *FEBS J*. 2012 Apr 1;279(7):1156–66.
226. Blesa J, Phani S, Jackson-Lewis V, Przedborski S. Classic and new animal models of Parkinson's disease. *J Biomed Biotechnol* [Internet]. 2012 [cited 2016 Jul 29];2012. Available from: <http://www.ncbi.nlm.nih.gov/pmc/articles/PMC3321500/>
227. Gubellini P, Kachidian P. Animal models of Parkinson's disease: An updated overview. *Rev Neurol (Paris)*. 2015 Nov;171(11):750–61.
228. Ungerstedt U, Ljungberg T, Steg G. Behavioral, physiological, and neurochemical changes after 6-hydroxydopamine-induced degeneration of the nigro-striatal dopamine neurons. *Adv Neurol*. 1974;5:421–6.
229. Ungerstedt U, Arbutnot GW. Quantitative recording of rotational behavior in rats after 6-hydroxydopamine lesions of the nigrostriatal dopamine system. *Brain Res*. 1970 Dec 18;24(3):485–93.
230. Ungerstedt U. 6-hydroxy-dopamine induced degeneration of central monoamine neurons. *Eur J Pharmacol*. 1968 Dec 1;5(1):107–10.
231. Martin GE, Myers RD, Newberg DC. Catecholamine release by intracerebral perfusion of 6-hydroxydopamine and desipramine. *Eur J Pharmacol*. 1976 Apr 1;36(2):299–311.
232. Cohen G. Oxy-radical toxicity in catecholamine neurons. *Neurotoxicology*. 1984;5(1):77–82.
233. Schober A. Classic toxin-induced animal models of Parkinson's disease: 6-OHDA and MPTP. *Cell Tissue Res*. 2004 Oct 1;318(1):215–24.

234. Blandini F, Armentero MT, Martignoni E. The 6-hydroxydopamine model: News from the past. *Parkinsonism Relat Disord.* 2008 Jul 1;14:S124–9.
235. Roeling TAP, Docter GJ, Voorn P, Melchers BPC, Wolters ECh, Groenewegen HJ. Effects of unilateral 6-hydroxydopamine lesions on neuropeptide immunoreactivity in the basal ganglia of the common marmoset, *Callithrix jacchus*, a quantitative immunohistochemical analysis. *J Chem Neuroanat.* 1995 Oct 1;9(3):155–64.
236. Valette H, Deleuze P, Syrota A, Delforge J, Crouzel C, Fuseau C, et al. Canine Myocardial Beta-Adrenergic, Muscarinic Receptor Densities After Denervation: A PET Study. *J Nucl Med.* 1995 Jan 1;36(1):140–6.
237. Poirier LJ. Histopathological changes associated with the intracerebral injection of 6-hydroxydopamine (6-OHDA) and peroxide (H2O2) in the cat and the rat. *J Neural Transm.* 1975 Sep 1;37(3):209–18.
238. Thiele SL, Warre R, Nash JE. Development of a Unilaterally-lesioned 6-OHDA Mouse Model of Parkinson's Disease. *J Vis Exp JoVE.* 2012 Feb 14;(60):3234.
239. Deumens R, Blokland A, Prickaerts J. Modeling parkinson's disease in rats: an evaluation of 6-ohda lesions of the nigrostriatal pathway. *Exp Neurol.* 2002 Jun;175(2):303–17.
240. Jeon BS, Jackson-Lewis V, Burke RE. 6-Hydroxydopamine Lesion of the Rat Substantia Nigra: Time Course and Morphology of Cell Death. *Neurodegeneration.* 1995 Jun 1;4(2):131–7.
241. Yuan H, Sarre S, Ebinger G, Michotte Y. Histological, behavioural and neurochemical evaluation of medial forebrain bundle and striatal 6-OHDA lesions as rat models of Parkinson's disease. *J Neurosci Methods.* 2005 May 15;144(1):35–45.
242. Sauer H, Oertel WH. Progressive degeneration of nigrostriatal dopamine neurons following intra-striatal terminal lesions with 6-hydroxydopamine: A combined retrograde tracing and immunocytochemical study in the rat. *Neuroscience.* 1994 Mar 1;59(2):401–15.
243. Ungerstedt U. Adipsia and aphagia after 6-hydroxydopamine induced degeneration of the nigro-striatal dopamine system. *Acta Physiol Scand Suppl.* 1971;367:95–122.
244. Carman LS, Gage FH, Shults CW. Partial lesion of the substantia nigra: relation between extent of lesion and rotational behavior. *Brain Res.* 1991 Jul 12;553(2):275–83.
245. Truong L, Allbutt H, Kassiou M, Henderson JM. Developing a preclinical model of Parkinson's disease: A study of behaviour in rats with graded 6-OHDA lesions. *Behav Brain Res.* 2006 Apr 25;169(1):1–9.
246. Giovanni A, Sieber BA, Heikkila RE, Sonsalla PK. Studies on species sensitivity to the dopaminergic neurotoxin 1-methyl-4-phenyl-1,2,3,6-tetrahydropyridine. Part 1: Systemic administration. *J Pharmacol Exp Ther.* 1994 Sep 1;270(3):1000–7.
247. Gerlach M, Riederer P, Przuntek H, Youdim MBH. MPTP mechanisms of neurotoxicity and their implications for Parkinson's disease. *Eur J Pharmacol Mol Pharmacol.* 1991 Dec 12;208(4):273–86.
248. Fox SH, Brotchie JM. Chapter 7 - The MPTP-lesioned non-human primate models of Parkinson's disease. Past, present, and future. In: Björklund A, Cenci MA, editors. *Progress in Brain Research [Internet]. Elsevier; 2010 [cited 2021 Sep 14]. p. 133–57. [Recent Advances in Parkinson'S Disease; vol. 184]. Available from: <https://www.sciencedirect.com/science/article/pii/S0079612310840075>*
249. Jackson-Lewis V, Przedborski S. Protocol for the MPTP mouse model of Parkinson's disease. *Nat Protoc.* 2007 Jan;2(1):141–51.
250. Sedelis M, Schwarting RKW, Huston JP. Behavioral phenotyping of the MPTP mouse model of Parkinson's disease. *Behav Brain Res.* 2001 Nov 8;125(1):109–25.
251. Vermilyea SC, Emborg ME. α -Synuclein and nonhuman primate models of Parkinson's disease. *J Neurosci Methods.* 2015 Nov 30;255:38–51.
252. Zhang Q shuang, Heng Y, Mou Z, Huang J yang, Yuan Y he, Chen N hong. Reassessment of subacute MPTP-treated mice as animal model of Parkinson's disease. *Acta Pharmacol Sin.* 2017 Oct;38(10):1317–28.

253. Jagmag SA, Tripathi N, Shukla SD, Maiti S, Khurana S. Evaluation of models of Parkinson's disease. *Neurodegeneration*. 2016;5:03.
254. Masliah E, Rockenstein E, Veinbergs I, Mallory M, Hashimoto M, Takeda A, et al. Dopaminergic Loss and Inclusion Body Formation in α -Synuclein Mice: Implications for Neurodegenerative Disorders. *Science*. 2000 Feb 18;287(5456):1265-9.
255. Richfield EK, Thiruchelvam MJ, Cory-Slechta DA, Wuertzer C, Gainetdinov RR, Caron MG, et al. Behavioral and Neurochemical Effects of Wild-Type and Mutated Human α -Synuclein in Transgenic Mice. *Exp Neurol*. 2002 May 1;175(1):35-48.
256. Rockenstein E, Mallory M, Hashimoto M, Song D, Shults CW, Lang I, et al. Differential neuropathological alterations in transgenic mice expressing α -synuclein from the platelet-derived growth factor and Thy-1 promoters. *J Neurosci Res*. 2002;68(5):568-78.
257. Emmer KL, Waxman EA, Covy JP, Giasson BI. E46K Human α -Synuclein Transgenic Mice Develop Lewy-like and Tau Pathology Associated with Age-dependent, Detrimental Motor Impairment. *J Biol Chem*. 2011 Oct 7;286(40):35104-18.
258. Cannon JR, Gekhman KD, Tapias V, Sew T, Dail MK, Li C, et al. Expression of human E46K-mutated α -synuclein in BAC-transgenic rats replicates early-stage Parkinson's disease features and enhances vulnerability to mitochondrial impairment. *Exp Neurol*. 2013 Feb;240:44-56.
259. Blesa J, Przedborski S. Parkinson's disease: animal models and dopaminergic cell vulnerability. *Front Neuroanat*. 2014 Dec 15;8:155.
260. Li Y, Liu W, Oo TF, Wang L, Tang Y, Jackson-Lewis V, et al. Mutant LRRK2R1441G BAC transgenic mice recapitulate cardinal features of Parkinson's disease. *Nat Neurosci*. 2009 Jul;12(7):826-8.
261. Fasano A, Romito LM, Daniele A, Piano C, Zinno M, Bentivoglio AR, et al. Motor and cognitive outcome in patients with Parkinson's disease 8 years after subthalamic implants. *Brain*. 2010 Sep 1;133(9):2664-76.
262. Dafsari HS, Reddy P, Herchenbach C, Wawro S, Petry-Schmelzer JN, Visser-Vandewalle V, et al. Beneficial effects of bilateral subthalamic stimulation on non-motor symptoms in Parkinson's disease. *Brain Stimulat*. 2016 Jan;9(1):78-85.
263. Contarino MF, Daniele A, Sibilia AH, Romito LMA, Bentivoglio AR, Gainotti G, et al. Cognitive outcome 5 years after bilateral chronic stimulation of subthalamic nucleus in patients with Parkinson's disease. *J Neurol Neurosurg Psychiatry*. 2006 Oct 20;78(3):248-52.
264. Giannicola G, Marceglia S, Rossi L, Mrakic-Sposta S, Rampini P, Tamma F, et al. The effects of levodopa and ongoing deep brain stimulation on subthalamic beta oscillations in Parkinson's disease. *Exp Neurol*. 2010 Nov;226(1):120-7.
265. Mueller K, Jech R, Růžička F, Holiga Š, Ballarini T, Bezdicek O, et al. Brain connectivity changes when comparing effects of subthalamic deep brain stimulation with levodopa treatment in Parkinson's disease. *NeuroImage Clin*. 2018 Jan 1;19:1025-35.
266. Barbe MT, Maarouf M, Alesch F, Timmermann L. Multiple source current steering - A novel deep brain stimulation concept for customized programming in a Parkinson's disease patient. *Parkinsonism Relat Disord*. 2014 Apr;20(4):471-3.
267. Vitek JL. Mechanisms of deep brain stimulation: Excitation or inhibition. *Mov Disord*. 2002 Mar 1;17(S3):S69-72.
268. Ashkan K, Rogers P, Bergman H, Ughratdar I. Insights into the mechanisms of deep brain stimulation. *Nat Rev Neurol*. 2017 Sep;13(9):548-54.
269. Anderson CJ, Sheppard DT, Huynh R, Anderson DN, Polar CA, Dorval AD. Subthalamic deep brain stimulation reduces pathological information transmission to the thalamus in a rat model of parkinsonism. *Front Neural Circuits* [Internet]. 2015 Jul 6 [cited 2019 Jul 10];9. Available from: <http://journal.frontiersin.org/Article/10.3389/fncir.2015.00031/abstract>
270. Dorval AD, Grill WM. Deep brain stimulation of the subthalamic nucleus reestablishes neuronal information transmission in the 6-OHDA rat model of parkinsonism. *J Neurophysiol*. 2014 May 15;111(10):1949-59.

271. McConnell GC, So RQ, Hilliard JD, Lopomo P, Grill WM. Effective deep brain stimulation suppresses low frequency network oscillations in the basal ganglia by regularizing neural firing patterns. *J Neurosci Off J Soc Neurosci*. 2012 Nov 7;32(45):15657–68.
272. Shi LH, Woodward DJ, Luo F, Anstrom K, Schallert T, Chang JY. High-frequency stimulation of the subthalamic nucleus reverses limb-use asymmetry in rats with unilateral 6-hydroxydopamine lesions. *Brain Res*. 2004 Jul 2;1013(1):98–106.
273. Rattka M, Fluri F, Krstić M, Asan E, Volkman J. A novel approach to assess motor outcome of deep brain stimulation effects in the hemiparkinsonian rat: Staircase and cylinder test. *J Vis Exp [Internet]*. 2016 May 31 [cited 2016 Jul 28];(111). Available from: <http://www.jove.com/video/53951/a-novel-approach-to-assess-motor-outcome-deep-brain-stimulation>
274. Oueslati A, Sgambato-Faure V, Melon C, Kachidian P, Gubellini P, Amri M, et al. High-frequency stimulation of the subthalamic nucleus potentiates L-dopa-induced neurochemical changes in the striatum in a rat model of Parkinson's disease. *J Neurosci*. 2007 Feb 28;27(9):2377–86.
275. Lindemann C, Krauss JK, Schwabe K. Deep brain stimulation of the subthalamic nucleus in the 6-hydroxydopamine rat model of Parkinson's disease: Effects on sensorimotor gating. *Behav Brain Res*. 2012 Apr 21;230(1):243–50.
276. Li XH, Wang JY, Gao G, Chang JY, Woodward DJ, Luo F. High-frequency stimulation of the subthalamic nucleus restores neural and behavioral functions during reaction time task in a rat model of Parkinson's disease. *J Neurosci Res*. 2009;NA-NA.
277. Alpaugh M, Saint-Pierre M, Dubois M, Aubé B, Arsenaault D, Kriz J, et al. A novel wireless brain stimulation device for long-term use in freely moving mice. *Sci Rep*. 2019 Apr 23;9(1):1–10.
278. Badstuebner K, Gimsa U, Weber I, Tuchscherer A, Gimsa J. Deep Brain Stimulation of Hemiparkinsonian Rats with Unipolar and Bipolar Electrodes for up to 6 Weeks: Behavioral Testing of Freely Moving Animals. *Park Dis [Internet]*. 2017;2017. Available from: <https://www.ncbi.nlm.nih.gov/pmc/articles/PMC512044/>
279. Chassain C, Melon C, Salin P, Vitale F, Couraud S, Durif F, et al. Metabolic, synaptic and behavioral impact of 5-week chronic deep brain stimulation in hemiparkinsonian rats. *J Neurochem*. 2016 Mar 1;136(5):1004–16.
280. Forni C, Mainard O, Melon C, Goguenheim D, Kerkerian-Le Goff L, Salin P. Portable microstimulator for chronic deep brain stimulation in freely moving rats. *J Neurosci Methods*. 2012 Jul 30;209(1):50–7.
281. Harnack D, Meissner W, Paulat R, Hilgenfeld H, Müller WD, Winter C, et al. Continuous high-frequency stimulation in freely moving rats: Development of an implantable microstimulation system. *J Neurosci Methods*. 2008 Jan 30;167(2):278–91.
282. Soto-Montenegro ML, Pascau J, Desco M. Response to deep brain stimulation in the lateral hypothalamic area in a rat model of obesity: In vivo assessment of brain glucose metabolism. *Mol Imaging Biol*. 2014 Dec 1;16(6):830–7.
283. Casquero-Veiga M, Bueno-Fernandez C, Romero-Miguel D, Lamanna-Rama N, Nacher J, Desco M, et al. Exploratory study of the long-term footprint of deep brain stimulation on brain metabolism and neuroplasticity in an animal model of obesity. *Sci Rep*. 2021 Mar 10;11(1):5580.
284. Casquero-Veiga M, Hadar R, Pascau J, Winter C, Desco M, Soto-Montenegro ML. Response to deep brain stimulation in three brain targets with implications in mental disorders: a PET study in rats. *PLoS ONE [Internet]*. 2016 Dec 29 [cited 2017 Mar 20];11(12). Available from: <http://www.ncbi.nlm.nih.gov/pmc/articles/PMC5199108/>
285. Klein J, Soto-Montenegro ML, Pascau J, Günther L, Kupsch A, Desco M, et al. A novel approach to investigate neuronal network activity patterns affected by deep brain stimulation in rats. *J Psychiatr Res*. 2011 Jul;45(7):927–30.
286. Nielsen MS, Andersen F, Cumming P, Møller A, Gjedde A, Sørensen JC, et al. Subthalamic high-frequency deep brain stimulation evaluated by positron emission tomography in a porcine Parkinson model. *Brain Res J*. 2012 Sep;5(3–4):309–25.

287. Paralikar K, Santa W, Iyer R, Thom A, Su X, Hovland E, et al. A fully implantable and rechargeable neurostimulation system for animal research. In: 2015 7th International IEEE/EMBS Conference on Neural Engineering (NER). 2015. p. 418–21.
288. Apetz N, Paralikar K, Neumaier B, Drzezga A, Wiedermann D, Iyer R, et al. Towards chronic deep brain stimulation in freely moving hemiparkinsonian rats: applicability and functionality of a fully implantable stimulation system. *J Neural Eng*. 2021 Jun 1;18(3):036018.
289. Benazzouz A, Gross C, Féger J, Boraud T, Bioulac B. Reversal of rigidity and improvement in motor performance by subthalamic high-frequency stimulation in MPTP-treated monkeys. *Eur J Neurosci*. 1993 Apr 1;5(4):382–9.
290. Bergman H, Wichmann T, DeLong MR. Reversal of experimental parkinsonism by lesions of the subthalamic nucleus. *Science*. 1990 Sep 21;249(4975):1436–8.
291. Moro E, Scerrati M, Romito LMA, Roselli R, Tonali P, Albanese A. Chronic subthalamic nucleus stimulation reduces medication requirements in Parkinson's disease. *Neurology*. 1999 Jan 7;53(1):85–85.
292. Kumar R, Lozano AM, Kim YJ, Hutchison WD, Sime E, Halket E, et al. Double-blind evaluation of subthalamic nucleus deep brain stimulation in advanced Parkinson's disease. *Neurology*. 1998 Jan 9;51(3):850–5.
293. Vingerhoets FJG, Villemure JG, Temperli P, Pollo C, Pralong E, Ghika J. Subthalamic DBS replaces levodopa in Parkinson's disease: Two-year follow-up. *Neurology*. 2002 Dec 2;58(3):396–401.
294. Udupa K, Chen R. The mechanisms of action of deep brain stimulation and ideas for the future development. *Prog Neurobiol*. 2015 Oct;133:27–49.
295. Martinez-Ramirez D, Hu W, Bona AR, Okun MS, Shukla AW. Update on deep brain stimulation in Parkinson's disease. *Transl Neurodegener*. 2015;4:12.
296. McIntyre CC, Anderson RW. Deep brain stimulation mechanisms: the control of network activity via neurochemistry modulation. *J Neurochem*. 2016 Jun 8;
297. Herrington TM, Cheng JJ, Eskandar EN. Mechanisms of deep brain stimulation. *J Neurophysiol*. 2016 Jan 1;115(1):19–38.
298. Kühn AA, Volkman J. Innovations in deep brain stimulation methodology. *Mov Disord Off J Mov Disord Soc*. 2016 Jul 12;
299. Mackovski N, Liao J, Weng R, Wei X, Wang R, Chen Z, et al. Reversal effect of simvastatin on the decrease in cannabinoid receptor 1 density in 6-hydroxydopamine lesioned rat brains. *Life Sci*. 2016 Jun 15;155:123–32.
300. Noor NA, Mohammed HS, Mourad IM, Khadrawy YA, Aboul Ezz HS. A promising therapeutic potential of cerebrolysin in 6-OHDA rat model of Parkinson's disease. *Life Sci*. 2016 Jun 15;155:174–9.
301. Shi K, Liu X, Qiao D, Hou L. Effects of treadmill exercise on spontaneous firing activities of striatal neurons in a rat model of Parkinson's disease. *Motor Control*. 2017 Jan;21(1):58–71.
302. Wang X, Yang HA, Wang XN, Du YF. Effect of siRNA-induced silencing of cellular prion protein on tyrosine hydroxylase expression in the substantia nigra of a rat model of Parkinson's disease. *Genet Mol Res [Internet]*. 2016 [cited 2016 Jul 28];15(2). Available from: <http://www.funpecrp.com.br/gmr/year2016/vol15-2/pdf/gmr7406.pdf>
303. Wang ZY, Lian H, Zhou L, Zhang YM, Cai QQ, Zheng LF, et al. Altered expression of D1 and D2 dopamine receptors in vagal neurons innervating the gastric muscularis externa in a Parkinson's disease rat model. *J Park Dis*. 2016 May 26;6(2):317–23.
304. Gerlach M, Riederer P. Animal models of Parkinson's disease: An empirical comparison with the phenomenology of the disease in man. *J Neural Transm*. 1996 Aug;103(8–9):987–1041.
305. He Z, Jiang Y, Xu H, Jiang H, Jia W, Sun P, et al. High frequency stimulation of subthalamic nucleus results in behavioral recovery by increasing striatal dopamine release in 6-hydroxydopamine lesioned rat. *Behav Brain Res*. 2014 Apr 15;263:108–14.

306. Temel Y, Visser-Vandewalle V, Aendekerk B, Rutten B, Tan S, Scholtissen B, et al. Acute and separate modulation of motor and cognitive performance in parkinsonian rats by bilateral stimulation of the subthalamic nucleus. *Exp Neurol*. 2005 May;193(1):43–52.
307. Pinnell RC, Pereira de Vasconcelos A, Cassel JC, Hofmann UG. A Miniaturized, Programmable Deep-Brain Stimulator for Group-Housing and Water Maze Use. *Front Neurosci* [Internet]. 2018 [cited 2019 Dec 4];12. Available from: <https://www.frontiersin.org/articles/10.3389/fnins.2018.00231/full>
308. Eberman K, Gomadam P, Jain G, Scott E. Material and Design Options for Avoiding Lithium Plating during Charging. *ECS Trans*. 2010 Dec 17;25(35):47–58.
309. Schallert T, Tillerson JL. Intervention Strategies for Degeneration of Dopamine Neurons in Parkinsonism. In: Emerich DF, Dean RL, Sanberg PR, editors. *Central Nervous System Diseases: Innovative Animal Models from Lab to Clinic* [Internet]. Totowa, NJ: Humana Press; 2000. p. 131–51. (Contemporary Neuroscience). Available from: https://doi.org/10.1007/978-1-59259-691-1_8
310. Schallert T, Fleming SM, Leasure JL, Tillerson JL, Bland ST. CNS plasticity and assessment of forelimb sensorimotor outcome in unilateral rat models of stroke, cortical ablation, parkinsonism and spinal cord injury. *Neuropharmacology*. 2000 Apr;39(5):777–87.
311. Qi J, Leahy RM, Cherry SR, Chatzioannou A, Farquhar TH. High-resolution 3D Bayesian image reconstruction using the microPET small-animal scanner. *Phys Med Biol*. 1998 Apr;43(4):1001–13.
312. Vollmar S, Hampl JA, Kracht L, Herholz K. Integration of functional data (PET) into brain surgery planning and neuronavigation. In: *Advances in Medical Engineering* [Internet]. Springer, Berlin, Heidelberg; 2007 [cited 2018 Feb 15]. p. 98–103. (Springer Proceedings in Physics). Available from: https://link.springer.com/chapter/10.1007/978-3-540-68764-1_16
313. Swanson, Larry W LW. *Brain maps : structure of the rat brain : a laboratory guide with printed and electronic templates for data, models and schematics* [Internet]. 2nd rev. ed. Amsterdam ; Oxford : Elsevier; 1998. Available from: <https://trove.nla.gov.au/version/39814314>
314. Smith S, Nichols T. Threshold-free cluster enhancement: Addressing problems of smoothing, threshold dependence and localisation in cluster inference. *NeuroImage*. 2009 Jan 1;44(1):83–98.
315. Paxinos G, Watson C. *The rat brain in stereotaxic coordinates* [Internet]. 2005 [cited 2018 Feb 15]. Available from: http://www.123library.org/book_details/?id=44462
316. Machado A, Rezaei AR, Kopell BH, Gross RE, Sharan AD, Benabid AL. Deep brain stimulation for Parkinson's disease: Surgical technique and perioperative management. *Mov Disord*. 2006;21(S14):S247–58.
317. Dowd E, Dunnett SB. Deficits in a lateralized associative learning task in dopamine-depleted rats with functional recovery by dopamine-rich transplants. *Eur J Neurosci*. 2004;20(7):1953–9.
318. Magistretti PJ, Pellerin L. Cellular mechanisms of brain energy metabolism and their relevance to functional brain imaging. Howseman A, Zeki S, editors. *Philos Trans R Soc Lond B Biol Sci*. 1999 Jul 29;354(1387):1155–63.
319. Jueptner M, Weiller C. Review: does measurement of regional cerebral blood flow reflect synaptic activity? Implications for PET and fMRI. *NeuroImage*. 1995 Jun;2(2):148–56.
320. Hamani C, Richter E, Schwab JM, Lozano AM. Bilateral Subthalamic Nucleus Stimulation for Parkinson's Disease: A Systematic Review of the Clinical Literature. *Neurosurgery*. 2005 Jun 1;56(6):1313–24.
321. Bakker M, Esselink RAJ, Munneke M, Limousin-Dowsey P, Speelman HD, Bloem BR. Effects of stereotactic neurosurgery on postural instability and gait in Parkinson's disease. *Mov Disord*. 2004 Sep;19(9):1092–9.
322. Ricchi V, Zibetti M, Angrisano S, Merola A, Arduino N, Artusi CA, et al. Transient effects of 80 Hz stimulation on gait in STN DBS treated PD patients: A 15 months follow-up study. *Brain Stimulat*. 2012 Jul;5(3):388–92.
323. Krack P, Batir A, Van Blercom N, Chabardes S, Fraix V, Ardouin C, et al. Five-Year Follow-up of Bilateral Stimulation of the Subthalamic Nucleus in Advanced Parkinson's Disease. *N Engl J Med*. 2003 Nov 13;349(20):1925–34.

324. Schupbach WMM. Stimulation of the subthalamic nucleus in Parkinson's disease: a 5 year follow up. *J Neurol Neurosurg Psychiatry*. 2005 Dec 1;76(12):1640–4.
325. Salin P, Manrique C, Forni C, Goff LKL. High-Frequency Stimulation of the Subthalamic Nucleus Selectively Reverses Dopamine Denervation-Induced Cellular Defects in the Output Structures of the Basal Ganglia in the Rat. *J Neurosci*. 2002 Jun 15;22(12):5137–48.
326. Bacci JJ, Absi EH, Manrique C, Baunez C, Salin P, Kerkerian-Le Goff L. Differential effects of prolonged high frequency stimulation and of excitotoxic lesion of the subthalamic nucleus on dopamine denervation-induced cellular defects in the rat striatum and globus pallidus. *Eur J Neurosci*. 2004 Dec 1;20(12):3331–41.
327. Melon C, Chassain C, Bielicki G, Renou JP, Goff LKL, Salin P, et al. Progressive brain metabolic changes under deep brain stimulation of subthalamic nucleus in parkinsonian rats. *J Neurochem*. 2015;132(6):703–12.
328. Meissner W, Guigoni C, Cirilli L, Garret M, Bioulac BH, Gross CE, et al. Impact of chronic subthalamic high-frequency stimulation on metabolic basal ganglia activity: a 2-deoxyglucose uptake and cytochrome oxidase mRNA study in a macaque model of Parkinson's disease. *Eur J Neurosci*. 2007 Mar 1;25(5):1492–500.
329. Rohleder C, Wiedermann D, Neumaier B, Drzezga A, Timmermann L, Graf R, et al. The functional networks of prepulse inhibition: Neuronal connectivity analysis based on FDG-PET in awake and unrestrained rats. *Front Behav Neurosci*. 2016;148.
330. Chang VC, Chou KL. Deep brain stimulation for Parkinson's disease: patient selection and motor outcomes. *Med Health R I*. 2006 Apr;89(4):142–4.
331. Pollak P. Chapter 9 - Deep brain stimulation for Parkinson's disease – patient selection. In: Lozano AM, Hallett M, editors. *Handbook of Clinical Neurology* [Internet]. Elsevier; 2013 [cited 2021 Oct 11]. p. 97–105. (Brain Stimulation; vol. 116). Available from: <https://www.sciencedirect.com/science/article/pii/B9780444534972000097>
332. Lang AE, Widner H. Deep brain stimulation for Parkinson's disease: Patient selection and evaluation. *Mov Disord*. 2002;17(S3):S94–101.
333. Herzog J, Fietzek U, Hamel W, Morsnowski A, Steigerwald F, Schrader B, et al. Most effective stimulation site in subthalamic deep brain stimulation for Parkinson's disease. *Mov Disord*. 2004;19(9):1050–4.
334. Paek SH, Yun JY, Song SW, Kim IK, Hwang JH, Kim JW, et al. The clinical impact of precise electrode positioning in STN DBS on three-year outcomes. *J Neurol Sci*. 2013 Apr 15;327(1–2):25–31.
335. Blomstedt P, Sandvik U, Linder J, Fredricks A, Forsgren L, Hariz MI. Deep brain stimulation of the subthalamic nucleus versus the zona incerta in the treatment of essential tremor. *Acta Neurochir (Wien)*. 2011 Dec 1;153(12):2329–35.
336. Fytagoridis A, Sandvik U, Åström M, Bergenheim T, Blomstedt P. Long term follow-up of deep brain stimulation of the caudal zona incerta for essential tremor. *J Neurol Neurosurg Psychiatry*. 2012 Mar 1;83(3):258–62.
337. Simola N, Morelli M, Carta AR. The 6-hydroxydopamine model of Parkinson's disease. *Neurotox Res*. 2007 Apr;11(3–4):151–67.
338. Martens HCF, Toader E, Decré MMJ, Anderson DJ, Vetter R, Kipke DR, et al. Spatial steering of deep brain stimulation volumes using a novel lead design. *Clin Neurophysiol*. 2011 Mar 1;122(3):558–66.
339. Deuschl G, Herzog J, Kleiner-Fisman G, Kubu C, Lozano AM, Lyons KE, et al. Deep brain stimulation: Postoperative issues. *Mov Disord*. 2006 Jun;21(S14):S219–37.
340. Boulet S, Lacombe E, Carcenac C, Feuerstein C, Sgambato-Faure V, Poupard A, et al. Subthalamic stimulation-induced forelimb dyskinesias are linked to an increase in glutamate levels in the substantia nigra pars reticulata. *J Neurosci*. 2006 Oct 18;26(42):10768–76.
341. Lee KJ, Shim I, Sung JH, Hong JT, Kim I sup, Cho CB. Striatal glutamate and GABA after high frequency subthalamic stimulation in parkinsonian rat. *J Korean Neurosurg Soc*. 2017 Mar 1;60(2):138–45.

342. Hefti F, Enz A, Melamed E. Partial lesions of the nigrostriatal pathway in the rat: Acceleration of transmitter synthesis and release of surviving dopaminergic neurones by drugs. *Neuropharmacology*. 1985 Jan 1;24(1):19–23.
343. Schüpbach WMM, Chastan N, Welter ML, Houeto JL, Mesnage V, Bonnet AM, et al. Stimulation of the subthalamic nucleus in Parkinson's disease: a 5 year follow up. *J Neurol Neurosurg Psychiatry*. 2005 Dec 1;76(12):1640–4.
344. Waldau B, Clayton DA, Gasperson LB, Turner DA. Analysis of the Time Course of the Effect of Subthalamic Nucleus Stimulation upon Hand Function in Parkinson's Patients. *Stereotact Funct Neurosurg*. 2011 Feb;89(1):48–55.
345. Merola A, Romagnolo A, Bernardini A, Rizzi L, Artusi CA, Lanotte M, et al. Earlier versus later subthalamic deep brain stimulation in Parkinson's disease. *Parkinsonism Relat Disord*. 2015 Aug;21(8):972–5.
346. Chang JY, Shi LH, Luo F, Zhang WM, Woodward DJ. Studies of the neural mechanisms of deep brain stimulation in rodent models of Parkinson's disease. *Neurosci Biobehav Rev*. 2007;31(5):643–57.
347. Darbakay Y, Forni C, Amalric M, Baunez C. High frequency stimulation of the subthalamic nucleus has beneficial antiparkinsonian effects on motor functions in rats, but less efficiency in a choice reaction time task. *Eur J Neurosci*. 2003 Aug 1;18(4):951–6.
348. Li Q, Ke Y, Chan DCW, Qian ZM, Yung KKL, Ko H, et al. Therapeutic deep brain stimulation in parkinsonian rats directly influences motor cortex. *Neuron*. 2012 Dec 6;76(5):1030–41.
349. Polar CA, Gupta R, Lehmkuhle MJ, Dorval AD. Correlation between cortical beta power and gait speed is suppressed in a parkinsonian model, but restored by therapeutic deep brain stimulation. *Neurobiol Dis*. 2018 Sep 1;117:137–48.
350. Sutton AC, O'Connor KA, Piliitsis JG, Shin DS. Stimulation of the subthalamic nucleus engages the cerebellum for motor function in parkinsonian rats. *Brain Struct Funct*. 2015 Nov 1;220(6):3595–609.
351. Brooks CMCC. The history of thought concerning the hypothalamus and its functions. *Brain Res Bull*. 1988 Jun 1;20(6):657–67.
352. Çavdar S, Şan T, Aker R, Şehrlif Ü, Onat F. Cerebellar connections to the dorsomedial and posterior nuclei of the hypothalamus in the rat. *J Anat*. 2001 Jan;198(Pt 1):37–45.
353. Onat F, Çavdar S. Cerebellar connections: hypothalamus. *The Cerebellum*. 2003 Dec 1;2(4):263–9.
354. de Git KCG, van Tuijl DC, Luijendijk MCM, Wolterink-Donselaar IG, Ghanem A, Conzelmann K, et al. Anatomical projections of the dorsomedial hypothalamus to the periaqueductal grey and their role in thermoregulation: a cautionary note. *Physiol Rep*. 2018 Jul 25;6(14):e13807.
355. Horst GJT, Luiten PGM. The projections of the dorsomedial hypothalamic nucleus in the rat. *Brain Res Bull*. 1986 Feb 1;16(2):231–48.
356. Ullah F, dos Anjos-Garcia T, Mendes-Gomes J, Elias-Filho DH, Falconi-Sobrinho LL, Freitas RL de, et al. Connexions between the dorsomedial division of the ventromedial hypothalamus and the dorsal periaqueductal grey matter are critical in the elaboration of hypothalamically mediated panic-like behaviour. *Behav Brain Res*. 2017 Feb;319:135–47.
357. Choi DC, Furay AR, Evanson NK, Ostrander MM, Ulrich-Lai YM, Herman JP. Bed Nucleus of the Stria Terminalis Subregions Differentially Regulate Hypothalamic–Pituitary–Adrenal Axis Activity: Implications for the Integration of Limbic Inputs. *J Neurosci*. 2007 Feb 21;27(8):2025–34.
358. Feldman S, Siegel RA, Weidenfeld J, Conforti N, Melamed E. Role of medial forebrain bundle catecholaminergic fibers in the modulation of glucocorticoid negative feedback effects. *Brain Res*. 1983 Feb 7;260(2):297–300.
359. Floyd NS, Price JL, Ferry AT, Keay KA, Bandler R. Orbitomedial prefrontal cortical projections to hypothalamus in the rat. *J Comp Neurol*. 2001;432(3):307–28.
360. Vogt BA, Miller MW. Cortical connections between rat cingulate cortex and visual, motor, and postsubicular cortices. *J Comp Neurol*. 1983;216(2):192–210.

361. van Groen T, Michael Wyss J. Connections of the retrosplenial granular cortex in the rat. *J Comp Neurol*. 1990;300(4):593–606.
362. Perlberg V, Lambert J, Butler B, Felfli M, Valabrègue R, Privat AL, et al. Alterations of the nigrostriatal pathway in a 6-OHDA rat model of Parkinson's disease evaluated with multimodal MRI. *PLoS One*. 2018;13(9):e0202597.
363. Chronister RB, Walding JS, Aldes LD, Marco LA. Interconnections between substantia nigra reticulata and medullary reticular formation. *Brain Res Bull*. 1988 Aug 1;21(2):313–7.
364. Vertes RP, Martin GF, Waltzer R. An autoradiographic analysis of ascending projections from the medullary reticular formation in the rat. *Neuroscience*. 1986 Nov 1;19(3):873–98.
365. Gerfen CR, Staines WA, Fibiger HC, Arbuthnott GW. Crossed connections of the substantia nigra in the rat. *J Comp Neurol*. 1982;207(3):283–303.
366. Shammah-Lagnado SJ, Costa MSMO, Ricardo JA. Afferent connections of the parvocellular reticular formation: A horseradish peroxidase study in the rat. *Neuroscience*. 1992 Sep 1;50(2):403–25.
367. Ter Horst GJ, Copray JCV, Liem RSB, Van Willigen JD. Projections from the rostral parvocellular reticular formation to pontine and medullary nuclei in the rat: Involvement in autonomic regulation and orofacial motor control. *Neuroscience*. 1991 Jan 1;40(3):735–58.
368. Huerta MF, Frankfurter A, Harting JK. Studies of the principal sensory and spinal trigeminal nuclei of the rat: Projections to the superior colliculus, inferior olive, and cerebellum. *J Comp Neurol*. 1983;220(2):147–67.
369. de Lahunta A, Glass E. Chapter 8 - Upper Motor Neuron. In: de Lahunta A, Glass E, editors. *Veterinary Neuroanatomy and Clinical Neurology (Third Edition)* [Internet]. Saint Louis: W.B. Saunders; 2009 [cited 2021 Nov 3]. p. 192–220. Available from: <https://www.sciencedirect.com/science/article/pii/B9780721667065000081>
370. Tang H, Wu GS, Xie J, He X, Deng K, Wang H, et al. Brain-wide map of projections from mice ventral subiculum. *Neurosci Lett*. 2016 Aug 26;629:171–9.
371. Insausti R, Herrero MT, Witter MP. Entorhinal cortex of the rat: Cytoarchitectonic subdivisions and the origin and distribution of cortical efferents. *Hippocampus*. 1997;7(2):146–83.
372. Schultz C, Engelhardt M. Anatomy of the Hippocampal Formation. *Hippocampus Clin Neurosci*. 2014;34:6–17.
373. Viskontas IV, Carr VA, Engel SA, Knowlton BJ. The neural correlates of recollection: Hippocampal activation declines as episodic memory fades. *Hippocampus*. 2009;19(3):265–72.
374. Maller JJ, Welton T, Middione M, Callaghan FM, Rosenfeld JV, Grieve SM. Revealing the Hippocampal Connectome through Super-Resolution 1150-Direction Diffusion MRI. *Sci Rep*. 2019 Feb 20;9(1):2418.
375. Brown TI, Ross RS, Tobyne SM, Stern CE. Cooperative interactions between hippocampal and striatal systems support flexible navigation. *NeuroImage*. 2012 Apr 2;60(2):1316–30.
376. Yao N, Cheung C, Pang S, Shek-kwan Chang R, Lau KK, Suckling J, et al. Multimodal MRI of the hippocampus in Parkinson's disease with visual hallucinations. *Brain Struct Funct*. 2016 Jan;221(1):287–300.
377. Gironell A, Kulisevsky J, Rami L, Fortuny N, García-Sánchez C, Pascual-Sedano B. Effects of pallidotomy and bilateralsubthalamic stimulation on cognitivefunction in Parkinson disease. *J Neurol*. 2003 Aug 1;250(8):917–23.
378. Ventre-Dominey J, Mollion H, Thobois S, Broussolle E. Distinct effects of dopamine vs STN stimulation therapies in associative learning and retention in Parkinson disease. *Behav Brain Res*. 2016 Apr 1;302:131–41.
379. Smeding HMM, Speelman JD, Koning-Haanstra M, Schuurman PR, Nijssen P, Laar T van, et al. Neuropsychological effects of bilateral STN stimulation in Parkinson disease: A controlled study. *Neurology*. 2006 Jun 27;66(12):1830–6.

380. Alegret M, Junqué C, Valdeoriola F, Vendrell P, Pilleri M, Rumià J, et al. Effects of Bilateral Subthalamic Stimulation on Cognitive Function in Parkinson Disease. *Arch Neurol*. 2001 Aug 1;58(8):1223-7.
381. Hacker CD, Perlmutter JS, Criswell SR, Ances BM, Snyder AZ. Resting state functional connectivity of the striatum in Parkinson's disease. *Brain*. 2012 Dec 1;135(12):3699-711.
382. Perciavalle V, Apps R, Bracha V, Delgado-García JM, Gibson AR, Leggio M, et al. Consensus Paper: Current Views on the Role of Cerebellar Interpositus Nucleus in Movement Control and Emotion. *The Cerebellum*. 2013 Oct;12(5):738-57.
383. Kelly RM, Strick PL. Cerebellar Loops with Motor Cortex and Prefrontal Cortex of a Nonhuman Primate. *J Neurosci*. 2003 Sep 10;23(23):8432-44.
384. Alexander GE, DeLong MR, Strick PL. Parallel Organization of Functionally Segregated Circuits Linking Basal Ganglia and Cortex. *Annu Rev Neurosci*. 1986;9:357-81.
385. Bostan AC, Dum RP, Strick PL. The basal ganglia communicate with the cerebellum. *Proc Natl Acad Sci*. 2010 May 4;107(18):8452-6.
386. Hoshi E, Tremblay L, Féger J, Carras PL, Strick PL. The cerebellum communicates with the basal ganglia. *Nat Neurosci*. 2005 Nov;8(11):1491-3.
387. Yu W, Krook-Magnuson E. Cognitive Collaborations: Bidirectional Functional Connectivity Between the Cerebellum and the Hippocampus. *Front Syst Neurosci*. 2015 Dec 22;9:177.
388. Aumann TD, Rawson JA, Finkelstein DI, Horne MK. Projections from the lateral and interposed cerebellar nuclei to the thalamus of the rat: A light and electron microscopic study using single and double anterograde labelling. *J Comp Neurol*. 1994;349(2):165-81.
389. Torquati T. Sulla presenza di una sostanza azotata nei germogli del semi di 'vicia faba'. *Arch Farm Sper*. 1913;(15):213-23.
390. Guggenheim M. Dioxypyphenylalanin, eine neue Aminosäure aus Vicia faba. 1913 Jan 1;88(4):276-84.
391. Holtz P. Dopadecarboxylase. *Naturwissenschaften*. 1939 Oct 1;27(43):724-5.
392. Montagu KA. Catechol Compounds in Rat Tissues and in Brains of Different Animals. *Nature*. 1957 Aug;180(4579):244-5.
393. Holtz P, Balzer H, Westermann E, Wezler E. Beeinflussung der Evipannarkose durch Reserpin, Iproniazid und biogene Amine. *Naunyn-Schmiedebergs Arch Für Exp Pathol Pharmacol*. 1957 Jul 1;231(4):333-48.
394. Sano I, Gamo T, Kakimoto Y, Taniguchi K, Takesada M, Nishinuma K. Distribution of catechol compounds in human brain. *Biochim Biophys Acta*. 1959 Jan 1;32:586-7.
395. Bertler Å, Rosengren E. Occurrence and distribution of dopamine in brain and other tissues. *Experientia*. 1959 Jan 1;15(1):10-1.
396. Ehringer H, Hornykiewicz O. Verteilung Von Noradrenalin Und Dopamin (3-Hydroxytyramin) Im Gehirn Des Menschen Und Ihr Verhalten Bei Erkrankungen Des Extrapyramidalen Systems. *Klin Wochenschr*. 1960 Dec 1;38(24):1236-9.
397. Birkmayer W, Hornykiewicz O. Der L-Dioxyphenylalanin (DOPA)-Effekt bei der Parkinson-Akinese. *Wien Klin Wschr*. 1961;(73):787-8.
398. Cotzias GC, Papavasiliou PS, Gellene R. Modification of Parkinsonism — Chronic Treatment with L-Dopa. *N Engl J Med*. 1969 Feb 13;280(7):337-45.
399. Cotzias GC, Van Woert MH, Schiffer LM. Aromatic Amino Acids and Modification of Parkinsonism. *N Engl J Med*. 1967 Feb 16;276(7):374-9.
400. Ahlskog JE, Muentert MD. Frequency of levodopa-related dyskinesias and motor fluctuations as estimated from the cumulative literature. *Mov Disord*. 2001;16(3):448-58.
401. Thanvi B, Lo N, Robinson T. Levodopa-induced dyskinesia in Parkinson's disease: clinical features, pathogenesis, prevention and treatment. *Postgrad Med J*. 2007 Jun 1;83(980):384-8.

402. Denny AP, Behari M. Motor fluctuations in Parkinson's disease. *J Neurol Sci.* 1999 May 1;165(1):18-23.
403. Mouradian MM, Junecos JL, Fabbrini G, Schlegel J, Bartko JJ, Chase TN. Motor fluctuations in Parkinson's disease: Central pathophysiological mechanisms, part II. *Ann Neurol.* 1988 Sep 1;24(3):372-8.
404. Contin M, Riva R, Martinelli P, Albani F, Avoni P, Baruzzi A. Levodopa Therapy Monitoring in Patients With Parkinson Disease: a Kinetic-Dynamic Approach. *Ther Drug Monit.* 2001 Dec;23(6):621-9.
405. Marsden CD, Parkes JD, Rees JE. A year's Comparison of Treatment of Patients with Parkinson's Disease with Levodopa Combined with Carbidopa versus Treatment with Levodopa Alone. *The Lancet.* 1973 Dec 29;302(7844):1459-62.
406. Rinne UK, Birket-Smith E, Dupont E, Hansen E, Hyyppä M, Marttila R, et al. Levodopa alone and in combination with a peripheral decarboxylase inhibitor benserazide (madopar®) in the treatment of Parkinson's disease. *J Neurol.* 1975 Dec 1;211(1):1-9.
407. Parkinson Study Group. Entacapone improves motor fluctuations in levodopa-treated Parkinson's disease patients. *Ann Neurol.* 1997;42:747-55.
408. Adler CH, Singer C, O'Brien C, Hauser RA, Lew MF, Marek KL, et al. Randomized, Placebo-Controlled Study of Tolcapone in Patients With Fluctuating Parkinson Disease Treated With Levodopa-Carbidopa. *Arch Neurol.* 1998 Aug 1;55(8):1089-95.
409. Parkinson Study Group. A Randomized Placebo-Controlled Trial of Rasagiline in Levodopa-Treated Patients With Parkinson Disease and Motor Fluctuations: The PRESTO Study. *Arch Neurol.* 2005 Feb 1;62(2):241-8.
410. Waters CH, Sethi KD, Hauser RA, Molho E, Bertoni JM. Zydys selegiline reduces off time in Parkinson's disease patients with motor fluctuations: A 3-month, randomized, placebo-controlled study. *Mov Disord.* 2004;19(4):426-32.
411. Koller WC, Hutton JT, Tolosa E, Capilldeo R, Group the CS. Immediate-release and controlled-release carbidopa/levodopa in PD: A 5-year randomized multicenter study. *Neurology.* 1999 Sep 1;53(5):1012-1012.
412. Chase TN, Engber TM, Mouradian MM. Palliative and prophylactic benefits of continuously administered dopaminomimetics in Parkinson's disease. *Neurology.* 1994 Jul;44(7 Suppl 6):S15-18.
413. Yeh KC, August TF, Bush DF, Lasseter KC, Musson DG, Schwartz S, et al. Pharmacokinetics and bioavailability of Sinemet CR: a summary of human studies. *Neurology.* 1989 Nov 1;39(11 Suppl 2):25-38.
414. Timpka J, Fox T, Fox K, Honig H, Odin P, Martinez-Martin P, et al. Improvement of dyskinesias with l-dopa infusion in advanced Parkinson's disease. *Acta Neurol Scand.* 2016;133(6):451-8.
415. Karlsborg M, Korbo L, Regeur L, Glad A. Duodopa pump treatment in patients with advanced Parkinson's disease. .6.
416. Shoulson I, Glaubiger GA, Chase TN. On-off response: Clinical and biochemical correlations during oral and intravenous levodopa administration in parkinsonian patients. *Neurology.* 1975 Dec 1;25(12):1144-1144.
417. LeWitt PA. Levodopa therapy for Parkinson's disease: Pharmacokinetics and pharmacodynamics. *Mov Disord.* 2014;30(1):64-72.
418. Newcomer TA, Rosenberg PA, Aizenman E. Iron-Mediated Oxidation of 3,4-Dihydroxyphenylalanine to an Excitotoxin. *J Neurochem.* 1995;64(4):1742-8.
419. Huot P, Fox SH, Brothchie JM. The serotonergic system in Parkinson's disease. *Prog Neurobiol.* 2011 Oct 1;95(2):163-212.
420. Politis M, Wu K, Loane C, Quinn NP, Brooks DJ, Rehncrona S, et al. Serotonergic Neurons Mediate Dyskinesia Side Effects in Parkinson's Patients with Neural Transplants. *Sci Transl Med.* 2010 Jun 30;2(38):38ra46-38ra46.

421. Nahimi A, Høltzermann M, Landau AM, Simonsen M, Jakobsen S, Alstrup AKO, et al. Serotonergic modulation of receptor occupancy in rats treated with l-DOPA after unilateral 6-OHDA lesioning. *J Neurochem.* 2012;120(5):806–17.
422. Tanaka H, Kannari K, Maeda T, Tomiyama M, Suda T, Matsunaga M. Role of serotonergic neurons in L-DOPA-derived extracellular dopamine in the striatum of 6-OHDA-lesioned rats. *NeuroReport.* 1999 Feb 25;10(3):631–4.
423. Navailles S, Bioulac B, Gross C, De Deurwaerdère P. Serotonergic neurons mediate ectopic release of dopamine induced by l-DOPA in a rat model of Parkinson's disease. *Neurobiol Dis.* 2010 Apr 1;38(1):136–43.
424. Bejjani BP, Arnulf I, Demeret S, Damier P, Bonnet AM, Houeto JL, et al. Levodopa-induced dyskinesias in Parkinson's disease: Is sensitization reversible? *Ann Neurol.* 2000;47(5):655–8.
425. Hilker R, Voges J, Thiel A, Ghaemi M, Herholz K, Sturm V, et al. Deep brain stimulation of the subthalamic nucleus versus levodopa challenge in Parkinson's disease: measuring the on- and off-conditions with FDG-PET. *J Neural Transm.* 2002 Oct 1;109(10):1257–64.
426. Nutt JG, Rufener SL, Carter JH, Anderson VC, Pahwa R, Hammerstad JP, et al. Interactions between deep brain stimulation and levodopa in Parkinson's disease. *Neurology.* 2001 Nov 27;57(10):1835–42.
427. Feigin A, Fukuda M, Dhawan V, Przedborski S, Jackson-Lewis V, Mentis MJ, et al. Metabolic correlates of levodopa response in Parkinson's disease. *Neurology.* 2001 Dec 11;57(11):2083–8.
428. Trugman JM, Anthony Hubbard C, Bennett JP. Dose-related effects of continuous levodopa infusion in rats with unilateral lesions of the substantia nigra. *Brain Res.* 1996 Jul 1;725(2):177–83.
429. Lundblad M, Picconi B, Lindgren H, Cenci MA. A model of l-DOPA-induced dyskinesia in 6-hydroxydopamine lesioned mice: relation to motor and cellular parameters of nigrostriatal function. *Neurobiol Dis.* 2004 Jun;16(1):110–23.
430. Winkler C, Kirik D, Björklund A, Cenci MA. l-DOPA-Induced Dyskinesia in the Intrastratial 6-Hydroxydopamine Model of Parkinson's Disease: Relation to Motor and Cellular Parameters of Nigrostriatal Function. *Neurobiol Dis.* 2002 Jul;10(2):165–86.
431. Ding Y, Restrepo J, Won L, Hwang DY, Kim KS, Kang UJ. Chronic 3,4-dihydroxyphenylalanine treatment induces dyskinesia in aphakia mice, a novel genetic model of Parkinson's disease. *Neurobiol Dis.* 2007 Jul 1;27(1):11–23.
432. Delfino MA, Stefano AV, Ferrario JE, Taravini IRE, Murer MG, Gershanik OS. Behavioral sensitization to different dopamine agonists in a parkinsonian rodent model of drug-induced dyskinesias. *Behav Brain Res.* 2004 Jul 9;152(2):297–306.
433. Pençe S. Paw Preference in Rats. *J Basic Clin Physiol Pharmacol.* 2002 Mar 1;13(1):41–50.
434. Signore P, Nosten-Bertrand M, Chaoui M, Roubertoux PL, Marchaland C, Perez-Diaz F. An assessment of handedness in mice. *Physiol Behav.* 1991 Apr 1;49(4):701–4.
435. Lacombe E, Carcenac C, Boulet S, Feuerstein C, Bertrand A, Poupard A, et al. High-frequency stimulation of the subthalamic nucleus prolongs the increase in striatal dopamine induced by acute l-3,4-dihydroxyphenylalanine in dopaminergic denervated rats. *Eur J Neurosci.* 2007;26(6):1670–80.
436. Eidelberg D, Moeller JR, Dhawan V, Spetsieris P, Takikawa S, Ishikawa T, et al. The Metabolic Topography of Parkinsonism. *J Cereb Blood Flow Metab.* 1994 Sep 1;14(5):783–801.
437. Ma Y, Tang C, Spetsieris PG, Dhawan V, Eidelberg D. Abnormal metabolic network activity in Parkinson's disease: Test—retest reproducibility. *J Cereb Blood Flow Metab.* 2007 Mar;27(3):597–605.
438. Haslinger B, Erhard P, Kämpfe N, Boecker H, Rummey E, Schwaiger M, et al. Event-related functional magnetic resonance imaging in Parkinson's disease before and after levodopa. *Brain.* 2001 Mar 1;124(3):558–70.
439. Becker G, Bahri MA, Michel A, Hustadt F, Garraux G, Luxen A, et al. Comparative assessment of 6-[18F]fluoro-L-m-tyrosine and 6-[18F]fluoro-L-dopa to evaluate dopaminergic presynaptic integrity in a Parkinson's disease rat model. *J Neurochem.* 2017;141(4):626–35.

440. Hume SP, Opacka-Juffry J, Myers R, Ahier RG, Ashworth S, Brooks DJ, et al. Effect of L-dopa and 6-hydroxydopamine lesioning on [11C]raclopride binding in rat striatum, quantified using PET. *Synapse*. 1995 Sep;21(1):45–53.
441. Lerner RP, Bimpisidis Z, Agorastos S, Scherrer S, Dewey SL, Cenci MA, et al. Dissociation of metabolic and hemodynamic levodopa responses in the 6-hydroxydopamine rat model. *Neurobiol Dis*. 2016 Dec;96:31–7.
442. Ohlin KE, Sebastianutto I, Adkins CE, Lundblad C, Lockman PR, Cenci MA. Impact of L-DOPA treatment on regional cerebral blood flow and metabolism in the basal ganglia in a rat model of Parkinson's disease. *NeuroImage*. 2012 May;61(1):228–39.
443. Buhmann C, Glauche V, Stürenburg HJ, Oechsner M, Weiller C, Büchel C. Pharmacologically modulated fMRI---cortical responsiveness to levodopa in drug-naive hemiparkinsonian patients. *Brain*. 2003 Feb 1;126(2):451–61.
444. Apetz N, Neumaier B, Drzezga A, Timmermann L, Endepols H. Modulation of brain network recruitment caused by STN DBS and L-DOPA in parkinsonian rats. In: *Nuklearmedizin - NuclearMedicine* [Internet]. Georg Thieme Verlag KG; 2019 [cited 2022 Jan 11]. p. P34. Available from: <http://www.thieme-connect.de/DOI/DOI?10.1055/s-0039-1683629>
445. Pasquereau B, Turner RS. Primary Motor Cortex of the Parkinsonian Monkey: Differential Effects on the Spontaneous Activity of Pyramidal Tract-Type Neurons. *Cereb Cortex*. 2011 Jun 1;21(6):1362–78.
446. Shepherd GMG. Corticostriatal connectivity and its role in disease. *Nat Rev Neurosci*. 2013 Apr;14(4):278–91.
447. Schwarting RKW, Huston JP. Unilateral 6-hydroxydopamine lesions of meso-striatal dopamine neurons and their physiological sequelae. *Prog Neurobiol*. 1996 Jun;49(3):215–66.
448. Schwarting R, Huston J. The unilateral 6-hydroxydopamine lesion model in behavioral brain research. Analysis of functional deficits, recovery and treatments. *Prog Neurobiol*. 1996 Oct;50(2–3):275–331.
449. Esposito F, Tessitore A, Giordano A, De Micco R, Paccone A, Conforti R, et al. Rhythm-specific modulation of the sensorimotor network in drug-naive patients with Parkinson's disease by levodopa. *Brain*. 2013 Mar 1;136(3):710–25.
450. Wu T, Wang L, Chen Y, Zhao C, Li K, Chan P. Changes of functional connectivity of the motor network in the resting state in Parkinson's disease. *Neurosci Lett*. 2009 Aug 21;460(1):6–10.
451. Mitchell A, Chakraborty S. What does the mediodorsal thalamus do? *Front Syst Neurosci*. 2013;7:37.
452. Inglis WL, Winn P. The pedunculo-pontine tegmental nucleus: Where the striatum meets the reticular formation. *Prog Neurobiol*. 1995 Sep 1;47(1):1–29.
453. Saper CB, Loewy AD. Projections of the pedunculo-pontine tegmental nucleus in the rat: evidence for additional extrapyramidal circuitry. *Brain Res*. 1982 Dec 9;252(2):367–72.
454. Beckstead RM, Domesick VB, Nauta WJH. Efferent connections of the substantia nigra and ventral tegmental area in the rat. *Brain Res*. 1979 Oct 19;175(2):191–217.
455. Kahn I, Shohamy D. Intrinsic connectivity between the hippocampus, nucleus accumbens, and ventral tegmental area in humans. *Hippocampus*. 2013;23(3):187–92.
456. Truttti AC, Mulder MJ, Hommel B, Forstmann BU. Functional neuroanatomical review of the ventral tegmental area. *NeuroImage*. 2019 May 1;191:258–68.
457. Morales M, Margolis EB. Ventral tegmental area: cellular heterogeneity, connectivity and behaviour. *Nat Rev Neurosci*. 2017 Feb;18(2):73–85.
458. Winn P. How best to consider the structure and function of the pedunculo-pontine tegmental nucleus: Evidence from animal studies. *J Neurol Sci*. 2006 Oct 25;248(1):234–50.
459. Gordon-Fennell A, Gordon-Fennell L, Desai S, Marinelli M. The Lateral Preoptic Area and Its Projection to the VTA Regulate VTA Activity and Drive Complex Reward Behaviors. *Front Syst Neurosci*. 2020 Nov 3;14:581830.

460. Swanson LW, Mogenson GJ, Gerfen CR, Robinson P. Evidence for a projection from the lateral preoptic area and substantia innominata to the 'mesencephalic locomotor region' in the rat. *Brain Res.* 1984 Mar;295(1):161–78.
461. Reichard RA, Parsley KP, Subramanian S, Stevenson HS, Schwartz ZM, Sura T, et al. The lateral preoptic area and ventral pallidum embolden behavior. *Brain Struct Funct.* 2019 Apr;224(3):1245–65.
462. Aronoff R, Matyas F, Mateo C, Ciron C, Schneider B, Petersen CCH. Long-range connectivity of mouse primary somatosensory barrel cortex: Long-range connectivity of barrel cortex. *Eur J Neurosci.* 2010 Jun 9;31(12):2221–33.
463. Mufson EJ, Mesulam MM. Insula of the old world monkey. II: Afferent cortical input and comments on the claustrum. *J Comp Neurol.* 1982 Nov 20;212(1):23–37.
464. Ghaziri J, Tucholka A, Girard G, Houde JC, Boucher O, Gilbert G, et al. The Corticocortical Structural Connectivity of the Human Insula. *Cereb Cortex.* 2017 Feb;27(2):1216–28.
465. Lin HC, Pan HC, Lin SH, Lo YC, Shen ETH, Liao LD, et al. Central Thalamic Deep-Brain Stimulation Alters Striatal-Thalamic Connectivity in Cognitive Neural Behavior. *Front Neural Circuits [Internet].* 2016 [cited 2022 Jan 13];9. Available from: <https://www.frontiersin.org/article/10.3389/fncir.2015.00087>
466. Schmidt SL, Brocker DT, Swan BD, Turner DA, Grill WM. Evoked Potentials Reveal Neural Circuits Engaged by Human Deep Brain Stimulation. *Brain Stimulat.* 2020;13(6):1706–18.
467. Younce JR, Campbell MC, Hershey T, Tanenbaum AB, Milchenko M, Ushe M, et al. Resting-State Functional Connectivity Predicts STN DBS Clinical Response. *Mov Disord.* 2021;36(3):662–71.
468. Shen L, Jiang C, Hubbard CS, Ren J, He C, Wang D, et al. Subthalamic Nucleus Deep Brain Stimulation Modulates 2 Distinct Neurocircuits. *Ann Neurol.* 2020 Dec;88(6):1178–93.
469. Donoghue JP, Herkenham M. Neostriatal projections from individual cortical fields conform to histochemically distinct striatal compartments in the rat. *Brain Res.* 1986 Feb 19;365(2):397–403.
470. McDonald AJ. Organization of amygdaloid projections to the prefrontal cortex and associated striatum in the rat. *Neuroscience.* 1991 Jan 1;44(1):1–14.
471. Mondillon L, Mermillod M, Musca SC, Rieu I, Vidal T, Chambres P, et al. The combined effect of subthalamic nuclei deep brain stimulation and l-dopa increases emotion recognition in Parkinson's disease. *Neuropsychologia.* 2012 Oct 1;50(12):2869–79.
472. Grafton ST, Turner RS, Desmurget M, Bakay R, Delong M, Vitek J, et al. Normalizing motor-related brain activity: Subthalamic nucleus stimulation in Parkinson disease. *Neurology.* 2006 Apr 25;66(8):1192–9.
473. Gopinath K, Krishnamurthy V, Cabanban R, Crosson BA. Hubs of Anticorrelation in High-Resolution Resting-State Functional Connectivity Network Architecture. *Brain Connect.* 2015 Jun 1;5(5):267–75.
474. Nutt JG, Carter JH, Lea ES, Sexton GJ. Evolution of the response to levodopa during the first 4 years of therapy. *Ann Neurol.* 2002;51(6):686–93.
475. Merola A, Zibetti M, Angrisano S, Rizzi L, Ricchi V, Artusi CA, et al. Parkinson's disease progression at 30 years: a study of subthalamic deep brain-stimulated patients. *Brain.* 2011 Jul 1;134(7):2074–84.
476. Tessitore A, Amboni M, Esposito F, Russo A, Picillo M, Marcuccio L, et al. Resting-state brain connectivity in patients with Parkinson's disease and freezing of gait. *Parkinsonism Relat Disord.* 2012 Jul 1;18(6):781–7.
477. Hilker R, Voges J, Weber T, Kracht LW, Roggendorf J, Baudrexel S, et al. STN-DBS activates the target area in Parkinson disease An FDG-PET study. *Neurology.* 2008 Feb 9;71(10):708–13.
478. Cerasa A, Koch G, Donzuso G, Mangone G, Morelli M, Brusa L, et al. A network centred on the inferior frontal cortex is critically involved in levodopa-induced dyskinesias. *Brain.* 2015 Feb 1;138(2):414–27.

479. Cerasa A, Novellino F, Quattrone A. Connectivity Changes in Parkinson's Disease. *Curr Neurol Neurosci Rep.* 2016 Aug 27;16(10):91.
480. Akram H, Wu C, Hyam J, Foltynie T, Limousin P, De Vita E, et al. l-Dopa responsiveness is associated with distinctive connectivity patterns in advanced Parkinson's disease. *Mov Disord.* 2017;32(6):874–83.

Acknowledgements

The completion of this dissertation would not have been possible without the help and support of the following people who contributed to this work in different ways:

First of all, I would like to thank my supervisor Prof. Dr. Heike Endepols from the bottom of my heart for always helping with words and deeds throughout the last six years, for listening to all my questions and problems (repeatedly), for constantly encouraging me and seeing the positive side of things, for being such a strong woman in science and a great role model, for not only accepting but supporting my boxing passion and being so forgiving with my complicated time schedule, and last but not least for her infinite patience. Without you, this work would have never been possible Heike.

I would also like to thank Prof. Dr. Lars Timmermann who first employed me at the University Hospital Cologne despite my unconventional athlete life style, introduced me to the fascinating field of Parkinson's disease, and established the connection to Prof. Dr. Endepols. Without him, I would not have had the opportunity to start this exciting PhD programme.

Dr. Elena Kordys I would like to thank for teaching me the surgical procedures crucial to my studies and for introducing me to the different experimental protocols. Similarly, I am very grateful for the analytical and statistical advice from Dr. Cathrin Rohleder who was always happy to help.

Special thanks are due to Kunal Paralikar from Medtronic, who did his best to help even from afar. His engineering knowledge and technical support regarding the stimulation system as well as his commitment to the project was irreplaceable. Beyond that, the pleasant and personal way of communication as well as his patience, support for and appreciation of my boxing career meant a lot to me.

Furthermore, I would like to express my gratitude to Dr. Dirk Wiedermann of the Max Planck Institute for Metabolism Research. His seemingly limitless knowledge and understanding of the MRI system and his vast experience with numerous technical problems made my day and saved precious time again and again.

Thanks is also due to Thomas Merker from the Scientific Workshop in the Medical Faculty of the University of Cologne. He supplied essential tools to prepare the stimulation systems and offered valuable advice.

I am extremely grateful for my former colleague and now good friend Stefanie Vus who helped making work fun, who was always there to discuss scientific questions, who shared my everyday struggles and achievements, and who always had my back. I also very much appreciate the other girls in the office, M.Sc. Olesia Bannykh, Dr. Felicia Krämer, Dr. Merle Hönig, and M.Sc. Julia Gollmann and would like to thank them for their constant professional advice and emotional support.

Furthermore, I would like to thank my fiancé Lukas Wilaschek for always believing in me and picking me up when I was down, and my very good friend Ursula Gottlob for always listening to my problems, making me laugh and taking my mind off things during tough times.

Lastly, I would particularly like to thank my parents Ute and Hannes Apetz as well as my brother Jan Apetz for constantly supporting me in doing what I love.